The *Ustilago maydis* forkhead transcription factor Fox1 is involved in the regulation of genes required for the attenuation of plant defenses during pathogenic development

Dissertation

zur

Erlangung des Doktorgrades

der Naturwissenschaften

(Dr. rer. nat.)

dem Fachbereich Biologie

der Philipps-Universität Marburg

vorgelegt von

Alexander Zahiri

aus Toronto, Kanada

Marburg/Lahn 2010

Vom Fachbereich Biologie

der Philipps-Universität Marburg als Dissertation

angenommen am: _____

Erstgutachter: Herr Prof. Dr. Jörg Kämper

Zweitgutachter: Herr Prof. Dr. Michael Bölker

Tag der mündlichen Prüfung am:_____

Declaration

I hereby declare that the dissertation entitled "The *Ustilago maydis* forkhead transcription factor Fox1 is involved in the regulation of genes required for the attenuation of plant defenses during pathogenic development" submitted to the Department of Biology, Philipps-Universität Marburg, is the original and independent work carried out by me under the guidance of the PhD committee, and the dissertation is not formed previously on the basis of any award of Degree, Diploma or other similar titles.

_____ _____

(Date and Place) (Alexander Zahiri)

The research pertaining this thesis was carried out at the Department of Organismic Interactions at the Max-Planck-Institute for Terrestrial Microbiology, Marburg, from October 2006 to April 2008, and Karlsruhe Institute of Technology, Institute for Applied Bioscience, Department of Genetics, from April 2008 to April 2010 under the supervision of Prof. Dr. Jörg Kämper.

Parts of this work are presented in the following submitted article:

Zahiri, A., Heimel, K., Wahl, R., Magnus, R., Kämper, J. (2010) The *Ustilago maydis* forkhead transcription factor Fox1 is involved in the regulation of genes required for the attenuation of plant defenses during pathogenic development. Submitted.

Abstract

The basidiomycete *Ustilago maydis* is a phytopathogenic fungus that causes common smut disease on maize. *U. maydis* is a dimorphic fungus that can exist as a non-pathogenic yeast-like haploid cell, or as a filamentous growing pathogenic dikaryon. As a biotrophic fungus, completion of the life cycle depends on living host tissue. The biotrophic interaction is initiated upon breaching of the host epidermal layer, and involves invagination of the host plasma membrane around hyphae to form an interaction zone. This is thought to facilitate nutrient acquisition by the fungus, as well as the translocation of fungal effector proteins into the plant cell. The establishment and maintenance of the biotrophic phase requires an adaptation to a multitude of nutritional/environmental conditions, and the response to host specific signals and defense reactions. Dynamic processes during the host interaction entail a complex regulatory network including a variety of different transcription factors, which work in concert to coordinate successful pathogenic development. While transcriptional regulators involved in the establishment of an infectious dikaryon and penetration into the host have been characterized, transcriptional regulators exclusively required for the post-penetration stages remained to be identified.

The potential forkhead transcription factor Fox1 has been identified by global gene expression profiling. Fox1 is specifically expressed *in planta* and required for biotrophic development. In particular, *U. maydis* Δ*fox1* mutant strains are unable to incite tumor formation, and infected leaf tissue displays increased anthocyanin levels. Expression analysis of the host response revealed the deregulation of genes required for plant cell growth and enlargement, and the induction of genes associated with the production of anthocyanins.

Microscopic analyses identified that unlike wild-type-hyphae, which are found frequently within the plant vasculature and mesophyll, hyphae of Δ*fox1* mutants predominantly aggregate within the plant vasculature and are rarely detected in the mesophyll. The reason behind this focused growth remains to be elucidated, however the Δ*fox1*-dependent repression of genes involved in sugar transport and processing could have a decisive effect on the ability of the fungus to grow in sugar-sparse plant tissue.

Global gene expression profiling identified Fox1 as a *b*-independent, plant specific regulator. *fox1*-dependent genes comprise those encoding secreted proteins, including potential effectors belonging to gene clusters required for virulence. As a

consequence, Δ*fox1*-hyphae trigger host defense reactions, including the overproduction and accumulation of H_2O_2 in and around infected cells, and a novel maize defense response phenotypically represented by the encasement of proliferating hyphae in a plant-produced matrix consisting of cellulose and callose.

Zusammenfassung

Der Basidiomycet *Ustilago maydis* ist ein phytopathogener Brandpilz, der den Maisbeulenbrand verursacht. *U. maydis* ist ein dimorpher Pilz, der sich in Form einer nichtpathogenen, saprophytischen haploiden Sporidie durch Knospung vermehren, oder phytopathogen, als stabiles dikaryotisches Filament innerhalb der Pflanze wachsen kann. Als biotropher Organismus ist die Komplettierung des Lebenszyklus vom Vorhandensein lebenden Wirtsgewebes abhängig. Die biotrophe Interaktion startet mit der Penetration der epidermalen Zellwand, gefolgt von einer Invagination der Wirts-Plasmamembran welche die Pilzhyphen schlauchartig umgibt, so dass eine apolplastische Interaktionszone entsteht. Diese sichert die Versorgung des Pilzes mit Nährstoffen, und bietet eine Grenzfläche für die Sekretion von pilzlichen Effektoren in die Wirtszelle. Die Etablierung und Aufrechterhaltung der kompatiblen Interaktion erfordert sowohl eine Anpassung des Pilzes an die veränderten Umwelt- und Nährstoffbedingungen, als auch das Umgehen oder die Suppression des pflanzlichen Abwehrssystems. Dynamische Prozesse während der Interaktion induzieren ein komplex reguliertes Netzwerk einschließlich einer Vielzahl von Transkritionsfaktoren welche die pathogene Entwicklung des Pilzes *in planta* koordinieren. Während bereits Transkriptionsregulatoren, welche die Entwicklung infektiöser dikaryotischer Hyphen und den Penetrationsmechanismus in die Wirtszelle regulieren charakterisiert wurden, konnten bisher noch keine Transkriptionsfaktoren identifiziert werden, die an der Regulation von Post-Penetrationsstadien beteiligt sind.

In einer genomweiten Expressionsanalyse konnte der potenzielle Forkhead Transkriptionsfaktor Fox1 identifiziert werden. Fox1 wird spezifisch *in planta* exprimiert und ist essentiell für eine kompatible Interaktion. *U. maydis fox1* Deletionsmutanten sind defizient bezüglich der Tumorbildung und infizierte Maispflanzen zeigen eine erhöhte Anthocyaninproduktion. Die Expressionsanalyse von infiziertem Wirtsgewebe zeigte Deregulierung von Genen deren Expression mit Zellwachstum und Zellausdehnung korreliert ist, sowie eine Induktion von Genen, die mit der Produktion von Anthocyaninen assoziiert sind.

Mikroskopische Untersuchungen zeigten, dass die Hyphen von *fox1* Deletionsstämmen überwiegend in den Leitbündeln akkumulieren, während Wildtyphyphen sowohl im Mesophyll als auch in den Leitbündeln aufzufinden sind. Die Ursache für dieses konzentrierte Wachstum ist bisher nicht bekannt. Allerdings könnte die Δ*fox1* abhängige Repression von Genen, involviert in Zuckertransport und

dessen Metabolisierung, einen entscheidenden Einfluss auf die Fähigkeit des Pilzes, in zuckerärmeren Arealen des pflanzlichen Wirtes zu wachsen, haben.

Weiterhin konnte in Expressionsanalysen gezeigt werden, dass Fox1 einen *b*-unabhängigen spezifisch *in planta* exprimierten Transkriptionsregulator darstellt. *fox1* regulierte Gene codieren für sekretierte Proteine einschließlich potenziellen Effektoren, die virulenzrelevanten Genclustern zugeordnet werden können. Als Konsequenz induzieren *fox1* Deletionsmutanten in der Wirtspflanze Abwehrreaktionen, die mit einer Akkumulation von H_2O_2 in und um infizierte Zellen herum einhergeht. Phänotypisch zeigt die Infektion mit Δ*fox1* Stämmen einen bisher für Mais unbeschriebenen Abwehrmechanismus, wobei proliferierende Hyphen von einer pflanzlichen Matrix aus überwiegend Cellulose und Callose umhüllt werden.

Glossary

A_{280}	absorbance at 280 nm
aa	amino acid
Amp	ampicillin
bp	base pair
^{o}C	degree Celsius
Cbx^{R}	carboxin-resistance
CM	complete medium
C-terminal	carboxyl-terminal
DAPI	4',6-diamidino-2-phenylindole
DIC	differential interference contrast
DMSO	dimethylsulfoxide
DNA	deoxyribonucleotide
dpi	days post infection
EDTA	ethylendiamintetraacetic acid
eGFP	enhanced green fluorescent protein
FBD	forkhead DNA-binding domain
f.c.	final concentration
g	gravity
h	hour
hph	hygromycin phosphotransferase gene
Hyg^{R}	hygromycin-resistance
kb	kilobase
ip	iron sulphur subunit of the succinate dehydrogenase locus
M	molar
mig	maize induced gene
min	minute
MM	minimal medium
mM	millimolar
MOPS	3-[N-morpholino] propanesulfonic acid
mRNA	messenger ribonucleic acid
N-terminal	amino-terminal
NLS	nuclear localization sequence
OD_{600}	optical density at 600 nm
ORF	open reading frame
PCR	polymerase chain reaction
PD	potato-dextrose
PEG	polyethylene glycol
$Phleo^{R}$	phleomycin-resistance
qRT-PCR	quantitative Real-Time Polymerase Chain Reaction
RNA	ribonucleic acid
SDS	sodium dodecyl sulfate
rpm	rotations per minute
TE	Tris-Cl + Na2-EDTA
T_m	melting temperature
Tris	trishydroxymethylamino-methane
U	unit (enzyme activity)
UTR	untranslated region
UV	ultraviolet light
v/v	volume per volume
WGA	wheat germ agglutinin
WT	wild-type
w/v	weight per volume

Table of contents

1 Introduction

1.1 *Ustilago maydis*, the causal agent of corn smut

Ustilago maydis is a phytopathogenic fungus that belongs to the Basidiomycetes, which include many other plant pathogens, as the smuts, bunts and rusts (Banuett, 1992). *U. maydis* is a specific pathogen of corn (*Zea mays*) and the causative agent of corn smut disease – it induces the neoplastic growth of plant tissue and subsequent tumor formation. This fungus is of particular importance as it is responsible for substantial losses of an economically important cultivar. However, unlike many other phytopathogenic basidiomycete fungi such as the bunts and rusts, *U. maydis* can be cultured under laboratory conditions. Furthermore, the availability of a fully annotated genome sequence and previously established molecular techniques for genetic manipulation make it an ideal model organism for the study of host-pathogen interactions.

1.2 The life cycle of *U. maydis*

U. maydis belongs to the group of biotrophic fungi that require living host tissue for proliferation. It is a dimorphic fungus that exists as a haploid non-pathogenic yeast-like cell, and as a filamentous growing pathogenic dikaryon (Banuett, 1992). The switch from the unicellular haploid to the pathogenic dikaryon is established upon fusion of two haploid cells with compatible *a*- and *b*-mating type loci. Cell fusion is achieved via a pheromone-receptor system encoded by the *a*-locus. Upon pheromone stimulation budding growth is arrested and conjugation tube formation is initiated (Spellig *et al*., 1994). The formation of the filamentous dikaryon and pathogenic development are controlled by the multiallelic *b*-locus that encodes the homeodomain transcription factors bE and bW. bE and bW form a heterodimeric complex (bE/bW) that serves as the master regulator of a transcription cascade that regulates host penetration and *in planta* development (Kahmann and Kämper, 2004; Wahl *et al*., 2010). Penetration of the plant cuticle is facilitated through appressoria, specialized infection structures that are involved in softening the plant cell wall, most likely via lytic enzymes (Snetselaar and Mims, 1993; Kahmann and Kämper, 2004; Doehlemann *et al*., 2008a). During penetration, the host plasma membrane invaginates and surrounds the invading hypha, which establishes a biotrophic

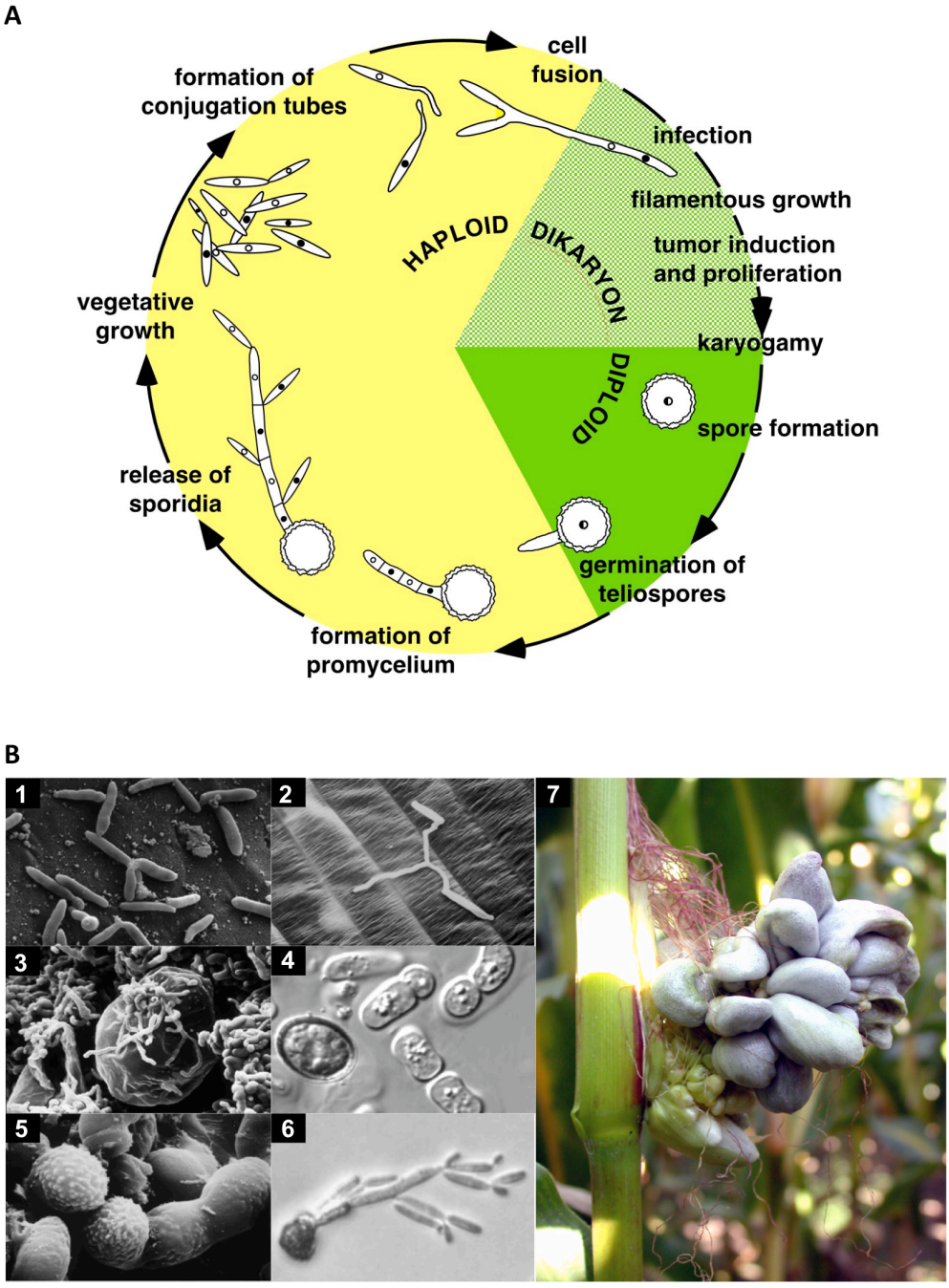

Figure 1. (A) A schematic diagram of the life cycle of *U. maydis* (see text for a detailed description). **(B)** The different developmental stages of the *U. maydis* life cycle are highlighted: (1) Yeast-like haploid sporidia dividing by budding (G. Wanner). (2) Fusion of two compatible haploid sporidia forming a filamentous dikaryotic hypha on the leaf surface (Snetselaar and Mims, 1993). (3) Mycelium proliferating within tumor tissue (K. Snetselaar). (4) Pre-sporulation stage, consisting of the fragmentation of hyphae followed by the rounding of cells (S. Huber). (5) Teliospore formation (Snetselaar and Mims, 1994). (6) The germination of a diploid teliospore resulting in the formation of haploid sporidia (S. Huber). (7) A tumor formed on a cob of corn (C. Basse).

interface between the invading hypha and plant cell (Bauer *et al*., 1997). Once inside the host, fungal hyphae grow inter- and intracellularly, leading to massive fungal proliferation resulting in the formation of tumors, which can develop on the leaves, stems, ears and tassels (Banuett, 1995; Doehlemann *et al*., 2008a). Within tumor tissue hyphae differentiate into segments. At this time-point karyogamy takes place, followed by the rounding of cells, resulting in the formation of thick-walled diploid teliospores (Banuett and Herskowitz, 1989; Snetselaar and Mims, 1993; Snetselaar and Mims, 1994). In the dormant state teliospores act as a dispersal agent, and are capable of remaining viable in dormancy for decades (Christensen, 1963; Banuett, 1995). Teliospore germination entails the formation and extension of a promycelium, the migration of the nucleus into the promycelium, followed by the completion of meiosis, and the formation of haploid sporidia (Christensen, 1963; Ramberg and McLaughlin, 1979).

1.3 The mating type loci of *U. maydis*

In *U. maydis* the morphological switch from the non-pathogenic haploid cell to the pathogenic dikaryon is controlled by a tetrapolar mating system, consisting of two genetically unlinked loci required for the determination of mating-type specificity (Kothe, 1996). These loci are the *a*-mating type locus that consists of two alleles, and the multiallelic *b*-mating type locus. The fusion of two compatible haploid cells is mediated by a pheromone/receptor based system encoded by the *a*-locus (Bölker *et al*., 1992; Urban *et al*., 1996). Each *a* allele encodes both a pheromone precursor (Mfa1 or Mfa2) and a pheromone receptor (Pra1 or Pra2). Fusion of two haploid cells can only take place when the pheromone receptor of one allele recognizes the pheromone of the other allele (Bölker *et al*., 1992). Upon pheromone recognition, compatible cells form conjugation tubes, which grow towards the pheromone source (Snetselaar *et al*., 1996). These conjugation tubes then fuse at the tips, followed by the migration of their individual nuclei into a common cytoplasmic space, generating a dikaryon (Bölker *et al*., 1992). After cell fusion, the decision to initiate the pathogenic program is mediated by the multiallelic *b*-locus, which has at least 19 different alleles (J. Kämper, unpublished). Each *b* allele encodes two homeodomain proteins, bEast (bE) and bWest (bW). Both proteins have N-terminal regions that harbor a variable domain, and C-terminal regions with a high degree of sequence similarity, which include the homeodomain motif (Gillissen *et al*., 1992; Kämper *et al*., 1995). bE and bW are able to dimerize forming the bE/bW heterodimeric complex, but only if the

dikaryon contains nuclei harboring different alleles of the *b*-mating type locus. The formation of the bE/bW complex is sufficient to initiate filamentous growth and pathogenic development (Bölker *et al*., 1995). In accordance with the onset of filamentous growth, the activation of bE/bW-complex also results in cell cycle arrest, which is only released upon penetration of the host plant (Mielnichuk *et al*., 2009).

1.4 The *b*-dependent regulatory cascade of *U. maydis*

The *U. maydis* bE/bW-heterodimer is a transcription factor, which triggers a complex regulatory cascade resulting in the dimorphic switch and the onset of pathogenic development. This cascade is triggered by the binding of the active heterodimer to conserved *b*-binding sequences (*bbs*) located in the promoter regions of directly regulated *b* target genes. Since the bE/bW-heterodimer is required for pathogenic development, it was proposed that direct *b* target genes would include pathogenicty factors. However, among the 20 known *b*-dependent genes, only a small fraction was identified to harbor the *bbs*-motif (Brachmann *et al*., 2001; Scherer *et al*., 2006). Since the majority of *b*-dependent genes are not directly regulated by the b-heterodimer, it was thought that the b-heterodimer directly regulates a small subset of genes (class I genes), which would include additional regulators that in turn regulate a larger portion of indirect *b* target genes (class II genes). To identify class I genes encoding potential regulators, DNA microarrays were used to monitor the global gene expression profile of *b*-inducible strains upon induction of the b-regulatory cascade (Heimel *et al*., submitted). This resulted in the identification of the gene *rbf1* (regulator of *b*-filament 1), which encodes a C_2H_2 zinc finger transcription factor. *rbf1* was also identified to be a direct target of the b-heterodimer, which is induced soon after *b*-induction (Heimel *et al*., submitted).

Rbf1 is vital for pathogenic development, as Δ*rbf1* mutant strains are unable to form appressoria and penetrate the plant cuticle (Heimel *et al*., submitted). Furthermore, Rbf1 was identified to be required for the regulation of more than 90% of all *b*-responsive genes (Heimel *et al*., submitted), identifying Rbf1 as the central regulatory switch of the *b*-regulatory network. Interestingly, the *rbf1*-dependent genes included genes encoding for additional regulators. Among theses were two genes encoding homeodomain transcription factors *hdp1* and *hdp2*, which were shown to be required for cell cycle arrest and pathogenic development respectively (Scherer, unpublished; Pothiratana, unpublished). The third gene, *biz1*, encodes a zinc finger transcription factor. Biz1 does not influence *b*-dependent filament formation, however

biz1 deletion mutants are severely impaired in the development of appressoria prior to plant penetration. Moreover, in the few instances were hyphae formed appressoria and penetrated the plant surface, proliferation did not extend beyond the epidermal layer (Flor-Parra *et al*., 2006). Even though the bE/bW-heterodimer, Rbf1, Hdp2 and Biz1 are all independently required for the establishment of the biotrophic phase, they are all initially expressed prior to plant penetration. Thus, additional *b*-independent regulators are most likely required for the progression of pathogenic development.

Previously, Zheng *et al.,* (2008) reported the identification of the *b*-independent C_2H_2 zinc finger transcription Mzr1, which is expressed during the biotrophic development and confers the induction of a subset of maize induced genes (*mig2* genes). Despite its role as a transcriptional activator *in planta*, deletion analysis revealed that *mzr1* was not essential for pathogenic development (Zheng *et al*., 2008). Even though Mzr1 had not effect on pathogenic development, it represents the first account of a *b*-independent transcriptional regulator that confers the induction of a specific subset of genes *in planta*. Therefore, it is conceivable that additional regulators are required for the completion of the *U. maydis* life cycle *in planta*. Such regulators may only be expressed at specific developmental stages, in a tissue specific fashion, under specific environmental/nutritional conditions, or upon perception of specific signals from the host plant.

1.5 Plant-induced fungal transcription factors in other phytopathogenic fungi

In phytopathogenic fungi, transcription factors have been implicated in the regulation of genes involved in specific stages of pathogenic development. The basic leucine zipper-like (bZIP-like) transcription factor TOXE of *Cochliobolus carbonum* regulates genes required for the production of HC-toxin that is highly virulent to selective maize genotypes (Pedley and Walton, 2001). In *Fusarium solani*, transcription factors CTF1α and CTF1β are required for the induction of cutinases involved in host penetration (Li *et al*., 2002), whereas a Zn_2Cys_6 transcription factor regulates expression of the pisatin demethylase *PDA1*, which detoxifies the host-produced isoflavonoid defense compound pisatin (Khan *et al*., 2003). More recently, the STE12-like transcription factor Clste12p of *Colletotrichum lindemuthianum* was shown to be required for invasive growth and pathogenic development. More specifically, Clste12p was shown to be required for the expression of genes encoding extracellular proteins, such as cell wall degrading enzymes, and proteins involved in the interaction of fungal cells with abiotic and biotic surfaces (Hoi *et al*., 2007).

1.6 *b*-dependent regulation

In *U. maydis* the b-heterodimer is set atop a regulatory cascade that initiates the pathogenic program. Activation of the b-heterodimer in axenic culture resulted in the regulation of 345 *b*-responsive genes, of which 206 genes were up-regulated and 139 genes down-regulated. Among the 345 *b*-regulated genes, only 239 were functionally classified. However, *b*-responsive genes included various deregulated genes involved in the cell cycle, which reinforced the observation that an active b-heterodimer leads to cell cycle arrest. Also among the *b*-responsive genes, were several genes with potential roles in the morphological switch from a budding haploid cell to a filamentous growing hypha. These included genes with predicted functions in cell wall synthesis and modification, as chitin synthases, and exo- and endoglucanases among others, suggesting an alteration in cell wall composition during the switch from a budding haploid cell to the filamentous growing hypha. Interestingly, a substantial portion of the *b*-responsive genes was predicted to encode secreted proteins (74 genes), which may play a role in the establishment of the biotrophic interaction (Heimel *et al*., submitted).

1.7 The *U. maydis* secretome and biotrophic development

The role of secreted effector proteins on the establishment and maintenance of pathogenic development of phytopathogenic bacteria, oomycetes and fungi is well documented (Birch *et al*., 2006; Catanzariti *et al*., 2006; Chisholm *et al*., 2006; Kamoun, 2006; Kämper *et al*., 2006; O'Connell and Panstruga, 2006; Ridout *et al*., 2006; Kamoun, 2007; Morgan and Kamoun, 2007). In *U. maydis,* as many as 750 genes are predicted to encode secreted proteins, most of which have not been ascribed a function (MUMDB; Müller *et al.,* 2008; Kämper *et al.,* 2006). A substantial portion of the genes that encode secreted proteins are organized into 12 gene clusters consisting of 3-26 genes, of which the majority are induced in tumor tissue (Kämper *et al*., 2006). Furthermore, 5 of the 12 clusters have been implicated in pathogenic development. Deletion strains of clusters 5B, 6A, 10A and 19A displayed different degrees of reduced virulence, whereas deletion of cluster 2A resulted in increased virulence (Kämper *et al*., 2006). Interestingly, only seven genes belonging to these clusters have also been shown to be up-regulated by the bE/bW-heterodimer (Kämper *et al*., 2006; Heimel *et al*., submitted), suggesting the need of additional regulators for

the complete induction of these clustered genes during *U. maydis* biotrophic development.

1.8 Fox1, a forkhead protein required for pathogenic development

Previously, DNA microarray experiments were conducted monitoring the gene expression profile of *U. maydis* during biotrophic development, resulting in a plethora of differentially expressed genes (Vranes *et al*., unpublished). In an attempt to identify additional regulators, the data set was examined for genes encoding proteins that harbored structural motifs observed in known transcription factors. This led to the identification of the gene, *fox1* (*um01523*), which encodes a protein with similarities to forkhead transcription factors. Deletion strains of *fox1* can form dikaryotic filaments that subsequently penetrate the plant, however, tumor development is severely impaired and teliospore formation is completely blocked. In addition, proliferating Δ*fox1*-hyphae trigger what appears to be a plant response, depicted by the encasement of hyphae in an optically dense matrix.

1.9 Forkhead transcription factors, a brief overview

Forkhead proteins makeup a transcription factor family that displays vast functional diversity, and are involved in a wide variety of biological processes (Carlsson and Mahlapuu, 2002). The name "Forkhead" was derived from the spiked-head structures observed in Drosophila forkhead mutant embryos, which are impaired in anterior and posterior gut formation (Weigel *et al*., 1989). Since their discovery in 1989, members of this gene family have been discovered in a variety of eukaryotic organisms. X-ray crystallography experiments determined that the 3-D structure of a forkhead domain consists of a helix-turn-helix core of three α-helices flanked by two loops (winged helix), resembling the shape of a butterfly (Clark *et al*., 1993). More specifically helix 1 and helix 2 are stacked on top of helix 3 (the recognition helix), which binds to the major groove of DNA (van Dongen *et al*., 2000). Wing 1 consists of two antiparallel *β*-strands that extend upwards in parallel to the DNA past the 3' end, while wing 2 has minor groove contact with the 5' end of the binding site (Clark *et al*., 1993). Within the forkhead family there is high conservation with respect to the three α-helices and *β*-strands, and less within the wings (Carlsson and Mahlapuu, 2002).

Forkhead proteins bind to DNA as monomers, with binding sites of 15-17 bp. Sequence specificity for such binding sites has previous been determined for several forkhead proteins using pools of short random-sequence duplexes (Pierrou *et al*., 1994). A seven-nucleotide core representing the major groove contact made by α-helix 3 was identified as RYMAAYA (R = A or G; Y = C or T; M = A or C), and is present in the majority of forkhead proteins (Overdier *et al*., 1994; Pierrou *et al*., 1994; Kaufmann *et al*., 1995), however, distantly related out-groups of forkhead proteins (FoxO subfamily) also bind to partial motif matches (Brunet *et al*., 1999; Kops and Burgering, 1999). In addition to the core sequence, flanking sequences on either side of the core are also required for high affinity binding (Overdier *et al*., 1994; Pierrou *et al*., 1994; Kaufmann *et al*., 1995; Roux *et al*., 1995). Distantly related forkhead proteins with differences in core and flanking sequences have demonstrated non-overlapping sequence specificity (Overdier *et al*., 1994), whereas others (FOXC1 and FOXD1) have partial target specificities (Pierrou *et al*., 1994).

Forkhead proteins generally act as transcriptional activators, however, examples of transcriptional repression have been documented in forkhead proteins FoxC2, FoxD2, FoxD3 and FoxG1 (Sutton *et al*., 1996; Freyaldenhoven *et al*., 1997; Bourguignon *et al*., 1998). The LIN-31 forkhead protein in C*aenorhabditis elegans* can function as a transcriptional activator or repressor depending on its phosphorylation state via MAP kinase signaling (Tan *et al*., 1998). Like many other types of transcription factors, activation regions involved in transcriptional activation have been mapped in numerous forkhead proteins, including FoxA2, FoxF1, FoxF2, and FoxN1 (Pani *et al*., 1992; Qian and Costa, 1995; Schuddekopf *et al*., 1996; Hellqvist *et al*., 1998; Mahlapuu *et al*., 1998). These activation regions can be numerous and are found in various locations relative to the forkhead domain. Unlike the DNA-binding domains, there is scarce conservation of activator and repressor domains between the different forkhead proteins, and in most cases an absence of distinct molecular features (specific amino acid enriched region) (Hellqvist *et al*., 1998; Mahlapuu *et al*., 1998).

1.10 Aim of this study

In *U. maydis*, transcriptional regulators involved in the establishment of the pathogenic dikaryon and subsequent penetration in to the host plant have been indentified. However, the knowledge of transcriptional regulators required during the post-penetration stages of pathogenic development is limited. Fox1 represents a potential forkhead transcription factor, which is exclusively expressed *in planta* and required for full virulence. The reduction in virulence is accompanied by the encasement of Δ*fox1*-hyphae in an optically dense matrix. This study will focus on the identification of downstream targets of Fox1, and use a reverse genetic approach to identify their specific roles with respect to the observed *fox1* mutant phenotypes. Furthermore this study will utilize DNA microarrays and microscopic analyses to examine the plants response in order to elucidate the source of the optically dense matrix.

2 Results

In *Ustilago maydis*, much is known about the regulators required for the onset of pathogenic development and subsequent penetration into the host, however, regulators required for the post-penetration stages of pathogenic development remain to be elucidated. DNA microarray experiments monitoring the *in planta* development of *U. maydis* (M. Vranes, unpublished; J. Kämper, personal communication) identified a small set of genes induced in the plant that encode potential regulators. One of these genes was *fox1*, which encodes a potential forkhead transcription factor that was found to be exclusively expressed *in planta*. Deletion of *fox1* resulted in a reduction in virulence and the encasement of hyphae in an optically dense matrix during biotrophic development.

2.1 Fox1, a putative forkhead transcription factor in *U. maydis*

The *U. maydis* gene *um01523* encodes a protein of 439 amino acids that contains 1) a domain from residues 130 to 223 with similarities to forkhead DNA-binding domains (FBD) belonging to described forkhead transcription factors, and 2) a serine-rich region from residues 312-403 (Figure 2A). Based on similarities to other forkhead transcription factors, the gene was named *fox1*. Sequence alignments with forkhead proteins from *Homo sapiens* and *Drosophila melanogaster* (Foxf1, Foxl1 and Slp1) support the presence of a helix-turn-helix core of three α-helices (H1, H2 and H3) flanked by two wings (W1 and W2, Figure 2B). Phylogenetic analysis comparing the amino acid sequence of Fox1 to 58 additional forkhead proteins revealed a distant evolutionary relationship within basidiomycetous fungi, and a closer evolutionary relationship within ascomycetes and higher eukaryotes respectively (Figure 3). The presence of a FBD would suggest that Fox1 could function as a transcription factor. Furthermore, NCBI protein blast identified five conserved DNA contact sites in the FBD, three of which are located at residue 3, 6 and 7 of the recognition helix (H3; Figure 2B), which are responsible for making direct base contacts in the major groove of DNA (Clark *et al*., 1993; Pierrou *et al*., 1994; Overdier *et al*., 1994; van Dongen *et al*., 2000).

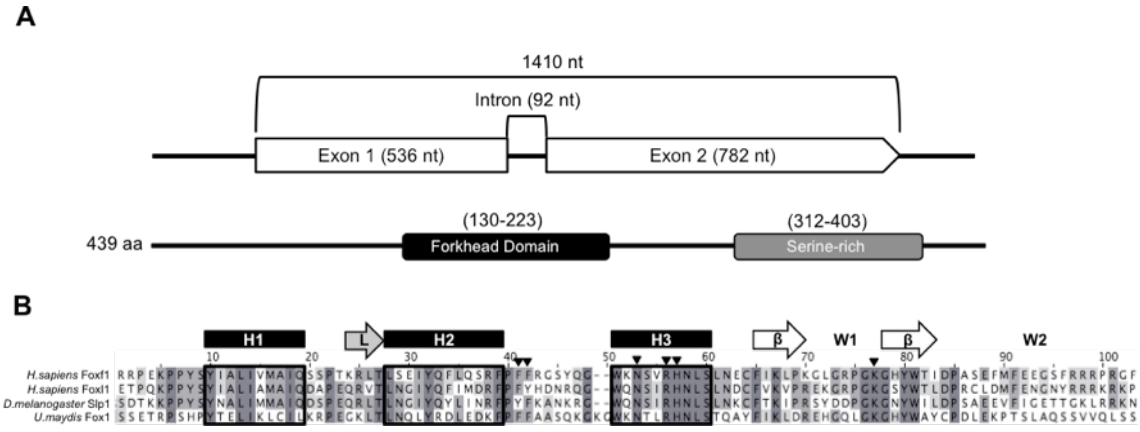

Figure 2. *fox1* encodes a forkhead protein. **(A)** Schematic presentation of the genomic sequences of *fox1* including a 92 bp intron, and the predicted protein structure of Fox1. The forkhead domain (aa 130-223; black box) and a serine-rich region (aa 312-403; grey box) are highlighted. **(B)** Protein sequence alignment of the *U. maydis* Fox1 forkhead DNA-binding domain (FBD) to FBDs of previously described forkhead proteins in *Homo sapiens* (Foxf1 and Foxl1) and *Drosophila melanogaster* (Slp1). The alignment confirms the presence of a helix-turn-helix core of three α-helices (H1, H2 and H3; black boxes) flanked by two wings (W1 and W2). Residues responsible for making contact to DNA are highlighted as black arrowheads, three of which are located at residue 3, 6 and 7 of the recognition helix (H3). The grey arrow represents a loop (L), and the two white arrows represent beta sheets (β).

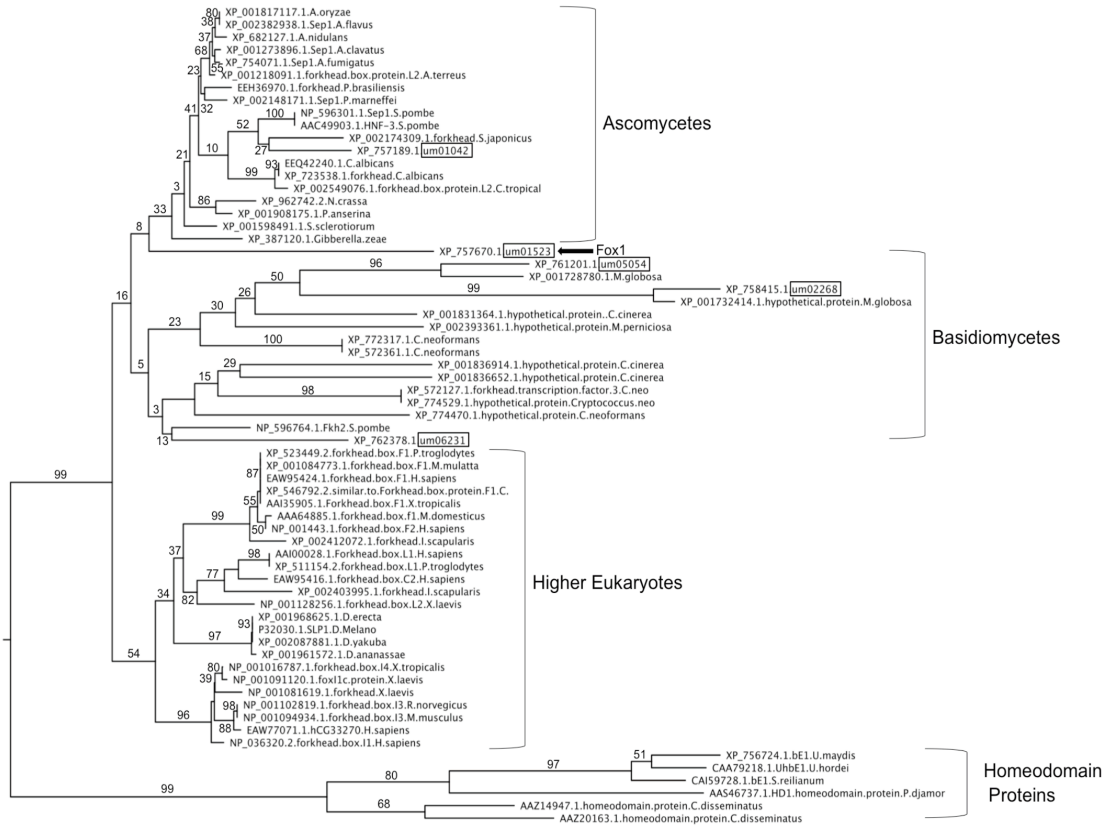

Figure 3. Phylogenetic tree comparing the Fox1 protein from *Ustilago maydis* to 58 forkhead proteins. The evolutionary relationship among forkhead proteins of basidiomycetous fungi including Fox1 of *U. maydis* display a less conserved phylogenetic resolution. Forkhead proteins from ascomycetes and higher eukaryotes display a more conserved phylogenetic resolution. The sequences of 6 homeodomain proteins from ascomycetous and basidiomycetous fungi were used as an out-group. *U. maydis* forkhead proteins are outlined with boxes, and Fox1 is labeled with a black arrow.

With respect to protein localization, SubLoc v1.0 predicted the subcellular localization of Fox1 to the nucleus (Reliability Index: RI = 9; Expected Accuracy = 98%). To verify nuclear localization, a Fox1-enhanced green fluorescent protein (eGFP) fusion under the control of the arabinose-inducible *crg1*-promoter (Bottin *et al*., 1996) was introduced into wild-type strains FB2 (*a2b2*) and AB31 (*a2 P crg1 :bW2,bE1*). After inducing strains FB2*Pcrg1:fox1:egfp* and AB31*Pcrg:fox1:egfp* for 5 hours in liquid array medium containing 1% arabinose as the sole carbon source, fluorescence microscopy identified the subcellular localization of the Fox1:eGFP fusion protein to the nucleus. (Figure 4A and 4B).

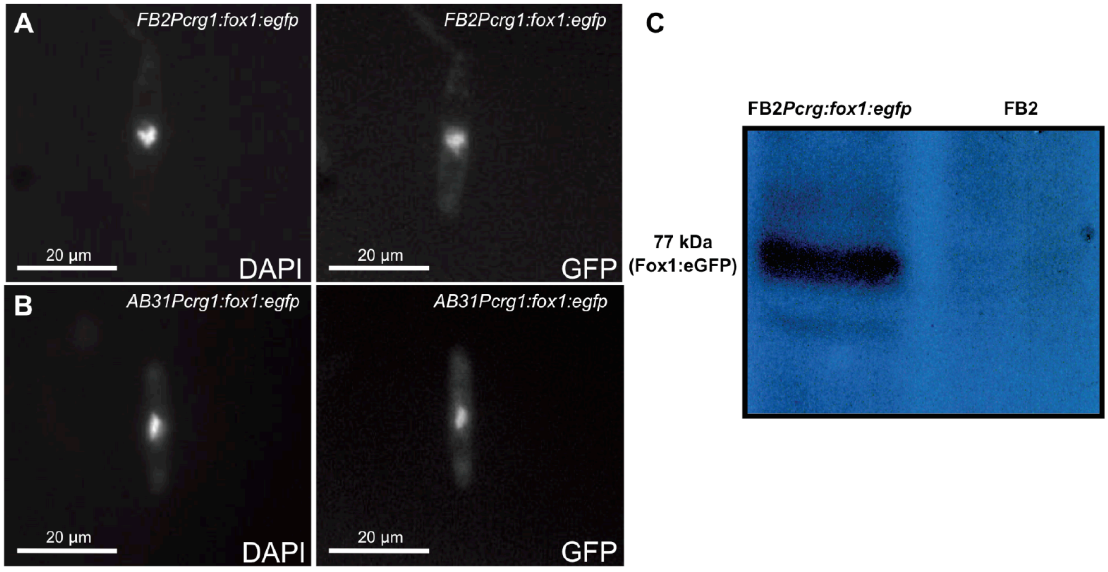

Figure 4. Fox1 is nuclear localized. **(A-B)** *fox1*-inducible strains FB2*Pcrg1:fox1:egfp* and AB31*Pcrg1:fox1:egfp* induced for 5 hours in liquid array medium containing 1% arabinose. Left panels show DAPI staining to visualize nuclei of haploid strains FB2*Pcrg1:fox1:egfp* and AB31*Pcrg1:fox1:egfp* grown in axenic culture. Right panels show the localization of Fox1:eGFP to the nucleus. **(C)** A Western blot of strains FB2*Pcrg1:fox1* and FB2 induced for 5 hours in liquid array medium containing 1% arabinose. The Left lane shows a 77 kDa band representing the intact Fox1:eGFP fusion protein in strain FB2*Pcrg1:fox1:egfp*, and no band present for the FB2 strain in the right lane.

2.2 Deletion of *fox1* has no effect on growth, mating and filament formation

Previous DNA microarray experiments indicated that the *fox1* gene was solely induced during biotrophic development (M. Vranes, unpublished; J. Kämper, personal communication). Quantitative Real-Time PCR (qRT-PCR) comparing the solopathogenic *U. maydis* strain SG200 in axenic culture to plants infected with SG200 at 1 day post-infection (dpi), 2 dpi, 4 dpi and 8 dpi confirmed the microarray results, and indicated that 4 dpi was the time-point *fox1* expression was at its highest level (Figure 5). Deletion of *fox1*, and the subsequent infection of maize plants with

FB1Δ*fox1* x FB2Δ*fox1* or SG200Δ*fox1* strains resulted in reduced virulence of *U. maydis*, and impaired tumor development *in planta*. Even though the involvement of Fox1 during pathogenic development is clearly evident, a thorough examination of Δ*fox1*-strains during developmental stages taking place outside of the plant was conducted to rule out any additional effects on *U. maydis* development.

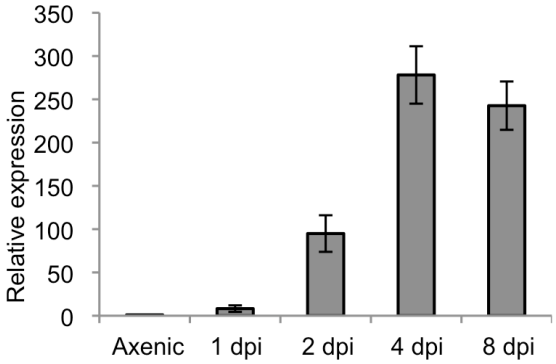

Figure 5. Expression analysis of *fox1* in the solopathogenic strain SG200. qRT-PCR was used to compare the relative expression of *fox1* in axenic culture (liquid array medium containing 1% glucose) to the expression in SG200 in infected maize leaves 1, 2, 4 and 8 dpi. Gene expression values are normalized relative to the constitutively expressed *actin* gene. Mean expression values are presented relative to the lowest level of expression. Error bars show the standard deviation of mean expression values of three biological replicates.

To determine if Fox1 has any influence over the saprophytic growth of *U. maydis*, *fox1* deletion strains FB1Δ*fox1*, FB2Δ*fox1* and SG200Δ*fox1* were grown in liquid culture and compared to their respective wild-type-strains FB1, FB2 and SG200. However, no morphological abnormalities were observed between Δ*fox1*-strains and their wild-type progenitor strains (Figure 6A). The next step was to determine if growth in the presence of different carbon sources had any effect on the growth rate of Δ*fox1*-strains. To examine this, *U. maydis* strains SG200Δ*fox1* and SG200 were grown in Minimal Medium supplemented with 1% sucrose, 1% glucose or 1% arabinose as the sole carbon source, and growth rate measured over an 8 hour time course. However, there was no difference in the rate of growth between SG200Δ*fox1* and SG200 strains, suggesting Fox1 has no effect on the growth rate of *U. maydis* under these tested conditions (Figure 6B). Finally, Δ*fox1*-strains were assayed for defects in mating and filament formation. Compatible haploid mixtures of FB1Δ*fox1* and FB2Δ*fox1* or FB1 and FB2, and solopathogenic strains SG200Δ*fox1* and SG200 with a cell density of OD_{600} ~1.0 were spotted on charcoal containing CM-glucose plates, which provide an environment for filament formation outside of the host plant. Under these conditions, Δ*fox1*-strains and their respective wild-type

counterparts were able to mate successfully, and no impairment in filament formation was detected (Figure 6C).

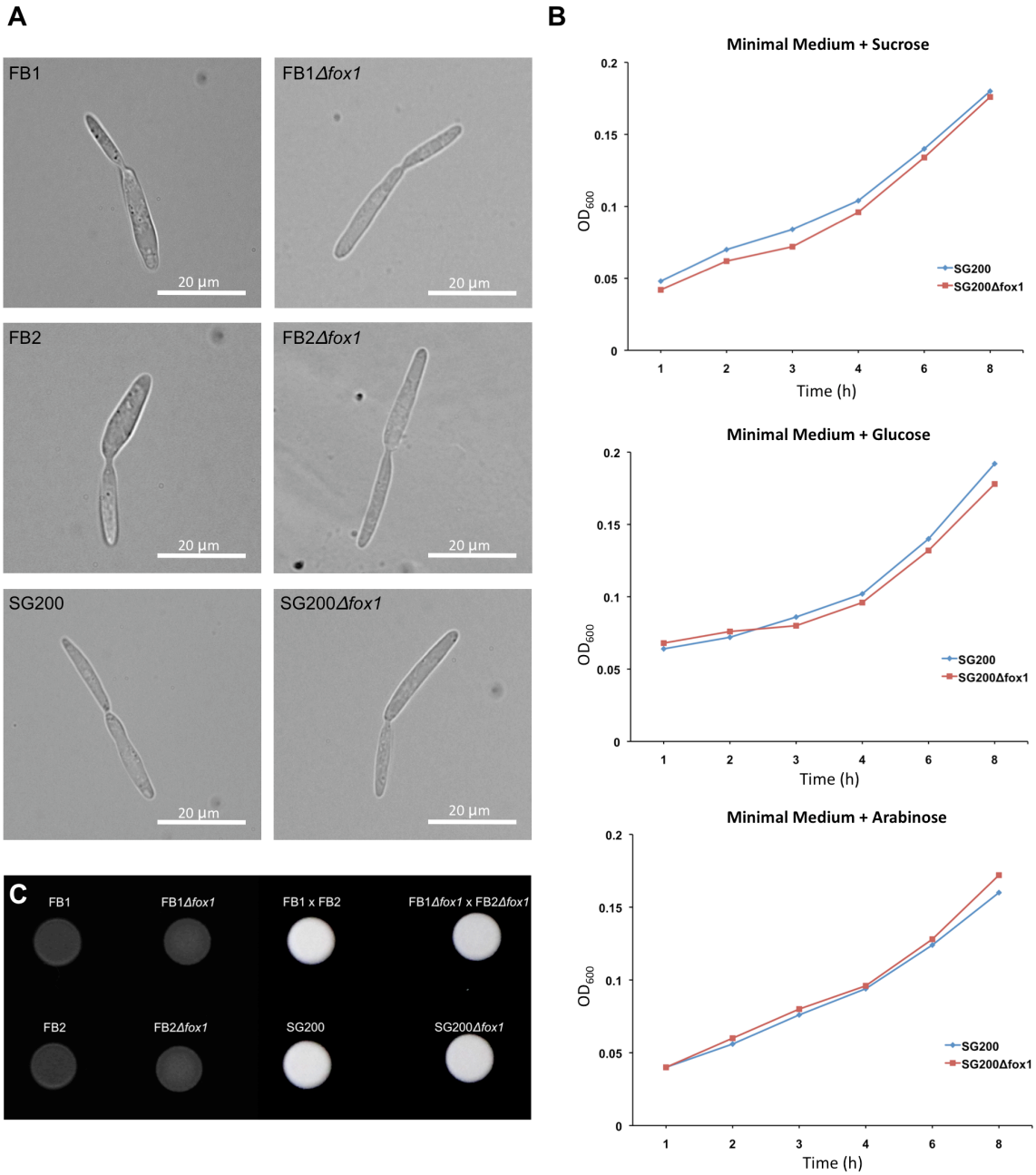

Figure 6. Δ*fox1*-strains have no effect on saprophytic growth, mating and filament formation. **(A)** *fox1* deletion strains FB1Δ*fox1*, FB2Δ*fox1* and SG200Δ*fox1* and wild-type-strains FB1, FB2 and SG200 grown in $YEPS_{Light}$ medium. No morphological abnormalities were observed in Δ*fox1*-strains when compared to the respective wild-type-strains. **(B)** An 8 hour time course study measuring the growth rate of *U. maydis* strains SG200Δ*fox1* and SG200 in Minimal Medium supplemented with either 1% sucrose, 1% glucose or 1% arabinose. No difference in the growth rate was observed between SG200Δ*fox1* and SG200 strains. **(C)** Mating and filament formation assay comparing compatible haploid mixtures of FB1Δ*fox1* x FB2Δ*fox1* and FB1 x FB2, and solopathogenic strains SG200Δ*fox1* and SG200 on charcoal containing CM-glucose plates. Δ*fox1*-strains like the respective wild-type-strains were able to mate and form filaments (depicted as white fuzzy spots). The haploid deletion strains FB1Δ*fox1*and FB2Δ*fox1* were individually spotted, and appear phenotypically identical to the respective wild-type-strains FB1 and FB2.

The lack of any defects in saprophytic growth, mating and filament formation are in line with the plant-specific expression profile of *fox1*.

2.3 Fox1 is required for full virulence during pathogenic development

Previously, *fox1* was deleted in strains FB1 (*a1b1*), FB2 (*a2b2*) and SG200. To address whether *fox1* is involved in pathogenic development, symptom development was monitored in maize plants infected with SG200Δ*fox1* or with a mixture of FB1Δ*fox1* x FB2Δ*fox1* in comparison with the respective wild-type control strains. No difference in disease symptom development was observed between Δ*fox1*- and wild-type-strain infected plants until 5 days post infection (dpi). However, at 7 dpi FB1Δ*fox1* x *FB2*Δ*fox1*- and SG200Δ*fox1*-infected plants displayed a severe impairment in tumor development (Figure 7A and 7B).

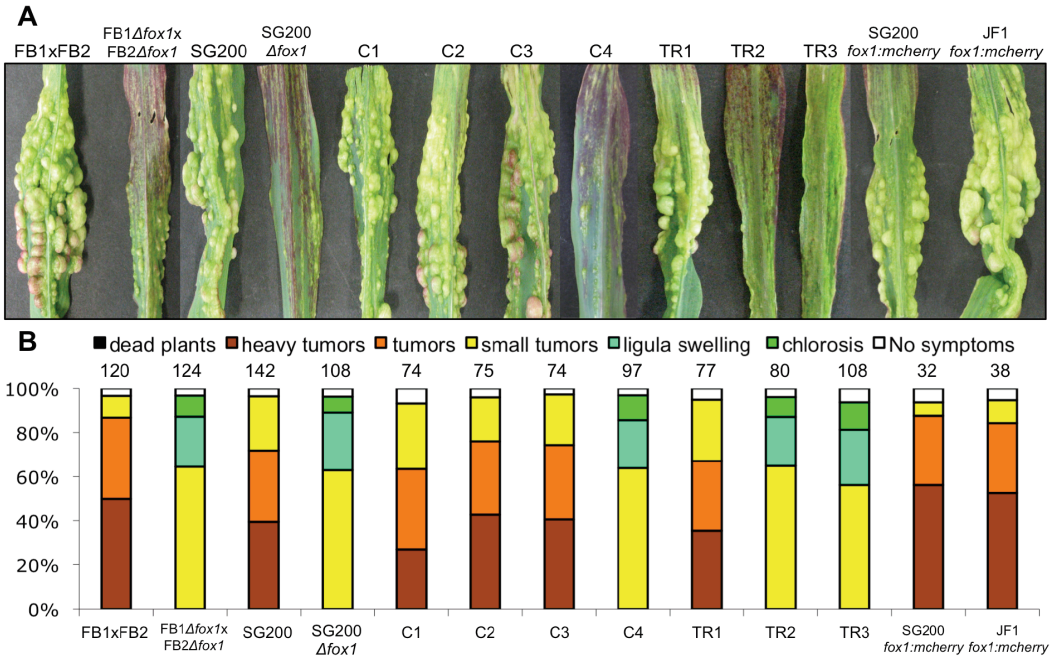

Figure 7. Fox1 is essential for the biotrophic development of *U. maydis*. **(A)** Disease symptoms of maize plants 7 dpi infected with *U. maydis* strains FB1 x FB2 (wild-type crosses), FB1Δ*fox1* x FB2Δ*fox1* (Δ*fox1* crosses), SG200 (wild-type), SG200Δ*fox1* (Δ*fox1*), Δ*fox1* complementation strains C1 (SG200Δ*fox1* $ip^r[P_{fox1}$:*fox1*$]ip^s$), C2 (SG200Δ*fox1* $ip^r[P_{mig2\text{-}5}$:*fox1*$]ip^s$), C3 (SG200Δ*fox1* $ip^r[P_{mig2\text{-}5}$:*fox1:egfp*$]ip^s$), C4 (SG200Δ*fox1* $ip^r[P_{mig2\text{-}5}$:*fox1*^{NS180,RS183,HS184}:*egfp*$]ip^s$), mutant strains TR1 (SG200*fox1*-79aa), TR2 (SG200*fox1*-139aa), TR3 (SG200*fox1*-216aa), and mcherry fusion strains SG200*fox1:mcherry* and JF1*fox1:mcherry*. **(B)** Disease rating of maize plants 7 days after infection with *U. maydis* strains FB1 x FB2, FB1Δ*fox1* x FB2Δ*fox1*, SG200, SG200Δ*fox1*, C1, C2, C3, C4, TR1, TR2, TR3, SG200*fox1:mcherry* and JF1*fox1:mcherry* (strain JF1 harbors an *egfp* gene under the control of the *mig2-5*-promoter, resulting in the cytosolic expression of eGFP *in planta*). Bars represent the percentage of infected plants with the symptom development indicated in the legend. Numbers represent the total number of plants infected with the corresponding strain.

In addition, Δ*fox1*-infected plants also displayed an increase in anthocyanin production when compared to their respective wild-type-infected plants. Quantification of the anthocyanin content, revealed that FB1Δ*fox1* x FB2Δ*fox1*-infected plants produced substantially more anthocyanin than FB1 x FB2-infected plants relative to mock infections (Figure 8).

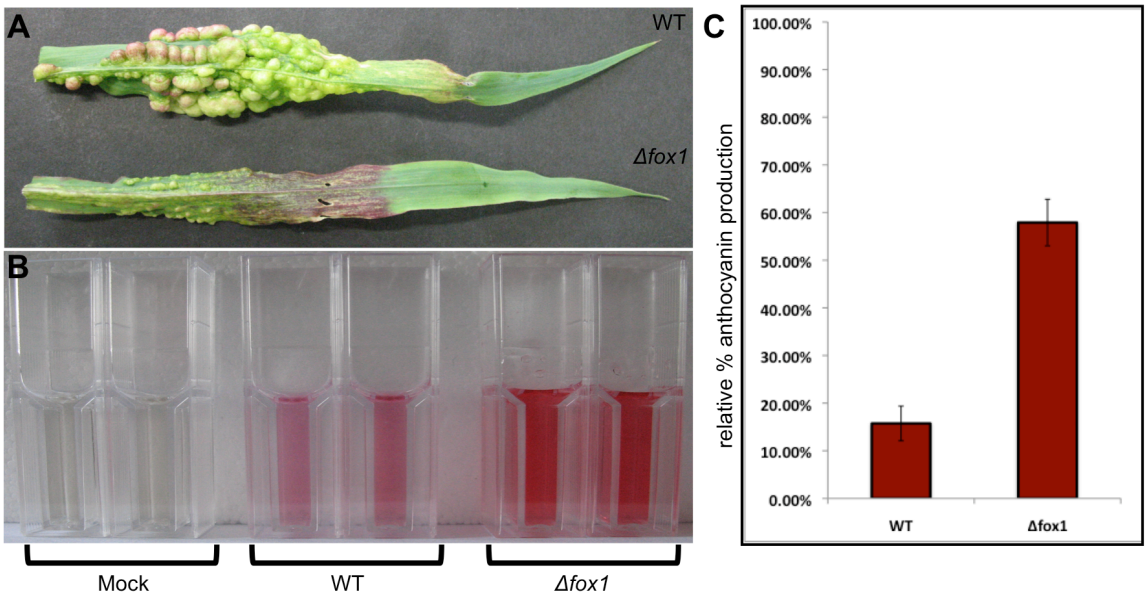

Figure 8. Maize plants infected with *U. maydis* Δ*fox1*-strains display increased anthocyanin production. **(A)** FB1Δ*fox1* x FB2Δ*fox1*-infected maize leaves show increased anthocyanin production when compared to their respective wild-type infections. **(B)** Visualization of anthocyanin extracted form the leaves of mock-infected, wild-type-infected, and FB1Δ*fox1* x FB2Δ*fox1*-infected plants. **(C)** Quantification of anthocyanin levels (Martin *et al*., 2002) in both wild-type- and FB1Δ*fox1* x FB2Δ*fox1*-infected plants leaves relative to non-infected mock controls.

To demonstrate that the observed mutant phenotype resulted from the *fox1* deletion, the native *fox1* gene with a 1078 bp 5´region was reintroduced into SG200Δ*fox1* (C1; SG200*Δfox1* $ip^r[P_{fox1}:fox1]ip^s$), which restored the virulence of the resulting strain to wild-type levels (Figure 7A and 7B). In addition, the *fox1* gene (C2; SG200Δ*fox1* $ip^r[P_{mig2\text{-}5}:fox1]ip^s$) and a *fox1:egfp* derivative (C3; SG200Δ*fox1* $ip^r[P_{mig2\text{-}5}:fox1:egfp]ip^s$), both driven by the *mig2-5*-promoter, which confers high gene expression *in planta* (Zheng *et al*., 2008) were introduced into SG200Δ*fox1*. Both strains were able to complement the Δ*fox1* mutation. Fluorescence microscopy of plant leaves infected with the C3 strain verified nuclear localization of Fox1:eGFP in proliferating fungal hyphae *in planta* (Figure 9A).

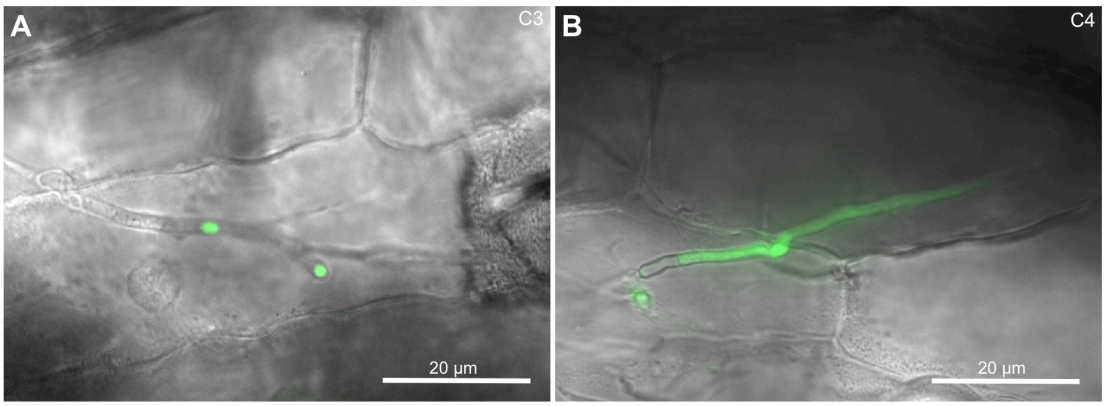

Figure 9. Fox1 is localized to the nucleus of proliferating hyphae during pathogenic development. **(A)** Intracellular hypha of the Δ*fox1* complementation strain C3 (SG200Δ*fox1* $ip^r[P_{fox1}$ *:fox1:egfp*$]ip^s$). Fox1:eGFP is localized to the nucleus of proliferating fungal hypha during pathogenic development. **(B)** Proliferating hypha of Δ*fox1* complementation strain C4 (SG200Δ*fox1* $ip^r[P_{mig2\text{-}5}$*:fox1*^{NS180,RS183,HS184}*:egfp*$]ip^s$), which harbors mutations at three residues in the forkhead DNA-binding domain demonstrated to be required for DNA-binding in previously characterized forkhead proteins. The Fox1^{NS180,RS183,HS184}:eGFP fusion protein was predominantly localized to the cytoplasm. Microscopic pictures A and B show an overlay of the GFP channel (green) and bright field projection (grey).

Localization of Fox1 under control of its native promoter was also attempted. A *fox1:mcherry* gene fusion was incorporated into the native *fox1*-locus in strains SG200 and JF1 (SG200 harboring an *egfp* gene under the control of the *mig2-5*-promoter in the *ip*-locus, resulting in the cytosolic expression of eGFP *in planta*) generating strains SG200*fox1:mcherry* and JF1*fox1:mcherry*. Both strains had similar disease rating as SG200 (Figure 7A and 7B), however the fluorescent signal was to weak to be detected in either strain by fluorescence microscopy (data not shown).

The forkhead DNA-binding domain (FBD) harbors three α-helices, with the third helix being involved in DNA-binding. Helix 3 of the *U. maydis* Fox1 contains three residues demonstrated to be required for DNA-binding in described forkhead transcription factors (Clark *et al*., 1993; Pierrou *et al*., 1994; Overdier *et al*., 1994; van Dongen *et al*., 2000). The conserved residues correspond to asparagine at position 180 (N180), arginine at position 183 (R183) and histidine at position 184 (H184) in Fox1. To determine if these residues were required for Fox1 function, PCR mutagenesis was implemented to mutate residues N180, R183 and H184 to an alanine, glycine and alanine respectively (Figure 10A). The resulting *fox1* mutant construct was fused to an *egfp* gene, placed under the control of the *mig2-5*-promoter (Zheng *et al*., 2008), and introduced into the *ip*-locus of SG200Δ*fox1* generating the strain C4 (SG200Δ*fox1* $ip^r[P_{mig2\text{-}5}$*:fox1*^{NS180,RS183,HS184}*:egfp*$]ip^s$). However, the C4 strain was not able to complement the Δ*fox1* mutation and plants infected with this strain displayed disease symptoms similar to SG200Δ*fox1*-infected plants (Figure 7A

and 7B), suggesting residues N180, R183 and H184 are required for Fox1 function. In addition, microscopic analysis of maize leaves infected with the C4 strain demonstrated that the Fox1^{NS180,RS183,HS184}:eGFP fusion protein was predominantly localized in the cytoplasm of proliferating hyphae (Figure 9B).

Fox1 has a serine-rich region downstream of the FBD, which is predicted to contain multiple conserved phosphorylation (MAPK, CDK, CK, GSK3, PKA and PKB) and protein interaction motifs (14-3-3 and FHA) within and flanking the serine-rich region. To determine if this region is required for Fox1 function, the native *fox1* gene was replaced with truncated versions of the gene. TR1 represents a deletion of the last 79 aa of Fox1 (including the last 43 aa of the serine-rich motif), in TR2 the entire serine-rich region was deleted, and in TR3 the entire serine-rich motif and an additional 89 aa up to the end of the FBD (Figure 10B). Plant infections with the different strains carrying the truncated versions of *fox1* revealed that TR1 induced symptoms similar to that of wild-type SG200 infections, while TR2 and TR3 displayed symptoms similar to SG200Δ*fox1*-infected plants (Figure 7A and 7B).

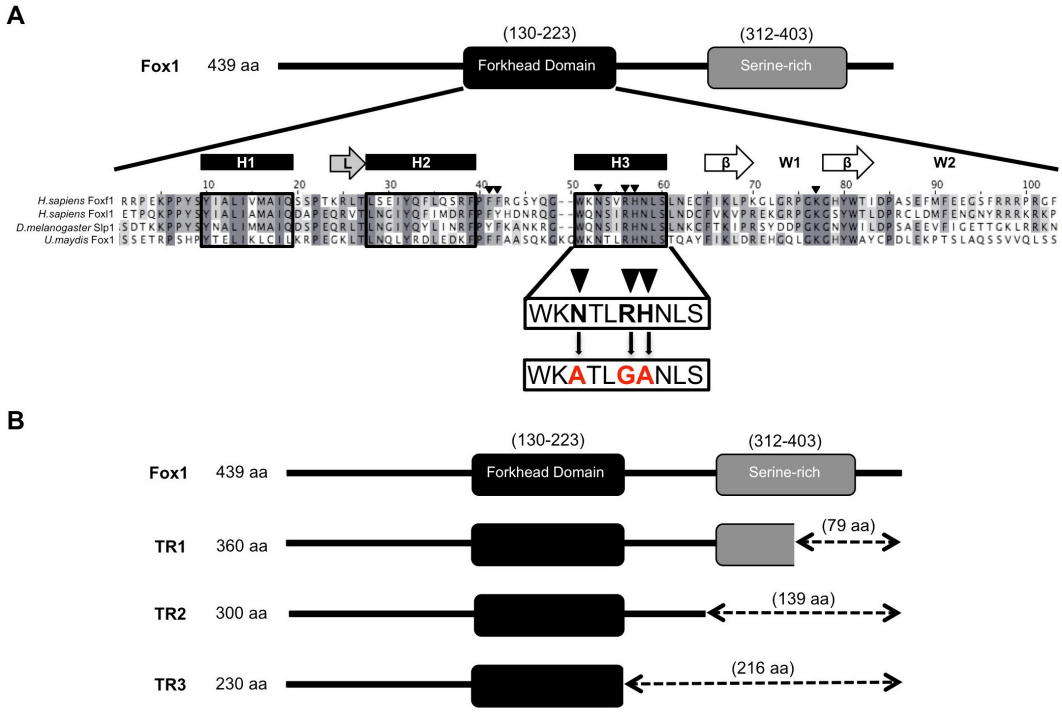

Figure 10. Illustration of the three amino acid substitutions in the third α-helix, and the three Fox1 protein truncations generated in this study. **(A)** Strain C4 was generated by mutating three positions of α-helix 3 (H3) of the Fox1 protein, previously shown to be required for direct DNA base contact (Clark *et al*., 1993; Overdier *et al*., 1994; Pierrou *et al*., 1994; Kaufmann *et al*., 1995). The following positions, asparagine at position 180 (N180), arginine 183 (R183) and histidine 184 (H184) were mutated to an alanine, glycine and alanine, respectively. **(B)** TR1 represents a deletion of the last 79 aa of Fox1 (including the last 43 aa of the serine-rich motif). In TR2 the entire serine-rich region was deleted, and in TR3 the entire serine-rich motif and an additional 89 aa up to the end of the forkhead domain.

2.4 Δ*fox1* mutants induce a novel *Zea mays* defense response

Previously, it has been demonstrated that Δ*fox1*-strains upon penetration into the host plant are encased in a thick-film-like substance in the epidermal layer (K. Heimel, personal communication). To examine at which stage of pathogenic development the encasement of Δ*fox1*-hyphae is initiated, a more detailed analysis was performed on hyphae during the infection process. Maize leaves infected with FB1Δ*fox1* x FB2Δ*fox1* were isolated daily from 2 to 9 dpi and stained with chlorazole black E to visualize fungal cells.

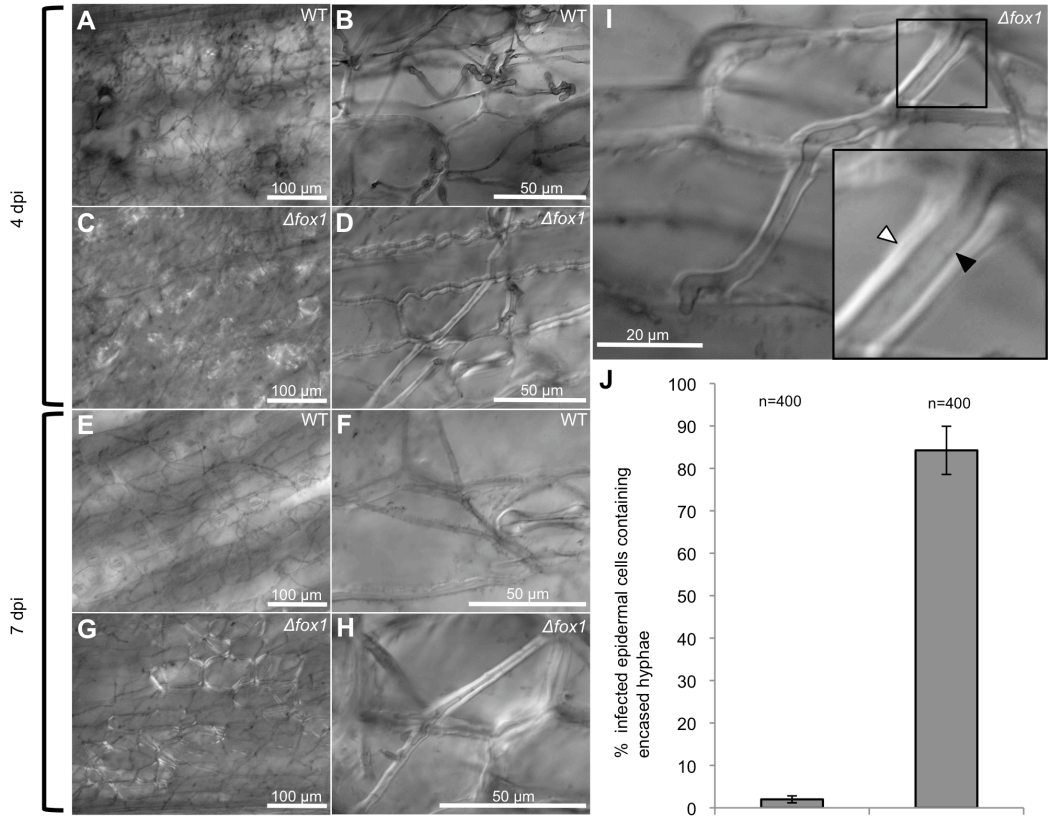

Figure 11. FB1Δ*fox1* x FB2Δ*fox1*-hyphae are encased in an optically dense matrix during pathogenic development. **(A-D)** Top view of maize leaves 4 days after infection with FB1 x FB2 (WT) and FB1Δ*fox1* x FB2Δ*fox1* (Δ*fox1*) strains, respectively. Initially the matrix surrounding Δ*fox1*-hyphae proliferating in the epidermal layer appeared as bright regions in select epidermal cells. **(E-H)** FB1 x FB2-hyphae and FB1Δ*fox1* x FB2Δ*fox1*-hyphae in infected maize leaves 7 dpi. The matrix encasing FB1Δ*fox1* x FB2Δ*fox1*-hyphae is more pronounced at 7 dpi when compared to FB1 x FB2-hyphae. **(I)** Magnified view of a FB1Δ*fox1* x FB2Δ*fox1*-hypha proliferating within the epidermal layer. The black arrowhead is pointing to the hypha, and the white arrowhead to the matrix. All fungal hyphae were visualized with chlorazole Black E. **(J)** A bar graph comparing the percentage of FB1Δ*fox1* x FB2Δ*fox1*-infected and FB1 x FB2-infected epidermal cells where encased proliferating hyphae can be observed. Infected maize leaves were harvested 7 dpi. A total of 8 infected leaves were harvested from 8 individual plants, and 50 infected epidermal cells monitored from each sample for a total of 400 cells. The number above each bar represents the number of infected epidermal cells observed for WT-infected and Δ*fox1*-infected leaf tissue. Error bars are indicated.

At 4 dpi, the tissue from plants infected with Δ*fox1*-strains showed the same appearance as that from plants infected with the wild-type-strains, with the exception of bright regions in select epidermal cells (Figure 11C). Closer inspection revealed that these bright regions were a result of the onset of fungal hyphae being encased by an optically dense matrix (Figure 11D). In contrast, the presence of encased fungal hyphae was extremely scarce in plant leaves infected with wild-type FB1 x FB2 crosses (Figure 11B). At 7 dpi, this phenotype was most prominent (Figure 11G, 11H and 11I), with ~ 82% of FB1Δ*fox1* x FB2Δ*fox1*-infected epidermal cells containing encased fungal hyphae compared to ~2% in wild-type infections (Figure 11J). The emergence of encased fungal hyphae at 4 dpi, which substantially increased in percentage at 7 dpi, suggest that the observed phenotype is a plant defense response.

2.5 Δ*fox1*-hyphae are encased in plant cell wall components

To test whether the matrix encasing the Δ*fox1*-hyphae was produced by the plant, FB1Δ*fox1* x FB2Δ*fox1*- and FB1 x FB2-infected plant leaves (4 dpi) were stained for cellulose and callose. Methylene blue revealed that the matrix encasing Δ*fox1*-hyphae most likely contains cellulose (Figure 12B and 12D), identifying that the encasement material is generated by the plant cell. In addition, unlike proliferating WT-hyphae aniline blue was able to stain encased Δ*fox1*-hyphae, indicating callose as a component of the matrix (Figure 12F).

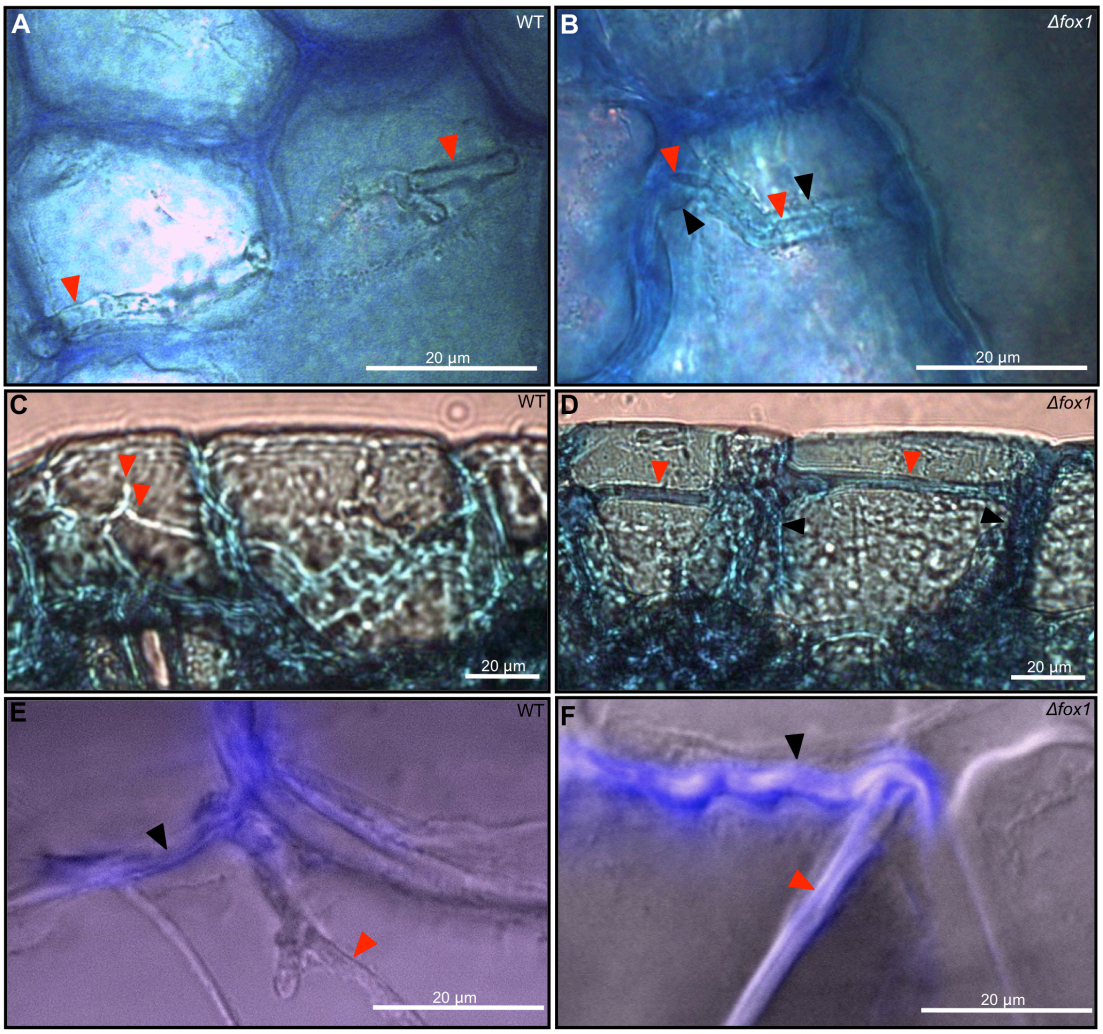

Figure 12. FB1Δ*fox1* x FB2Δ*fox1*-hyphae are encased in a plant-produced matrix consisting of cellulose and callose. **(A-B)** Infected maize leaves 4 dpi. Top view of intracellular proliferating fungal hyphae of *U. maydis* strains FB1 x FB2 (WT), and FB1Δ*fox1* x FB2Δ*fox1* (Δ*fox1*) respectively. Cellulose was visualized by methylene blue staining. A proliferating Δ*fox1*-hypha is encased in a cellulose-containing matrix. Proliferating hyphae are labeled with red arrowheads, and the encasement matrix is labeled with black arrowheads. **(C-D)** Methylene blue stained cross-sections of WT and FB1Δ*fox1* x FB2Δ*fox1*-infected maize leaves 4 dpi. Unlike the WT-hyphae, FB1Δ*fox1* x FB2Δ*fox1*-hyphae are completely encased in the plant-produced matrix, and appear blue in color due to the presence of cellulose in the encasement matrix. FB1Δ*fox1* x FB2Δ*fox1*-hyphae and the respective WT-hyphae are labeled with red arrowheads. **(E-F)** Top view of WT- and FB1Δ*fox1* x FB2Δ*fox1*-hyphae proliferating through epidermal cells of maize leaves 4 dpi. Callose was visualized with aniline blue staining. Unlike WT-hyphae, the matrix surrounding Δ*fox1*-hyphae stained whitish-blue in color, indicating that callose is a component of the encasement matrix. Proliferating hyphae are labeled with red arrowheads, and the plant cell wall is labeled with black arrowheads. Microscopic images E-F show an overlay of the DAPI channel (blue) and bright field projection (grey).

2.6 Δ*fox1*-hyphae induce the accumulation of reactive oxygen species

The observation that Δ*fox1*-hyphae are encased in a plant-produced matrix during *in planta* development suggests that the intimacy of the biotrophic interface between pathogen and host has been disrupted. The identification of cellulose and callose as components of this optically dense matrix determined that this is in fact the host plant responding to pathogen invasion. If this is the case, then the host plant must be able to detect invading Δ*fox1*-hyphae prior to their encasement during the early stages of the initial invasion process. One of the initial lines of plant defense against microbial invasion is the overproduction and accumulation of reactive oxygen species (ROS), as H_2O_2 at invasion sites. To determine if Δ*fox1*-hyphae trigger this initial plant defense response, maize leaves infected with *U. maydis* strains SG200Δ*fox1* or SG200 were harvested 2 dpi when most hyphae have just penetrated into the plant epidermal layer, and stained with diamino-benzidine (DAB) to visualize the accumulation of H_2O_2. DAB staining of SG200Δ*fox1*-infected plant tissue revealed a very strong accumulation of H_2O_2 in and around epidermal cells containing proliferating Δ*fox1*-hyphae (Figure 13B), and no accumulation at invasion sites of SG200-infected plants (Figure 13A). The data suggest that unlike wild-type-hyphae, Δ*fox1*-hyphae trigger an initial plant defense response within the epidermal cells.

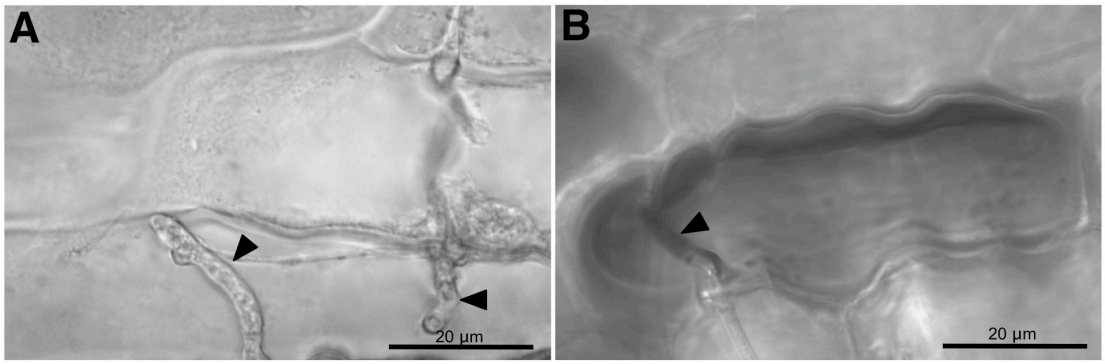

Figure 13. Δ*fox1*-hyphae elicit a strong accumulation of H_2O_2 in infected and neighboring epidermal cells. **(A)** SG200 (WT) hyphae (Black arrowheads) growing in epidermal cells. No accumulation of H_2O_2 was observed in WT-infected plant cells. **(B)** Proliferating SG200Δ*fox1* (Δ*fox1*) hypha (black arrowhead) elicits a strong accumulation of H_2O_2 in infected and neighboring epidermal cell, represented by a dark cloudy haze.

2.7 Δ*fox1*-hyphae predominantly aggregate within the plant vasculature

To examine the later stages of pathogenic development, confocal microscopy was utilized to ease the visualization of proliferating hyphae in living plant tissue. Maize plants infected with FB1Δ*fox1* x FB2Δ*fox1* or FB1 x FB2 crossings were harvested at 5 and 7 dpi. FB1Δ*fox1* x FB2Δ*fox1*- and FB1 x FB2-hyphae were stained with WGA-AF488, and plant structures were visualized with propidium iodide. Confocal microscopy revealed that FB1 x FB2-hyphae accumulated around the vascular bundles, but were also found frequently in mesophyll cells (Figure 14A, 14C). However, FB1Δ*fox1* x FB2Δ*fox1*-hyphae predominantly aggregated within the plant vasculature, and were rarely seen proliferating in the mesophyll (Figure 14B, 14D). More specifically, Δ*fox1*-hyphae were concentrated in the bundle sheath cells of the vascular bundles (Figure 14D).

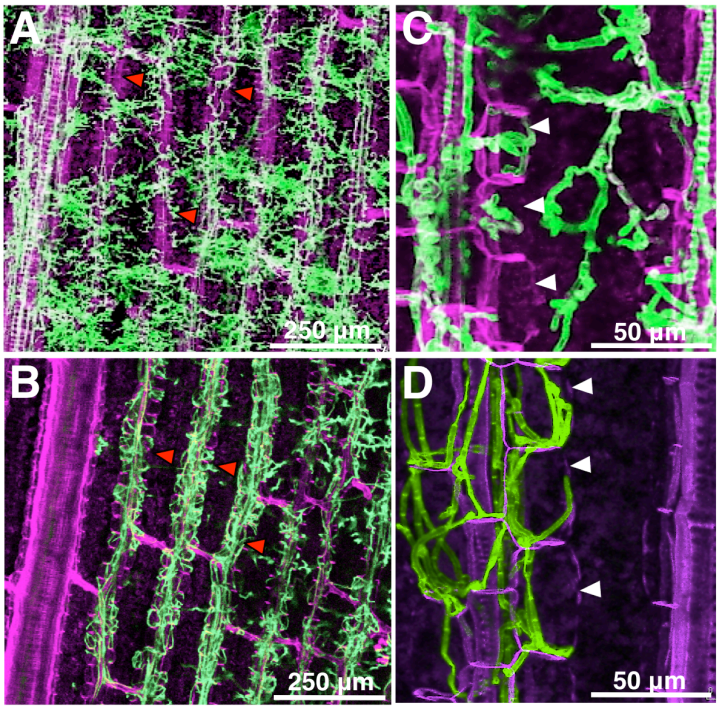

Figure 14. Δ*fox1*-hyphae predominantly aggregate within the plant vasculature. (**A)** Top view of a maize leaf infected with FB1 x FB2 (WT) strains 5 dpi. Fungal hyphae (green) are seen proliferating through the plant mesophyll and vascular bundles (red arrowheads). (**B)** FB1Δ*fox1* x FB2Δ*fox1* (Δ*fox1*) infected maize leaf 5 dpi. Fungal hyphae are predominantly found growing within the vascular bundles (red arrowheads), and rarely in the mesophyll. **(C)** Magnified view of a maize leaf infected with WT-hyphae. **(D)** A magnified view of a maize leaf revealed that Δ*fox1*-hyphae are mainly concentrated in the bundle sheath cells (white arrowheads) of the vascular bundles. In all images plant structures appear purple. All images are maximum projection stacks taken with a confocal microscope.

2.8 Δ*fox1*-hyphae induce transcriptional changes in the maize transcriptome

To gain a comprehensive view of the genes involved in the induction of plant defenses by Δ*fox1*-strains, microarray analyses were conducted on Δ*fox1*-infected leaf tissue. In a previous study, the global transcriptional response of maize after infection with SG200 at 12 hpi, 24 hpi, 2 dpi, 4 dpi, and 8 dpi has been described (Doehlemann *et al*., 2008b). Using identical experimental conditions, SG200Δ*fox1*-infected maize plants were compared to SG200-infected plants at 4 dpi. The 4 dpi time-point was selected due to the initial emergence of encased hyphae. For DNA microarray expression analysis, 7-day-old maize plants were infected with strain SG200Δ*fox1*. Infected leaf tissue was harvested 4 dpi, and RNA isolated for subsequent microarray hybridizations. The global gene expression profile of maize plants infected with SG200Δ*fox1*-hyphae was compared to the expression profile of maize leaves infected with strain SG200 (4 dpi; Doehlemann *et al*., 2008b).

Since infected maize leaves consist of a heterogeneous mixture of plant cells, including, uninfected, infected, and infected cells with encased fungal hyphae, background noise was expected to attenuate the true expression levels of the genes responsible for this plant defense phenotype. Therefore, the PageMan software (http://mapman.mpimp-golm.mpg.de/pageman/) was utilized to analyze all differentially expressed genes regardless of the degree of fold change, in order to provide a visual model depicting enriched biological processes (Table 1). The enrichment analysis revealed down-regulated genes associated with the metabolism of plant hormones such as auxins and gibberellins, and up-regulated genes involved in anthocyanin production, more specifically, the metabolism of phenylpropanoids and flavonoids. In addition, there was an enrichment of down-regulated genes involved in cell wall degradation and modification, and up-regulated genes involved in cellulose synthesis (Table 1).

The next step involved a more detailed analysis of the microarray data, in order to identify specific genes belonging to the enriched functional categories identified in the PageMan analysis. Microarray data was analyzed using Affymetrix Micro Array Suite 5.1. Further analysis was carried out using the R bioconductor package (http://www.bioconductor.org/), and dChip1.3 software package (http://biosun1.harvard.edu/complab/dchip/). Only genes with changes greater than 2-fold, and a corrected *P*-value <0.001 were considered significant (see Materials and Methods for a detailed explanation of the gene expression filter criteria). In

SG200Δ*fox1*-infected plants, 458 genes were differentially regulated (369 down-regulated and 89 up-regulated) when compared to SG200-infected plants (Supplemental Table 1). Several individual genes were identified that were at least 2-fold up- or down-regulated, which fell under the enriched biological processes identified in the PageMan analysis (Table 2; see Materials and Methods for details for filter criteria; significantly regulated genes are summarized in Supplemental Table 1).

Table 1. SG200Δ*fox1*-induced changes of the maize transcriptome.

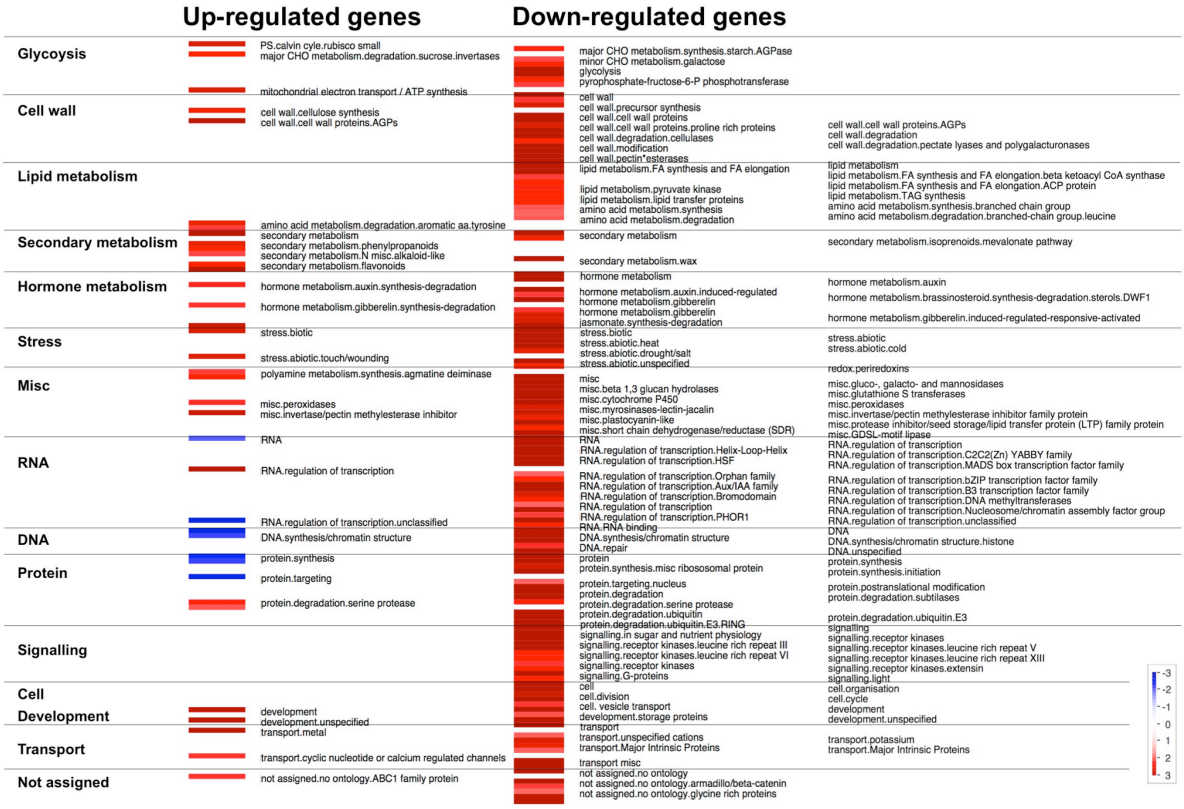

An overview of the differentially expressed maize genes in SG200Δ*fox1*-infected plants compared to SG200-infected plants 4 dpi, visualized by PageMan (http://mapman.mpimp-golm.mpg.de/pageman/). Up-regulated (left column) and down-regulated genes (right-column) are grouped according to their proposed biological function. Over-representation analysis (ORA) calculates if specific subgroups are over- or under-represented, if the probability is > 3.0 or < -3.0 (z-scores; converted *P*-value, where a z-score of 1.96 represents a *P*-value of 0.05). The probability of over-representation (red) or under-representation (blue) of differentially expressed genes within the different biological processes is color-coded for up- and down-regulated genes respectively (see color scale bar). Refer to the PageMan manual for a detailed description of statistical analysis (http://mapman.mpimp-golm.mpg.de/pageman/help/help.html#Statistics).

The down-regulation of genes involved in the metabolism of auxins and gibberellins, as well as the down-regulation of numerous genes involved in cell wall modification and degradation, including 7 expansins (Table 2), most likely reflects the inability of Δ*fox1*-strains to induce the formation of tumors. The induction of genes involved in

anthocyanin production corroborates the increased anthocyanin content in Δ*fox1*-infected leaf tissue (Table 2; Figure 8). Interestingly, two genes encoding putative *Zea mays* cellulose synthase catalytic subunits (*ZmCesA11*; ZmAffx.13.1S1_s_at and *ZmCesA12*; ZmAffx.5.1.S1_at) were identified as being up-regulated (Table 2). These two *Z. mays* cellulose synthases are the prime candidate genes responsible for the production of cellulose forming a constrictive barrier around Δ*fox1*-hyphae proliferating within the epidermal layer (Figure 12B and 12D).

Table 2. Microarray analysis of *Z. mays* genes differentially expressed after infection with strain SG200Δ*fox1*. Genes presented in this table represent enriched functional categories.

Array Probe Set	Annotation[a]	Fold Change[b] *Δfox1* vs WT
Cellulose synthesis		
ZmAffx.13.1.S1_s_at	*Zea mays* cellulose synthase catalytic subunit 11 (CesA11)	3.3
ZmAffx.5.1.S1_at	*Zea mays* cellulose synthase catalytic subunit 12 (CesA12)	2.8
Anthocyanin production		
Zm.19108.1.S1_at	(*Arabidopsis thaliana*) T45624 flavonoid 3-hydroxylase-like protein	2.8
Zm.3406.1.S1_at	4CL 4-coumarate coenzyme A ligase	2.4
Cell Wall modification and degradation		
Zm.14507.3.A1_a_at	*Zea mays* glycosyl hydrolases family 16 protein	-98.4
Zm.13537.1.S1_at	Endoglucanase 1 precursor (Endo-1,4-beta-glucanase)	-33.7
Zm.11734.1.A1_a_at	*Zea mays* polygalacturonase inhibitor 1	-25.0
Zm.5108.1.A1_at	*Zea mays* xyloglucan endotransglucosylase/hydrolase protein 23	-21.7
Zm.13944.3.S1_a_at	*Zea mays* beta-expansin 8 (expB8)	-20.1
Zm.7152.1.A1_at	hypothetical protein with pectinesterase activity	-13.4
Zm.11734.2.S1_x_at	*Zea mays* polygalacturonase inhibitor 1 precursor	-13.0
Zm.5822.1.A1_at	*Zea mays* beta-expansin 4 (expB4) precursor	-9.5
Zm.6626.1.A1_at	*Zea mays* polygalacturonase	-8.8
Zm.6419.1.A1_at	*Zea mays* xyloglucan endotransglucosylase/hydrolase	-7.7
Zm.669.1.S1_at	*Zea mays* alpha-expansin 5 (expA5)	-6.7
Zm.9565.1.A1_at	*Zea mays* beta-expansin 3 (expB3)	-6.3
Zm.13728.1.S1_at	*Zea mays* alpha-expansin 4 (expA4)	-6.2
Zm.1747.1.A1_at	*Zea mays* beta-expansin 5 (expB5)	-4.7
Zm.665.1.S1_at	*Zea mays* alpha-expansin 1 (expA1)	-3.9
Hormone signaling		
Zm.5020.1.S1_at	*Zea mays* IAA12 - auxin-responsive Aux/IAA family member	-18.1
Zm.3080.1.A1_at	*Zea mays* IAA13 - auxin-responsive Aux/IAA family member	-4.0
Zm.4896.1.A1_at	*Zea mays* IAA13 - auxin-responsive Aux/IAA family member	-2.2
Zm.10176.1.A1_at	*Zea mays* gibberellin-regulated protein 1	-12.6
Zm.8468.1.A1_at	*Zea mays* gibberellin receptor GID1L2	-7.0

(a) Gene annotations were provided by MapMan.
(b) Fold changes give the relative mean expression of maize plants infected with the strain SG200Δ*fox1* (4 dpi; Doehlemann *et al.*, 2008 b) compared to the mean expression of maize plants infected with the respective wild-type-strains (4 dpi). Fold changes were calculated using dChip1.3 and values >2 and <-2 with a corrected *P*-value < 0.001 were considered as significant (see Materials and Methods).

2.9 Ectopic expression of *fox1* has no effect on saprophytic growth

To identify putative Fox1 targets, strains were generated where *fox1* could be induced in axenic culture for subsequent microarray experiments. The *fox1* gene was expressed under the control of the arabinose-inducible *crg1*-promoter (Bottin *et al.*, 1996) and introduced into the *ip*-locus of *U. maydis* wild-type-strains FB2 and AB31, generating *fox1*-inducible-strains FB2*Pcrg:fox1* and AB31*Pcrg:fox1* respectively. After 5 hours of growth under inducing conditions, no morphological differences were observed between *fox1*-inducible-strains and their respective wild-type-strains (Figure 15A-15D). The induction of *fox1* upon medium shift was confirmed by Northern analysis in strains FB2*Pcrg:fox1* and AB31*Pcrg:fox1* (Figure 15E). A custom Affymetrix *U. maydis* array was used to compare the expression profile of strains FB2*Pcrg:fox1* and FB2 grown 5 hours under inducing conditions. Transcriptional analysis identified *fox1* as the lone induced gene (93-fold; Figure 15F), indicating that Fox1 does not act as a transcriptional regulator under the tested conditions. A similar microarray experiment comparing AB31*Pcrg:fox1* and AB31 induced cultures was abandoned, since ectopic expression of *fox1* in the AB31 background had no effect on cell morphology.

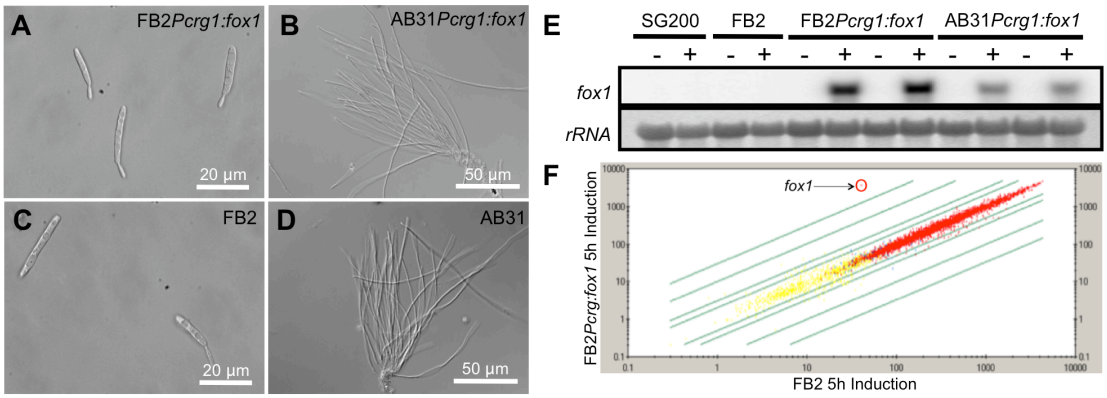

Figure 15. *fox1*-inducible-strains FB2*Pcrg1:fox1* **(A)** and AB31*Pcrg1:fox1* **(B)**, and their progenitor strains FB2 **(C)** and AB31 **(D)** grown under inducing conditions for 5 hours in liquid array medium containing 1% arabinose. No morphological differences were observed between *fox1*-inducible-strains and their wild-type counterparts. **(E)** Induction of the *fox1* transcript can be observed in both *fox1*-inducible-strains. Two independently generated strains were used to confirm the *fox1* induction of strains FB2*Pcrg1:fox1* and AB31*Pcrg1:fox1*. The 18S rRNA was used as a loading control. *fox1*-inducible-strains FB2*Pcrg1:fox1*, AB31*Pcrg1:fox1*, and wild-type-strains SG200 and FB2 after 5 hours growth under uninducing (-) conditions (liquid array medium + 1% glucose) and inducing (+) conditions (liquid array medium + 1% arabinose). **(F)** Scatter plot of the signals on a log scale comparing *U. maydis* strains FB2*Pcrg1:fox1* and FB2 induced for 5 hours in liquid array medium containing 1% arabinose. The *fox1* gene was the only gene significantly induced (93-fold). 2, 5, 10 and 50-fold change lines are represented.

2.10 Fox1 is involved in the regulation of secreted proteins during pathogenic development

The deletion of *fox1* has no effect on the saprophytic growth of *U. maydis*. In addition, the ectopic expression of the *fox1* gene did not result in detectable morphological effects in axenic culture, while gene expression profiling of *fox1*-inducible-strains confirmed Fox1 was not functional during saprophytic growth. In order to address the function of Fox1 as a transcriptional activator or repressor, and to identify putative target genes of Fox1, microarray analysis was performed comparing the expression profiles of FB1Δ*fox1* and FB2Δ*fox1* crossings, and of FB1 and FB2 crossings *in planta*, since *fox1* deletion strains displayed a substantial reduction in virulence and elicited the induction of host plant defenses.

Based on the expression profile of *fox1*, microarray experiments were conducted comparing infected plant leaves 5 dpi. This time-point was chosen due to the presence of encased Δ*fox1*-hyphae, and because it was the earliest time-point ample fungal material was present in infected leaf tissue for *U. maydis* array detection (J. Kämper and M. Vranes, personal communication). For the microarray expression analysis, 7-day-old maize plants were infected with either a mixture of FB1Δ*fox1* and FB2Δ*fox1* or FB1 and FB2 haploid cells. Infected leaf tissue was harvested at 5 dpi, and RNA isolated for subsequent microarray hybridizations. The resulting gene expression image data was analyzed using Affymetrix Micro Array Suite 5.1. Additional analysis was performed using the R bioconductor package (http://www.bioconductor.org/), and dChip1.3 software package (http://biosun1.harvard.edu/complab/dchip/). Only genes with expression changes greater than two-fold, and a corrected *P*-value <0.01 were considered significant (see Materials and Methods for a detailed explanation of gene expression filter criteria). A total of 141 genes (130 down-regulated and 11 up-regulated; Supplemental Table 2) were identified that showed a significantly altered expression (>2-fold, corrected *P*-value <0.01) as a result of deleting *fox1*. Enrichment analysis using the Blast2Go tool (Conesa *et al*., 2005) did not reveal an over-representation of functional categories. However, several genes encoding proteins involved in sugar processing and transport were down-regulated in the Δ*fox1* arrays (Table 3; Supplemental Table 2), among these a glucoamylase precursor (*um04064*; -21.5), a trehalase precursor (*um02212*; -4.1-fold), an invertase (*um01945*; -2.9-fold) and a putative glucose transporter (*um06076*; -2.4-fold). In a previous study, the high-affinity sucrose transporter Srt1

has been shown to be required for full fungal virulence (Wahl *et al*., 2010). The same sucrose transporter (*srt1*; *um02374*) was also present in the Δ*fox1* arrays, however it was just shy of the 2-fold cut off with a fold change of -1.95 (Data not shown). Notably, several genes from the phenylpropanoid pathway were also observed to be down-regulated, as a phenylalanine ammonia-lyase (*um00078*; -5.9), 4-coumarate:CoA ligase (*um01171*; -14.3-fold), 4-coumarate:CoA ligase 1 (*um06153*; -8.1-fold), chorismate mutase (*um04220*; -4.6-fold), and chorismate synthase (*um11329*; -3-fold) (Supplemental Table 2). Interestingly, 38 of the differentially regulated genes encode for proteins predicted to be secreted (33 down-regulated and 5 up-regulated; Table 4; Supplemental Table 2), which represents an enrichment from ~13% (expected) to ~27% (*P*-value = 4.86 x 10^{-6}; normalized to the total number of genes for secreted proteins detectable under the experimental conditions).

Table 3. Microarray analysis of *U. maydis* genes differentially expressed involved in sugar processing and transport in Δ*fox1* mutant strains during biotrophic development.

Array Probe Set	Gene[a]	Annotation[a]	Target P[b]	Cluster[c]	Fold change[d]
W125um144G_at	um04064	related to Glucoamylase precursor			-21.5
W15um272G_at	um03615	related to Glucose oxidase	RC=2	9A	-7.6
C35um214G_at	um12045	related to alpha glucosidase II beta subunit	RC=3		-4.2
W15um126G_at	um02212	related to trehalase precursor	RC=2		-4.1
W155um003G_at	um01945	probable SUC2 - invertase (sucrose hydrolyzing enzyme)	RC=1		-2.9
W5um057G_at	um06076	putative glucose transporter			-2.4

(a) Genes and annotations are derived from MUMDB (http://mips.helmholtz-muenchen.de/genre/proj/ustilago/).
(**b)** Represents the reliability class (RC) of the protein sequences containing a signal peptide. RC-values range from 1-5. A lower RC-value indicates a stronger prediction that the protein is secreted.
(c) Identifies the genes belonging to previously identified genes cluster described in Kämper *et al* (2006).
(d) Fold changes give the relative mean expression of FB1Δ*fox1* x FB2Δ*fox1*-infections (5 dpi) compared to the mean expression in wild-type-infections (5 dpi).

2.11 Deletion analysis of *fox1*-dependent genes encoding potential effectors

To identify gene(s) responsible for the induction of plant defenses during *in planta* development of Δ*fox1*-hyphae, the three most down-regulated genes encoding potential secreted effectors, *um03046* (-105.1-fold), *um12258* (-85.1-fold) and *um05027* (-59.6-fold) were deleted in SG200, and assayed for pathogenicity. Both SG200Δ*um05027* and SG200Δ*um12258* strains displayed disease ratings similar to SG200, while SG200Δ*um03046* showed a slight reduction in virulence (Figure 16A and 16B). However, microscopic analysis of infected leaf tissues revealed no phenotypic abnormalities in proliferating hyphae in either of the three deletion strains when compared to SG200 (Data not shown).

The deletion analyses suggest that in addition to *um03046* there must be additional *fox1*-regulated gene(s) that are responsible for the induction of host defenses and reduced virulence. Six of the genes down-regulated in response to the *fox1* deletion encode for potentially secreted proteins that belong to three of the clusters that have been linked to pathogenic development (Table 4; Supplemental Table 2) (Kämper *et al*., 2006): *um02533* (-5.7-fold) in cluster 6A, *um03751* (-6.4-fold) and *um03752* (-8.5-fold) in cluster 10A, and *um05308* (-3.8-fold), *um05312* (-4.4-fold) and *um05314* (-4.3-fold) in cluster 19A. It is conceivable that the *fox1*-dependent combined deregulation of several genes has attributed to the reduced virulence of Δ*fox1*-hyphae. In particular, the deregulation of genes encoding secreted effectors most likely interferes with the suppression of host defense pathways that result in the observed host defense responses, such as the production of H_2O_2 and the encasement of Δ*fox1*-hyphae. Fox1 represents the first *U. maydis* plant-induced transcription factor involved in the regulation of genes required for biotrophic development.

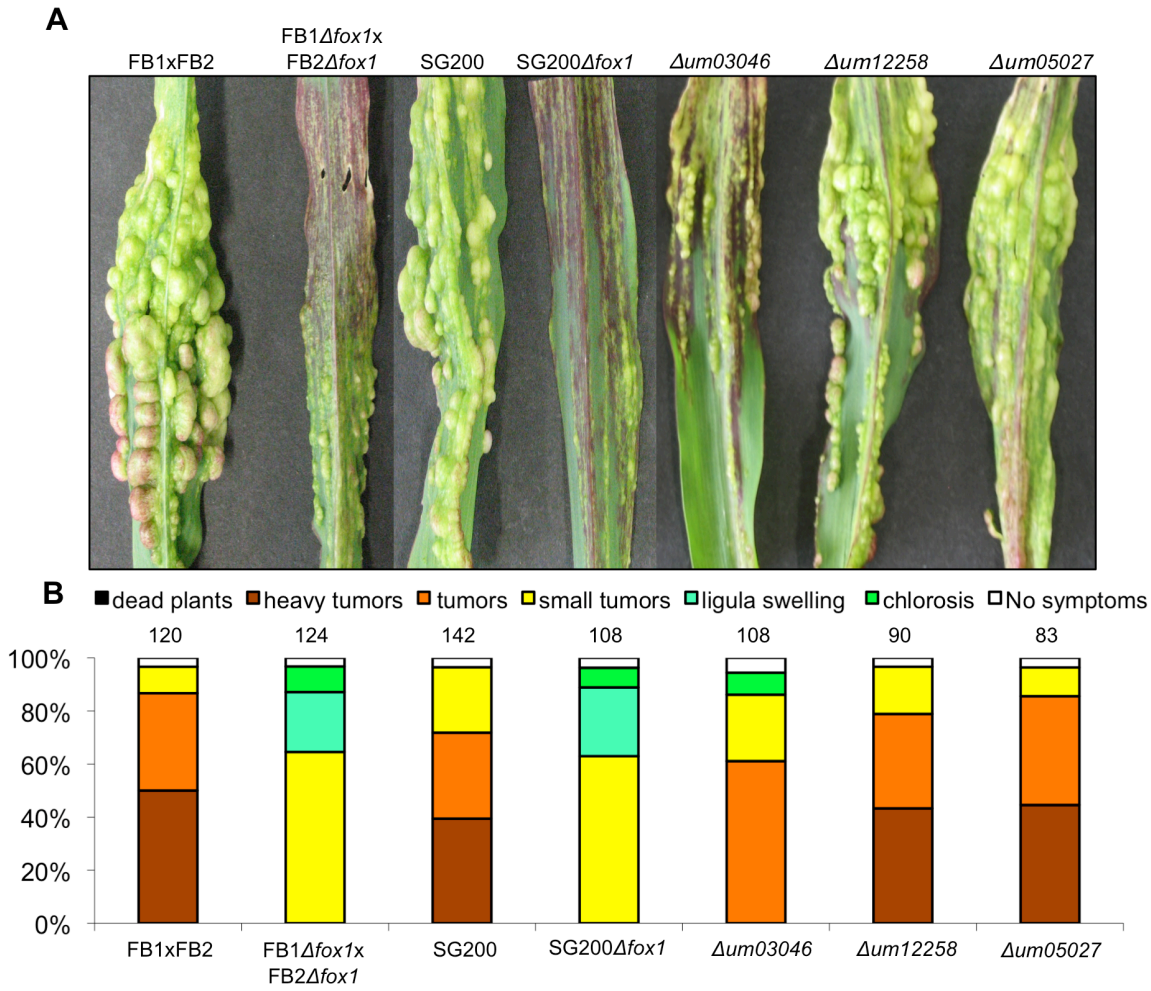

Figure 16. Deletion analysis of *fox1*-dependent genes encoding potential secreted effectors during biotrophic development. **(A)** Disease symptoms of maize plants 7 dpi with *U. maydis* strains FB1 x FB2 (wild-type crosses), FB1Δ*fox1* x FB2Δ*fox1* (Δ*fox1* crosses), SG200 (wild-type), SG200Δ*fox1* (Δ*fox1*), and mutant strains SG200Δ*um03046*, SG200Δ*um12258* and SG200Δ*um05027*. **(B)** Disease rating of maize plants 7 dpi with *U. maydis* strains FB1 x FB2, FB1Δ*fox1* x FB2Δ*fox1*, SG200, SG200Δ*fox1*, SG200Δ*um03046*, SG200Δ*um12258* and SG200Δ*um05027*. Bars represent the percentage of infected plants with the symptom development indicated in the legend. Numbers represent the total number of plants infected with the corresponding strain.

Table 4. Microarray analysis of *U. maydis* genes differentially expressed encoding proteins predicted to be secreted in Δ*fox1* mutant strains during biotrophic development.

Array Probe Set	Gene[a]	Annotation[a]	Target P[b]	Cluster[c]	Virulence of Cluster Deletion Mutants *In Planta*[d]	Fold change[e]
C55um250G_at	um03046*	hypothetical protein	RC=1			-105.1
W5um167G_at	um12258*	hypothetical protein	RC=1			-85.1
W135um170G_at	um05027*	hypothetical protein	RC=1			-59.6
C27um006G_at	um02297	conserved hypothetical Ustilago-specific protein	RC=1			-22.5
W55um076G_at	um03349	putative protein	RC=2			-13.7
W125um140G_at	um03752	conserved hypothetical Ustilago-specific protein	RC=2	10A	Reduced	-8.5
C26um006G_at	um02298	hypothetical protein	RC=2			-7.6
W15um272G_at	um03615	related to Glucose oxidase	RC=2	9A	Unaffected	-7.6
W150um188G_at	um04815	hypothetical protein	RC=1			-6.7
W126um140G_at	um03751	hypothetical protein	RC=1	10A	Reduced	-6.4
W6um060G_at	um02135	hypothetical protein	RC=2			-6.3
W115um154G_at	um02533	hypothetical protein	RC=2	6A	Reduced	-5.7
W140um005G_at	um05819	hypothetical protein	RC=1			-5.4
C95um098G_at	um00154	related to Para-nitrobenzyl esterase	RC=1			-4.9
W225um010G_at	um01235	hypothetical protein	RC=1	2A	Increased	-4.7
C64um125G_at	um05312	hypothetical protein	RC=1	19A	Markedly Reduced	-4.4
W27um245G_at	um05926	conserved hypothetical Ustilago-specific protein	RC=1			-4.4
C55um125G_at	um05314	hypothetical protein	RC=1	19A	Markedly Reduced	-4.3
C35um214G_at	um12045	related to alpha glucosidase II beta subunit	RC=3			-4.2
W15um126G_at	um02212	related to trehalase precursor	RC=2			-4.1
C100um139G_at	um01334	hypothetical protein	RC=2			-4.0
W5um146G_at	um05964	related to esterase	RC=1			-3.9
C80um125G_at	um05308	hypothetical protein	RC=1	19A	Markedly Reduced	-3.8
W20um273G_at	um06273	probable NCP1 - NADPH-cytochrome P450 reductase	RC=1			-3.7
C55um089G_at	um10816	conserved hypothetical protein	RC=2			-3.4
C72um008G_at	um04354	hypothetical protein	RC=1			-3.3
C65um173G_at	um11484	hypothetical protein	RC=1			-3.2
W155um003G_at	um01945	probable SUC2 - invertase (sucrose hydrolyzing enzyme)	RC=1			-2.9
W10um056G_at	um01888	probable serine-type carboxypeptidase F precursor	RC=2	3A	Unaffected	-2.9
C34um264G_at	um04033	hypothetical protein	RC=1			-2.9
W5um110G_at	um00581	conserved hypothetical protein	RC=1			-2.8
W21um006G_at	um02299	hypothetical protein	RC=1			-2.7
C20um081G_at	um03232	conserved hypothetical Ustilago-specific protein	RC=1			-2.4
C125um125G_at	um10553	hypothetical protein	RC=1	19A	Markedly Reduced	2.5
C56um060G_at	um02119	hypothetical protein	RC=1			2.7
W70um070G_at	um02473	hypothetical protein	RC=2	5B	Non-pathogenic	2.7
C20um245G_at	um05930	hypothetical protein	RC=1			3.2
C15um245G_at	um05931	hypothetical protein	RC=1			3.4

(*) Indicates that the gene was deleted in this study.
(a) Genes and annotations are derived from MUMDB (http://mips.helmholtz-muenchen.de/genre/proj/ustilago/)**.**
(b) Represents the reliability class (RC) of the protein sequences containing a signal peptide. RC-values range from 1-5. A lower RC-value indicates a stronger prediction that the protein is secreted.
(c) Identifies the genes belonging to previously identified genes cluster described in Kämper *et al* (2006).
(d) Virulence phenotype observed for *U. maydis* mutants deleted for the entire gene cluster as described in Kämper *et al* (2006). Phenotypes for individual gene deletions within each gene cluster are not available.
(e) Fold changes give the relative mean expression of FB1Δ*fox1* x FB2Δ*fox1*-infections (5 dpi) compared to the mean expression in wild-type-infections (5 dpi).

3 Discussion

In *Ustilago maydis,* the establishment and maintenance of the biotrophic interface requires dynamic alterations in gene expression profiles. These alterations can occur as a result of environmental stimuli, altered nutrient conditions, or the perception of host-specific signals. Such external cues enable the fungus to activate the appropriate transcriptional regulators, resulting in the induction of specific genes required to adapt to the dynamic environment of its host. Fox1 represents a potential forkhead transcription factor that is exclusively expressed *in planta*. Fox1 is required for full virulence and the suppression of host defenses. The function of Fox1 during biotrophic development and its involvement in the attenuation of host defenses, as well as the plants response to invasion will be discussed.

3.1 Fox1, a potential forkhead transcription factor

Fox1 most likely functions as a transcriptional regulator, since the protein harbors a conserved forkhead DNA-binding domain (FBD), with sequence similarity to previously described forkhead transcription factors in higher eukaryotes that was shown to confer sequence specific binding (Overdier *et al*., 1994; Pierrou *et al*., 1994; Kaufmann *et al*., 1995). In addition, the Fox1:eGFP fusion protein localizes to the nucleus during saprophytic growth and biotrophic development. Furthermore, the recognition helix (H3) of Fox1 contains three conserved residues that represent the principle contact surface of H3 to target DNA (Clark *et al*., 1993; Boura *et al*., 2007). Attempts to complement the Δ*fox1*-phenotype with a Fox1:eGFP fusion protein harboring mutations at the three residues not only failed to restore virulence, it also resulted in a cytoplasmic eGFP signal. A likely explanation is that the mutations lead to protein instability, resulting in the degradation of Fox1 and the cytoplasmic localization of the eGFP. Even though the involvement of these residues in making base contacts has not been shown, they are clearly required for Fox1 function.

3.2 Fox1 is required for the biotrophic development of *U. maydis*

Neither deletion nor overexpression of *fox1* led to any morphological defects, alterations in growth rate or impact on gene expression, suggesting Fox1 has no effect during saprophytic growth. Furthermore, gene expression profiling indicates that *fox1* is exclusively expressed during biotrophic development, independent of the bE/bW-heterodimer. The bE/bW-heterodimer is neither sufficient to induce *fox1* expression in axenic culture, nor required for *fox1* expression during biotrophic development: *fox1* is only moderately (-2.5 fold) down-regulated in response to inactivation of a temperature-sensitive bE protein *in planta* (Wahl *et al*., 2010; Heimel *et al*., submitted). The lack of *fox1* expression and functionality in axenic culture, its plant specific expression, and the only observable phenotype of Δ*fox1*-strains occurring *in planta*, suggest that Fox1 is involved in the regulation of genes specifically required during the biotrophic stage of *U. maydis*. The mode in which transcriptional regulation via Fox1 is achieved is still unknown, however, it is feasible that Fox1 is activated in a tissue specific fashion, or upon the perception of plant-specific signals, as secondary metabolites.

3.3 The serine-rich region of Fox1 is required for function

Since ectopic expression of *fox1* in axenic culture has no influence on the gene expression profile, it must be assumed that in addition to its transcriptional regulation, Fox1 is also regulated either via posttranslational modifications, and/or via the interaction with cofactors present only under the specific developmental/environmental conditions within the host plant. A comparable mechanism has been described for the *Saccharomyces cerevisiae* forkhead protein Fkh2 that is involved in the cell cycle-dependent transcriptional regulation. Fkh2 binds cooperatively with the MADS-box protein Mcm1 to G_2/M-specific promoters; in addition, activation requires the phosphorylation of Fkh2 by the cyclin dependent kinase Cdc28, which promotes the interaction of Fkh2 with the coactivator Ndd1 (Spellman *et al*., 1998; Koranda *et al*., 2000; Hollenhorst *et al*., 2001; Darieva *et al*., 2003; Reynolds *et al*., 2003; Pic-Taylor *et al*., 2004; Darieva *et al*., 2006; Pondugula *et al*., 2009). The mechanism by which the *U. maydis* Fox1 protein is activated still remains to be elucidated; however, the serine-rich region is a likely candidate for an interaction-domain. Removal of the first half of this region had no effect on pathogenic development, however, removal of the entire serine-rich motif resulted in

disease symptoms similar to SG200Δ*fox1* infections, indicating, that the first 48 amino-acids of this motif are essential for Fox1 function. The presence of multiple potential phosphorylation sites and protein interaction motifs suggest that Fox1 may be activated via a kinase pathway, or through protein-protein interactions with cofactors only present during the biotrophic development of *U. maydis*.

3.4 Reprogramming of the host plant as a result of impaired tumor development

Δ*fox1*-strains are severely impaired in tumor development during biotrophic development. Transcriptome analysis of maize plants infected with the SG200Δ*fox1* strain displayed substantial transcriptional reprogramming compared to SG200 infections. Moreover, majority of the differentially regulated genes were reduced in expression. In line with the impaired tumor development of Δ*fox1*-strains *in planta*, genes involved in phytohormone response and signaling were also down-regulated. Recently, it was shown that maize genes involved in auxin-synthesis and -response are transcriptionally induced upon *U. maydis* infection during tumor development (Doehlemann *et al*., 2008b); in addition, elevated levels of gibberellins have been shown to promote cell elongation (Salas Fernandez *et al*., 2009). Transcriptome analysis of SG200Δ*fox1*-infected plants identified differentially expressed genes encoding proteins involved in auxin (AUX) response, as well as gibberellin (GA) signaling. Thus, the deregulation of genes involved in hormone response and signaling in the Δ*fox1*-infected plants is most likely a result of impaired tumor development.

In the same line is the observation that numerous genes involved in plant cell wall modification and degradation were also repressed, including 7 genes encoding expansins. Expansins are plant proteins that belong to a superfamily consisting of four sub-families, α-expansin (EXPA), β-expansin (EXPB), expansin-like A (EXLA) and expansin-like B (EXLB). Expansins are essential for plant cell enlargement, and numerous developmental processes involved in cell wall modification (reviewed in Sampedro and Cosgrove, 2005). The largest families are the EXPA and EXPB, which have been implicated in cell wall loosening during cell enlargement (McQueen-Mason *et al*., 1992; Cosgrove *et al*., 1997). In maize, individual expansins are expressed in specific tissues (Wu *et al*., 2001). A more recent study, which examined the association of specific expansins with growth in maize, determined, among the 33

maize expansin genes, 19 were expressed during the leaf elongation zone (Muller *et al*., 2007). Furthermore, they could be organized into three distinct clusters involved in cell division, maximal leaf expansion, and cell wall differentiation. The involvement of AUXs and GAs in the stimulation of plant growth was previously discussed. In tomato plants, exogenous application of AUX and GA resulted in substantial induction of expansin *LeExp2* mRNA levels in hypocotyls (Caderas *et al*., 2000). These findings suggest that the reduced expression of expansins observed in Δ*fox1*-infected plants may have a direct correlation to the reduced expression of genes involved in AUX and GA signaling.

Additional repressed genes involved in cell wall modification and degradation included, xyloglucan endotransglucosylases (XETs) involved in maintaining stability during cell expansion (Smith and Fry, 1991; Xu *et al*., 1995; Purugganan *et al*., 1997; Campbell and Braam, 1999), and an endoglucanase that is involved in the degradation of non-cellulosic β-glucans (Hatfield and Nevins, 1986; Hatfield and Nevins, 1987) subsequently leading to cell wall loosening. Furthermore, endoglucanase activity is also enhanced via auxin signaling in maize coleoptile cell walls (Inouhe and Nevins, 1991). In addition, a probable pectinesterase was also observed, which is involved in the cell wall loosening and degradation by promoting the activity of cell wall hydrolases, such as endopolygalacturonases (Micheli, 2001).

Thus the down-regulation of additional genes involved in the cell wall synthesis and modification, such as xyloglucan endotransglucosylases, endoglucanases and pectinesterases may also reflect the reduced tumor development. The inability of Δ*fox1* mutants to development mature tumors, is most likely due to the host responding to fungal invasion, and subsequently regaining developmental control.

3.5 Δ*fox1*-strains trigger host defense responses

While there is no apparent response of maize plants to the infection with wild-type *U. maydis* strains, the infection with *fox1* deletion strains triggers (1) the accumulation of reactive oxygen species as H_2O_2, (2) the accumulation of anthocyanin and (3) the encasement of hyphae in a cellulose/callose-containing matrix. All these reactions can be interpreted as defense reactions. The overproduction and accumulation of H_2O_2 and other reactive oxygen species (ROS) has been shown to act as an intercellular signal resulting in a hypersensitive response (HR), which can lead to the induction of systemic acquired resistance (SAR) or programmed cell death (PCD) (Alvarez *et al*., 1998; Kuzniak and Urbanek, 2000; Talarczyk and Hennig, 2001; Mateo *et al*., 2004). Previous studies indicate that while H_2O_2 triggered HR may facilitate necrotrophic growth, it can impede the spread of biotrophic plant pathogens (Govrin and Levine, 2000; Hückelhoven and Kogel, 2003). This restriction of growth may be a result of H_2O_2 stimulating the cross-linking of cell wall proteins, resulting in reinforced plant cell walls (Brisson *et al*., 1994). It has been shown that H_2O_2 can form barriers against invading pathogens through the oxidative coupling of feruloyl-polysaccharides in maize cell walls (Encina and Fry, 2005). With respect to the biotrophic development of *U. maydis*, the accumulation of ROS resulting in PCD must be prevented in the establishment of a biotrophic interaction.

The observed overproduction and accumulation of H_2O_2 in and around plant cells infected with Δ*fox1*-hyphae could be interpreted as the inability of the fungus to detoxify H_2O_2. This was demonstrated in *U. maydis* strains with a deleted *yap1* gene, which encodes a homologue to the *S. cerevisiae* response regulator to oxidative stress. *yap1* mutants displayed increased H_2O_2 sensitivity and reduced virulence, indicating the need of the fungus to detoxify H_2O_2 during biotrophic development (Hipskind *et al*., 1996; Molina and Kahmann, 2007). However, when compared to DAB staining of plant tissue infected with *yap1* mutants, the accumulation of H_2O_2 at invasion sites of Δ*fox1*-hyphae is drastically increased. Unlike Δ*yap1*-hyphae, which only trigger a very localized H_2O_2 response, the H_2O_2 response to invading Δ*fox1*-hyphae was demonstrated to not only completely engulf invaded epidermal cells, but also neighboring cells. This elevated ROS response clearly indicates that the plant is not only recognizing the invading hyphae, it is responding aggressively.

Even though the accumulation of ROS is an initial host defense response against pathogen invasion, it is quite toxic and can damage the host cell. As a result, the plant must be able to protect its cells from this oxidative burst. In maize, a common response to invading fungal pathogens is the accumulation of anthocyanins. It has been suggested that this accumulation may be an attempt to protect infected maize cells from oxidative stress resulting from the induction of ROS (Hipskind *et al*., 1996). Similarly, it has been suggested that anthocyanins function as antioxidants in cotton tissue in response to hypersensitivity triggered by pathogen attack (Kangatharalingam *et al*., 2002). A substantial increase in anthocyanin production was observed in Δ*fox1*-infected leaf tissue in comparison wild-type infections. Transcriptome analyses of SG200Δ*fox1*-infected plant tissue confirmed the induction of genes encoding a 4-coumarate:CoA ligase (4CL) and a putative flavonoid-3',5'-hydroxylase (F3'5'H), which are both key enzymes in the phenylpropanoid pathway (Lee and Douglas, 1996; Ferrer *et al*., 2008). The observable increase in anthocyanin production and induction of key genes required for the biosynthesis of anthocyanins, suggest the accumulation of these secondary metabolites may function as antioxidants involved in attenuating the potential damaging effects of the oxidative burst observed in plant cells infected with Δ*fox1*-hyphae.

The inability of Δ*fox1*-hyphae to produce mature tumors resulted in the down-regulation of numerous genes involved in plant cell wall growth and modification. Intriguingly, in the presence of numerous repressed genes involved in plant cell enlargement, two genes encoding cellulose synthases (*ZmCesA11* and *ZmCesA12*) were induced. It is conceivable that these two genes are not associated with tumor development, but may function in a direct response to the invading pathogen. The observed expression data is further corroborated by methylene blue staining of plant tissue infected with Δ*fox1*-hyphae, which confirmed cellulose as a component of the plant-produced-barrier encasing Δ*fox1*-hyphae in epidermal cells. This result was further reinforced by Δ*fox1*-infected leaf tissue stained with lugol's iodine (M. Rath, personal communication). Furthermore, aniline blue staining also confirmed callose as a component. It is also worth noting that a gene encoding a callose synthase-like protein was induced (up-regulated 1.54-fold; data not shown), however, it did not pass the 2-fold cutoff requirement.

Modifications at the plant cell wall in response to invading pathogens are well documented. Such modifications include the accumulation of phenolic compounds at the cell wall, synthesis of lignin-like polymers for cell wall reinforcement, and the

formation of thick barriers at invasion sites called papillae (reviewed in Hückelhoven, 2007). Such barriers are composed of a variety of plant cell wall components including cellulose, callose, phenolics, pectins, glycoproteins and thionins (Aist, 1976; Snyder and Nicholson, 1990; Thordal-Christensen *et al*., 1997; Bolwell *et al*., 2002). Moreover, comparable cellulose-containing encasements have been observed around the haustoria of *Phytophthora parasitica* in tobacco (Hanchey and Wheeler, 1971). Callose encasements were observed in Arabidopsis plants infected with the powdery mildew fungus *Golovinomyces orontii* (Jacobs *et al*., 2003), and in an incompatible interaction between *Uromyces phaseoli* and cowpea; in the latter case the encasement was linked to the termination of fungal growth (Heath and Heath, 1971). In the natural host barley, callose encasements of *Blumeria graminis f. sp. hordei* haustoria were never observed (Meyer *et al*., 2009). However, in an incompatible interaction with the non-host Arabidopsis, nearly all haustoria were partially encased, suggesting the inability of *B. graminis* to suppress the formation of these encasements in an incompatible interaction. Thus, the encasement of Δ*fox1*-hyphae in a cellulose- and callose-containing matrix may be interpreted as a plant-produced structural barrier in response to pathogen invasion.

Previously, 12 members of the cellulose synthase (CesA) gene family were isolated in maize (Appenzeller *et al*., 2004). They determined that three cellulose synthase genes (*ZmCesA10-12*) had amino acid sequences similar to Arabidopsis CesA family members involved in secondary cell wall formation (Turner and Somerville, 1997; Taylor *et al*., 1999; Taylor *et al*., 2000; Tanaka *et al*., 2003; Taylor *et al*., 2003; Zhong *et al*., 2003), and thought to encode the catalytic subunits of the cellulose synthase complex located at the plasma membrane (Kimura *et al*., 1999). *ZmCesA10-12* are predominantly expressed in the maize stalk tissue with a high abundance of secondary cellulose depositions to reinforce the cell walls and thus to increase stalk strength (Appenzeller *et al*., 2004). Interestingly, a US patent entitled "Maize cellulose synthases and uses thereof" describes the isolation of *Z. mays* cellulose synthases *ZmCesA10*, *11*, and *12* genes, there involvement in secondary wall synthesis, and how transgenic maize lines may result in increased stalk strength. (Dhugga KS, Wang H, Tomes D, Helentjaris TG, inventors; 2002 July 31. Maize cellulose synthases and uses thereof. United States patent US 6,930,225). The induction of cellulose synthase genes *ZmCesA11* and *ZmCesA12* in SG200Δ*fox1*-infected leaf tissue, can argue a second function of these genes in plant defense, i.e. the deposition of cellulose in response to pathogen attack. From the observations

made in this study, it is quite possible that such transgenic maize lines may not only increase stalk strength, but also increase host resistance to invading pathogens.

3.6 Δ*fox1*-hyphae predominantly aggregate within the plant vasculature

Δ*fox1*-hyphae penetrate through the epidermal layer and predominantly aggregate within the plant vasculature, and rarely in the mesophyll. This focused growth to the vascular bundles may be a result of different tissue-specific defense reactions, which may be more severe in the epidermal layer and by that restrict the hyphae to the vasculature. The observation of several down-regulated *U. maydis* genes involved in sugar processing and transport may be a secondary effect of the growth in the sugar-rich vascular bundles. However, it is also possible that the focused growth in the plant vasculature is a direct effect of a Δ*fox1*-dependent down-regulation of genes required for sugar processing and transport, which may hinder the ability of the fungus to grow in a sugar-sparse environment (Table 3; Supplemental Table 2).

3.7 The phenylpropanoid pathway and *U. maydis* biotrophic development

Gene expression analysis of *fox1* deletion strains *in planta*, identified the *fox1*-dependent deregulation of several genes from the phenylpropanoid pathway, as phenylalanine ammonium lyase (PAL), 4-Coumarate:CoA ligase (4CL) and chorismate mutase (CM). While in plants the products of this pathway, as flavonoids and anthocyanins with respect to pathogen defense is well documented, its role in fungi has yet to be determined. Although tempting to speculate, a role in pathogenic development can be excluded, since the deletion of PAL, which conveys the key reaction for the pathway, has no effect on the pathogenic development of *U. maydis* (Kim *et al*., 2001). However, it has been shown that *U. maydis* cultures display lower PAL activity when grown on medium containing readily processed sugars, as sucrose, glucose and mannose (Kim *et al*., 2001). Thus, the deregulation of genes from the phenylpropanoid pathway may be a result of the focused growth of Δ*fox1*-hyphae to the sucrose-rich plant vasculature.

3.8 Fox1 is involved in the regulation of secreted pathogenicity factors

The plant-specific induction and activation of *fox1* is in line with the genes deregulated upon *fox1* deletion *in planta*, the majority of which are induced in tumor tissue (Kämper *et al*., 2006). From these genes, only seven are induced in response to the b-heterodimer in axenic culture (Heimel *et al*., submitted; Supplemental Table 2), and another nine genes show an altered expression upon inactivation of a temperature sensitive *bE* allele *in planta* (Wahl *et al*., 2010). These expression patterns imply an interdependency of different regulatory pathways. It is conceivable that pathogenic development is initiated by the formation of an active bE/bW-heterodimer, and upon plant penetration additional regulators like Fox1 are then activated to integrate specific signals within the plant, and to regulate specific subsets of genes, some of which are also regulated by the bE/bW-heterodimer. The consequence of this regulatory network is that not all of the genes that are deregulated upon the deletion of *fox1* are directly regulated by Fox1; indeed bioinformatics approaches were not able to define a common DNA-binding motif in the promoter regions of genes down-regulated upon the deletion of *fox1* (data not shown).

It is likely that the observed phenotype of the *fox1* deletion strains *in planta* is a result of the deregulation of genes required for the establishment of the biotrophic interaction and adaptation to the host environment, which is supported by the identification of several *fox1*-dependent genes encoding potential effectors. The role of effectors as virulence factors in plant-pathogenic fungi and oomycetes is well documented (Birch *et al*., 2006; Catanzariti *et al*., 2006; Kamoun, 2006; Kämper *et al*., 2006; O'Connell and Panstruga, 2006; Kamoun, 2007; Morgan and Kamoun, 2007), and it is proposed that these effectors play a pivotal role in the interference with host defense and in reprogramming the host to satisfy the needs of the invading pathogen. In *U. maydis*, various genes encoding for potential effectors are arranged in clusters that are specifically induced during biotrophic development, and it has been shown that the deletion of individual clusters affects pathogenic development (Kämper *et al*., 2006). Fox1 is involved in the regulation of six genes encoding potential effectors in three pathogenicity-relevant gene clusters. Even though these gene clusters have been implicated in pathogenic development, the function of the individual genes remains unknown. However, Fox1 is also required for the regulation of potential effector genes not belonging to defined gene clusters. Individually, all the genes regulated by Fox1 may not play a critical role in biotrophic development, but the simultaneous deregulation of several effector genes with potential redundant

functions could have an impact on virulence. Thus, the single deletion of the *fox1*-dependent gene *um03046* only resulted in a very slight reduction in virulence, while the concerted deregulation of all the *fox1*-dependent effector genes would result in the induction of plant defenses and the encasement of Δ*fox1*-hyphae.

The observation that Fox1 is involved in the regulation of only a fraction of the plant-induced effector genes suggests the requirement of additional regulatory circuits for successful biotrophic development. It is possible that additional yet to be described transcription factors are involved in the regulation of different effector genes at specific stages in pathogenic development, in response to environmental cues, and/or in a tissue-specific fashion. As a biotrophic pathogen, the requirement of such effectors would be detrimental in the establishment of a biotrophic relationship. Unlike necrotophic fungi, *U. maydis* has a very limited supply of plant cell wall degrading enzymes (Kämper *et al*., 2006). It is likely that secreted proteins are involved in either the modification, or localized degradation of the plant cell wall to assist with the initial penetration and subsequent cell-to-cell proliferation (Doehlemann *et al*., 2008a; Müller *et al*., 2008). Once inside the host, effectors would be required for the establishment and maintenance of the biotrophic interface, and the suppression of plant defenses. Finally, additional effectors may be required to promote the survival of the fungus through the manipulation of plant cell metabolism in order to provide an ideal environment for colonization and subsequent tumor development.

Fox1 represents the first *b*-independent, *in planta* specific regulator involved in the regulation of effectors required for the establishment and maintenance of the biotrophic interface. The simultaneous deregulation of *fox1*-dependent genes impedes the ability of *U. maydis* to adapt to the host plant environment, resulting in the induction of initial host defenses and the subsequent encasement of proliferating hyphae in a plant-produced fungal barrier. Future research will be focused on identifying the signaling pathway(s) that lead to *fox1*-induction, and to dissect the *fox1*-responsive genes and their particular function in suppression of plant defense reactions.

4 Materials and Methods

4.1 Materials and source of supplies

4.1.1 Chemicals, buffers and solutions, media, enzymes and kits

Chemicals

All chemicals used in this study were of research grade, and were obtained from Ambion, Sigma Aldrich, Merck, Fluka, Seakem, Difco, BD Biosciences, BioRad, Amersham, Pharmacia, Sigma, Invitrogen, Vector Laboratories and Carl-Roth.

Solutions and buffers

All standard solutions and buffers used in this study were prepared as described in Ausubel *et al*. (1987) and Sambrook *et al*. (1989). All additional specific solution solutions and buffers are listed in the corresponding method sections.

Media

For *E. coli* cultures, dYT liquid medium and YT solid Medium were used (Ausubel *et al*., 1987; Sambrook *et al*., 1989). Ampicillin was added to a final concentration of 100 μg/ml.

dYT liquid medium
16 g Trypton-Pepton (Difco)
10 g Yeast-Extract (Difco)
5 g NaCl
Add H_2O to 1 l and autoclave

YT solid medium
0.8 % (w/v) Trypton-Pepton (Difco)
0.5 % (w/v) Yeast-Extract (Difco)
0.5 % (w/v) NaCl
1.3 % (w/v) Agar (Roth)
Add H_2O to 1 l and autoclave
Plates were left at room temperature for at least 12 hours prior to usage.

dYT-glycerol medium
16 g Trypton-Pepton (Difco)
10 g Yeast-Extract (Difco)
5 g NaCl
800 ml (v/v) 87% Glycerine (f.c. 69,6%)
Add H_2O to 1 l and autoclave

For *U. maydis*, the media used in this study are described in the following section.

CM-medium (Holliday, 1974; Banuett and Herskowitz, 1989)
2.5 g Casamino acids (Difco)

1 g Yeast-Extract (Difco)
10 ml Vitamin solution (Holliday, 1974)
62.5 ml Salt solution (Holliday, 1974)
0.5 g DNA degr. Free Acid (Sigma, D-3159)
1.5 g NH4NO3
Add H_2O to 980 ml. Adjust pH to 7.0 with 5M NaOH, and autoclave.
20 ml 50% (w/v) Glucose solution (f.c. 1% CM-Glc) or 40 ml 25% Arabinose solution (f.c. 1% CM-Ara).
For CM-solid medium, Agar (Difco) was added to a final concentration of 2%.

PD-solid medium
24 g Potato Dextrose Broth (Difco)
20 g Agar (Difco)
Add H_2O to 1 l and autoclave.

PD-solid medium
24 g Potato Dextrose Broth (Difco)
10 g Charcoal (Sigma C-9157)
20 g Agar (Difco)
Add H_2O to 1 l and autoclave.

$YEPS_L$-medium modified from (Tsukuda *et al*., 1988):
10 g Yeast-Extract (Difco)
10 g Bacto-Peptone (Difco)
10 g Sucrose
Add H_2O to 1 l.

Salt solution (Holliday, 1974):
16 g KH2PO4
4 g Na_2SO4
8 g KCl
4 g $MgSO_4$ x $7H_2O$
1.32 g $CaCl_2$ x $2H_2O$
8 ml Trace elements
Add H_2O up to 1 l and sterile filter

Trace element solution (Holliday, 1974):
60 mg H_3BO_3
140 mg $MnCl_2$ x 4 H_2O
400 mg $ZnCl_2$
40 mg $NaMoO_4$ x 2 H_2O
100 mg $FeCl_3$ x 6 H_2O
40 mg $CuSO_4$ x 5 H_2O
Add H_2O up to 1 l and sterile filter

Vitamin solution (Holliday, 1974):
100 mg Thiamin (Sigma T-4625)
50 mg Riboflavin (Sigma R-4500)
50 mg Pyridoxine (Sigma P-9755)
200 mg Calcium pantothenate (Sigma P-2250)
500 mg p-Aminobenzoic-acid (Sigma A-9878)
200 mg Nicotinic acid (Sigma N-4126)
200 mg Choline chloride (Sigma C-1879)
1000 mg myo-Inositol (Sigma I-5125)
Add H_2O up to 1 l and sterile filter

NM-medium:
0.3% (w/v) KNO_3
6.25% (v/v) Salt solution (Holliday, 1974)
Sterile filtrated 50% (w/v) glucose, 25% (w/v) arabinose, or 50% (w/v) sucrose solution was added to a final concentration of 1%. pH was adjusted to 7.0 with 5M NaOH and sterile filtered.

Array-minimal medium (Scherer *et al*., 2006):
62.5 ml Salt solution (Holliday, 1974)
30 mM L-Glutamine

Add H_2O up to 980 ml, adjust pH to 7.0 with 5M NaOH and Sterile filter
20 ml 50% (w/v) glucose solution (f.c. 1%) or 40 ml 25% (w/v) arabinose solution (f.c. 1%) was added to a final concentration of 1%.

Regeneration Agar (Schulz *et al*., 1990):
a) Top-Agar:
1.5 % (w/v) Bacto-Agar (Difco)
1M Sorbitol (Sigma S-1876)
in $YEPS_L$ -Medium (described above)
b) Bottom-Agar: The same as a), with the additional of 400µg/ml Hygromycin or 4 µg/ml Carboxin

NSY-glycerol medium
8 g Nutrient Broth (Difco)
1 g Yeast-Extract (Difco)
5 g Sucrose (Roth)
800 ml 87% Glycerol (f.c. 69.6%)
Add H_2O up to 1 l

Enzymes

All restriction enzymes, *Taq* DNA polymerase, T4 DNA ligase, Antarctic Phosphatase, Klenow Fragment and Labeling buffer were obtained from NEB. Phusion™ High-Fidelity DNA polymerase was obtained from Finnzymes.

Kits and miscellaneous materials used in this study

The following kits were used in this study as described by the supplier: TOPO TA Cloning Kit (Invitrogen) was used to directly clone PCR products. QiaQuick PCR purification Kit (Qiagen) was used to purify PCR products. QiaQuick Gel Extraction Kit (Qiagen) was used to purify DNA fragments from agarose gels. QIAprep Spin MiniPrep Kit (Qiagen) was used to isolate and purify plasmid DNA before sequencing. RNeasy Kit (Qiagen) was used to purify total RNA to be used in qRT-PCR and microarray experiments. TURBO DNA-*free*™ (Ambion) was used for removal of DNA prior to first-strand cDNA synthesis. SuperScript® III First-Strand Synthesis SuperMix (Invitrogen) was used for first-strand cDNA synthesis. Platinum® SYBR® Green qPCR SuperMix-UDG (invitrogen) was used for qRT-PCR. BioArray-HighYield-RNA Transcript Labeling Kit (Enzo) was used for cRNA synthesis. MicroSpinTM S-300 HR Columns were used for purification of P^{32} labeled probes. DIG-High Prime was used for the nonradioactive labeling of DNA with DIG-11-dUTP alkali-labile. ECL Plus Western Blot detection reagent (GE Healthcare) was

used for chemiluminescene detection.

4.1.2 Oligonucleotides

All oligonucleotides in this study were purchased from Eurofins MWG Synthesis GmbH. The nucleotide sequences are presented form the 5'-end to the 3'-end.

The following oligonucleotides were used for amplifying the left borders (LB) and right borders (RB) for the construction of deletion-, protein fusion-, and truncation-constructs, inserts for over-expression, complementation and point mutation constructs (Brachmann *et al*., 2001; Brachmann *et al*., 2004; Kämper, 2004; Zheng *et al*., 2008), and for quantitative Real-Time PCR.

Table 5: Oligonucleotides used in this study:

Names of primers	Primer sequences (5' to 3')
***um03046* deletion construct**	
Δ03046-lb-for	GTTTAAGACGTGACGTTCGGCGAA
Δ03046-lb-rev	GTTGGCCATCTAGGCCATCC GCGACATTCGTGATCCATCC
Δ03046-rb-for	GTTGGCCTGAGTGGCCGG CGATTGCCGGATAGAAGTGAACT
Δ03046-rb-rev	TAACCTGCGGCGATCTCCCTG CAG
Δ03046-nested-for	TGCCGATCGTGTCTGTTGTTGTCA
Δ03046-nested-rev	AGTAGGGTCCATTCACGGCCACAGC
***um05027* deletion construct**	
Δ05027-lb-for	CCACATCCACAGACAGTAGCCAAC
Δ05027-lb-rev	GTTGGCCATCTAGGCCCAACCTGAGTAGCATGGACAAA
Δ05027-rb-for	GTTGGCCTGAGTGGCCGAAACCAGCTGCATCTGCAC
Δ05027-rb-rev	TCGTGGACGAAGCGTCACAGA TCC
Δ05027-nested-for	CAACCAAGGCCACGTCTTCCACAC
Δ05027-nested-rev	TTCCTACCTGTCTGGGACCGCTTC
***um12258* deletion construct**	
Δ12258-lb-for	ACTGTCCATTGGACCGGCGAAAAC
Δ12258-lb-rev	GTTGGCCATCTAGGCCTAGA ACGCTTCCGTGCTCTCTCGCA
Δ12258-rb-for	GTTGGCCTGAGTGGCCTTTGGGCCACAACGTTTACGAGAA
Δ12258-rb-rev	TCGAAAAGCGTCTAGCTAATGCACG
Δ12258-nested-for	AAAGCCAACAAAGCACCAAGCGTA
Δ12258-nested-rev	CGCTATCTCCTTGAAGCGGTATTAC
***Fox1 mcherry:ha*-fusion construct**	
mcherry-for	GTAGGCCAACGCGGCCACCATG GTGAGCAAGGGCGAGGAGGAT
mcherry-rev	GTAGGCGCGCCTTAAGCGTAATCTGGAACATCGTATGGGTA
fox1-mch-lb-for	CTCACAGCAATCCATCTTCGTC
fox1-mch-lb-rev	GATGGCCGCGTTGGCCTGACGCCTCGAGATAGGGTTAGAGA
fox1-mch-rb-for	GATGGCCTGAGTGGCCGGTTTCAGTTTGCTTGCGACTC
fox1-mch-rb-rev	TGGTTTACCTGTTCTTGGGTCC
fox1-mch-nested-for	CATAGGTACCGATAGCCG ATCC
fox1-mch-nested-rev	CTTAGTCACCCACTCCCTCCTC

Table 5: Oligonucleotides used in this study, continued:

Names of primers	Primer sequences (5' to 3')
***fox1* overexpression plasmid construct**	
fox1-NdeI-for	GTGCATATGTACTGGGCCAAGTCCCACGAC
fox1-NotI-rev	GCGGCCGCCTAACGCCTCGAGATAGGGTTAGA
***fox1 eGFP*-fusion overexpression plasmid construct**	
fox1-NdeI-for	GTGCATATGTACTGGGCCAAGTCCCACGAC
fox1-SfiI-rev	GTGGGCCGCGTTGGCCCGACGCCTCGAGATAGGGTTAGAGAG
***fox1* with 1078 bp native promoter region complementation plasmid construct**	
fox1-np-XbaI-for	GGCTCTAGAGCATGGATGTCATCACTCATATC
fox1-AflII-rev	GTTCTTAAGCTA ACGCCTCGAGATAGGGTTAG
***fox1* under control of the *mig2-5* promoter complementation plasmid construct**	
fox1-NcoI-for	GCCGCCATGGACTGGGCCAAGTCCCACGAC
fox1-AflII-rev	GTTCTTAAGCTA ACGCCTCGAGATAGGGTTAG
***fox1 eGFP*-fusion under control of the *mig2-5* promoter complementation plasmid construct**	
fox1-NcoI-for	GCCGCCATGGACTGGGCCAAGTCCCACGAC
fox1-NcoI-rev	AACCCATGGCACGCCTCGAGATAGGGTTAGAG
***fox1* truncation 1 (TR1: Fox1-79aa) construct**	
TR1-lb-for	CCAGACCTTCCATGTCTCTCAG
TR1-lb-rev	GTTGGCCATCTAGGCCCTATAAAGATGAGAGCTGCACAACC
TR-rb-for	GTTGGCCTGAGTGGCCGGTTTCAGTTTGCTTGCGACTC
TR-rb-rev	TGGTTT ACCTGTTCTTGGGTCC
TR-nested-for	GCGTGGCCACTAGTGAAGAGTAG
TR-nested-for	CTTAGTCACCCACTCCCTCCTC
***fox1* truncation 2 (TR2: Fox1-139aa) construct**	
TR2-lb-for	CCAGACCTTCCATGTCTCTCAG
TR2-lb-rev	GTTGGCCATCTAGGCCCTAACGAAATTTGGGCGCCAACCG
TR-rb-for	GTTGGCCTGAGTGGCCGGTTTCAGTTTGCTTGCGACTC
TR-rb-rev	TGGTTT ACCTGTTCTTGGGTCC
TR-nested-for	GCGTGGCCACTAGTGAAGAGTAG
TR-nested-for	CTTAGTCACCCACTCCCTCCTC
***fox1* truncation 3 (TR3: Fox1-216aa) construct**	
TR3-lb-for	CCAGACCTTCCATGTCTCTCAG
TR3-lb-rev	GTTGGCCATCTAGGCCCTAGTCATACGCAGAAGAGGGCTG
TR-rb-for	GTTGGCCTGAGTGGCCGGTTTCAGTTTGCTTGCGACTC
TR-rb-rev	TGGTTT ACCTGTTCTTGGGTCC
TR-nested-for	GCGTGGCCACTAGTGAAGAGTAG
TR-nested-for	CTTAGTCACCCACTCCCTCCTC
***fox1* construct with mutations at 3 residues required for direct base contacts to DNA**	
fox1-NcoI-for	GCCGCCATGGACTGGGCCAAGTCCCACGAC
fox1-FBD-mutations-rev	GGCTGGAAGGCCACACTTGGCGCCAACTTGTCAACGC
fox1-FBD-mutations-for	GCGTTGACAAGTTGGCGCCAAGTGTGGCCTTCCAGCC
fox1-NcoI-rev	AACCCATGGCACGCCTCGAGATAGGGTTAGAG
Quantitative real-time PCR (qRT-PCR) gene specific primers	
rt-fox1-for	AGGCGCAGATCTGATTGTCTCTGG
rt-fox1-rev	CAATGTCCGACAAGGAGGATGTGG
rt-actin-for	CATGTACGCCGGTATCTCG
rt-actin-rev	CTCGGGAGGAGCAACAATC

Strains

Escherichia coli strains

E. coli TOP10 (Invitrogen) (F^- *mcr*A Δ(*mrr-hsd*RMS-*mcr*BC) Φ80*lacZ*ΔM15 Δ*lac*X74 *deo*R nupG *rec*A1 *ara*D139 Δ (*ara-leu*)7697 *gal*U *gal*K *rps*L(Str^R) *end*A1 λ) which is a derivative of *E. coli* K12 or *E. coli* Mach1 (Invitrogen) (Δ*rec*A1398 *end*A1*ton*A Φ80Δ*lac*M15 Δ*lac*X74 *hsd*R(r_K^- m_K^+)) which is a derivative of *E. coli* W strains (ATCC 9637, S. A. Waksman) were used for cloning purposes.

Maize variety (*Zea mays* spec.)

For all pathogenicity assays, the maize variety Early Golden Bantam (Old Seed Company, Madison Wisconsin, USA) was used.

Ustilago maydis strains

All *U. maydis* strains used in this study are listed in Tables 6 and 7. Table 6 shows all of the strains provided at the beginning of this study. Table 7 shoes all of the strains generated in this study.

Table 6: Progenitor strains used in this study

Strain	Relevant Genotype	Resistance	Reference
AB31	*a2* P_{crg}*:bW2,bE1*	-	(Brachmann *et al*., 2001)
FB1	*a1 b1*	-	(Banuett and Herskowitz, 1989)
FB2	*a2 b2*	-	Banuett and Herskowitz (1989)
SG200	*a1mfa2 bW2bE1*	-	(Bölker *et al*., 1995)
JF1	*a1mfa2 bW2bE1 ip*^{r}[$P_{mig2\text{-}5}$*:egfp*]*ip*^{s}	$Phleo^R$, Cbx^R	(Farfsing *et al*., 2005)
FB1Δ*fox1*	*a1 b1* Δ*fox1*	Hyg^R	(Zahiri *et al*., submitted)
FB2Δ*fox1*	*a2 b2* Δ*fox1*	Hyg^R	(Zahiri *et al*., submitted)
SG200Δ*fox1*	*a1mfa2 bW2bE1* Δ*fox1*	$Phleo^R$, Hyg^R	(Zahiri *et al*., submitted)

Table 7. Strains generated in this study.

Strain	Relevant Genotype	Resistance	Progenitor
FB2*Pcrg1:fox1:egfp*	*a2 b2 ip^r[P$_{crg1}$:fox1:egfp]ip^s*	Cbx^R	FB2
AB31*Pcrg1:fox1:egfp*	*a2 P$_{crg1}$:bW2,bE1 ip^r[P$_{crg}$:fox1:egfp]ip^s*	Phleo^R, Cbx^R	AB31
FB2*Pcrg1:fox1*	*a2 b2 ip^r[P$_{crg}$:fox1]ip^s*	Cbx^R	FB2
AB31*Pcrg1:fox1*	*a2 P$_{crg1}$:bW2,bE1 ip^r[P$_{crg}$:fox1]ip^s*	Phleo^R, Cbx^R	AB31
SG200*fox1:mcherry*	*a1mfa2 bW2bE1 fox1:mcherry*	Phleo^R, Hyg^R	SG200
JF1*fox1:mcherry*	*a1mfa2 bW2bE1 fox1:mcherry ip^r[P$_{mig2-5}$:egfp]ip^s*	Phleo^R, Hyg^R, Cbx^R	JF1
C1	*a1mfa2 bW2bE1 Δfox1 ip^r[P$_{fox1}$:fox1]ip^s*	Phleo^R, Hyg^R, Cbx^R	SG200Δ*fox1*
C2	*a1mfa2 bW2bE1 Δfox1 ip^r[P$_{mig2-5}$:fox1]ip^s*	Phleo^R, Hyg^R, Cbx^R	SG200Δ*fox1*
C3	*a1mfa2 bW2bE1 Δfox1 ip^r[P$_{mig2-5}$:fox1:egfp]ip^s*	Phleo^R, Hyg^R, Cbx^R	SG200Δ*fox1*
C4	*a1mfa2 bW2bE1 Δfox1 ip^r [P$_{mig2-5}$:fox1^{NS180,RS183,HSI84}:egfp]ip^s*	Phleo^R, Hyg^R, Cbx^R	SG200Δ*fox1*
TR1	*a1mfa2 bW2bE1 fox1-79aa*	Phleo^R, Hyg^R	SG200
TR2	*a1mfa2 bW2bE1 fox1-139aa*	Phleo^R, Hyg^R	SG200
TR3	*a1mfa2 bW2bE1 fox1-216aa*	Phleo^R, Hyg^R	SG200
SG200Δ*um03046*	*a1mfa2 bW2bE1 Δum03046*	Phleo^R, Hyg^R	SG200
SG200Δ*um12258*	*a1mfa2 bW2bE1 Δum12258*	Phleo^R, Hyg^R	SG200
SG200Δ*um05027*	*a1mfa2 bW2bE1 Δum05027*	Phleo^R, Hyg^R	SG200

4.1.3 Plasmids and plasmid constructs

pCR.2.1-TOPO (invitrogen): Used for the direct cloning of PCR products.

pBS-hhn (Kämper, 2004): Used to construct gene deletions of *um03046, um12258, um05027, um04813-um04816, um04813, um04814, um04815, um04816*, *fox1* truncations *fox1-79aa, fox1-139aa and fox1-216aa*, and *fox1:mcherry:ha* fusions. Contains a 1,884 bp-*Sfi*I restriction sites harboring a hygromycin resistance cassette (Hyg^R). The *hph* gene is flanked by the *hsp70*-promoter and the T*nos*-terminator.

p123-VCP1 (A. Djamei, unpublished): Used for amplification of the 748 bp *Asc*I-*Sfi*I *mcherry:ha* fragment.

pMF3-h (Brachmann *et al*., 2004): Used to construct the *fox1:mcherry:ha* fusions. Contains a 3,730 bp *Sfi*I-fragment harboring the *egfp* gene and Hyg^R. The *egfp* gene is followed by the T*nos*-terminator. The *Sfi*I-fragment is used for C-terminal eGFP fusions. The *hph* gene is flanked by the *hsp70*-promoter and the T*nos*-terminator.

pRU11Δ*Not*I (Zahiri *et al*., submitted): Used to construct the *fox1* gene overexpression *crg1:fox1*. A pRU11 (Brachmann *et al*., 2001) derivative in which the *Not*I site at position 6474 has been removed by a fill in reaction.

pJF1 (Farfsing *et al*., 2005): Used to construct the *fox1:egfp* fusion over-expression *mig2-5:fox1:egfp*. Contains a 1,634 bp *Xba*I-*Afl*II-fragment harboring the *mig2-5*-promoter and *egfp* gene. The *Nde*I-fragment is used for C-terminal eGFP fusions under the control of the *mig2-5*-promoter. The *egfp* gene is followed by the T*nos*-terminator.

4.1.4 Plasmids and plasmid constructs generated in this study

pRU11-1c-*fox1*: Was used for the integration of the *fox1* ORF under the control of the arabinose-inducible *crg1*-promoter (Brachmann *et al*., 2001) into the *ip*-locus of FB2 and AB31, generating FB2*Pcrg1:fox1* and AB31*Pcrg1:fox1*. A 1,333 bp *Nde*I-*Not*I-fragment *fox1* ORF was amplified from cDNA of FB1 x FB2 infected tumor tissue 5 dpi using primers fox1-NdeI-for and fox1-NotI-rev and incorporated into pRU11Δ*Not*I. pRU11-1c-*fox1* was linearized with *Ssp*I and introduced into the *ip*-locus of strains FB2 and AB31 as described by Brachmann *et al*., (2001). Initiation and termination of transcription are mediated by the *crg1*-promoter and T*nos*-terminator respectively. pRU11-1c-*fox1* contains the ip^r and ip^s locus for homologous integration and selection.

pRU11-1c-*fox1:egfp*: Was used for the integration of *fox1:egfp* under the control of the arabinose-inducible *crg1*-promoter (Brachmann *et al*., 2001) into the *ip*-locus of FB2 and AB31, generating FB2*Pcrg1:fox1:egfp* and AB31*Pcrg1:fox1:egfp*. A 1,344 bp *Nde*I-*Sfi*I-fragment *fox1* gene without stop codon was amplified from cDNA of FB1 x FB2 infected tumor tissue 5 dpi using primers fox1-NdeI-for and fox1-SfiI-rev, and integrated together with a 1 kb *egfp*-T*nos Sfi*I-*Not*I-fragment into the respective *Nde*I-*Not*I sites of pRU11D*Not*I, linearized with *Ssp*I, and integrated into the *ip*-locus of strains FB2 and AB31 as described by Brachmann *et al*., (2001). Initiation and termination of transcription are mediated by the *crg1*-promoter and T*nos*-terminator respectively. pRU11-1c-*fox1:egfp* contains the ip^r and ip^s locus for homologous integration and selection.

pJF1-*Nat-fox1*: Was used for the complementation of the *fox1* deletion by integration of *fox1* under the control of the *native-fox1*-promoter into the *ip*-locus of SG200Δ*fox1* generating C1. The 1,634 bp *Xba*I-*Afl*II *mig2-5:egfp* fragment was removed from pJF1 (Farfsing *et al*., 2005) using *Xba*I and *Afl*II, and replaced with *fox1* and 1078 bp

of the *fox1* promoter region, generated by PCR amplification using primers fox1-np-XbaI-for and fox1-AflII-rev, and integrated into the respective *Xba*I-*Afl*II sites of pJF1, linearized with *Ssp*I, and integrated into the *ip*-locus of strain SG200Δ*fox1* as described by Brachmann *et al*., (2001). Initiation and termination of transcription are mediated by the *native-fox1*-promoter and T*nos*-terminator respectively. pJF1-*Nat-fox1* contains the ip^r and ip^s locus for homologous integration and selection.

pJF1-*fox1*: Was used for the complementation of the *fox1* deletion by integration of *fox1* under the control of the *mig2-5*-promoter into the *ip*-locus of SG200Δ*fox1* generating C2. The 765 bp *Nco*I-*Afl*II *egfp* fragment of pJF1 was replaced by a 1,335 bp *Nco*I-*Afl*II *fox1* gene generated by PCR amplification using primers fox1-NcoI-for and fox1-AflII-rev, linearized with *Ssp*I, and integrated into the *ip*-locus of strain SG200Δ*fox1* as described by Brachmann *et al*., (2001). Initiation and termination of transcription are mediated by the *mig2-5*-promoter and T*nos*-terminator respectively. pJF1 -*fox1* contains the ip^r and ip^s locus for homologous integration and selection.

pJF1-*fox1:egfp*: Was used for the complementation of the *fox1* deletion by integration of *fox1:egfp* under the control of the *mig2-5*-promoter into the *ip*-locus of SG200Δ*fox1* generating C3. To express *fox1:egfp* under control of the *mig2-5*-promoter, the 1,344 bp *fox1* gene without stop codon flanked by *Nco*I sites was generated by PCR amplification using primers fox1-NcoI-for and fox1-NcoI-rev was integrated into the respective *Nco*I-sites of pJF1, linearized with *Ssp*I, and integrated into the *ip*-locus of strain SG200Δ*fox1* as described by Brachmann *et al*., (2001). Initiation and termination of transcription are mediated by the *mig2-5-fox1*-promoter and T*nos*-terminator respectively. pJF1- *fox1:egfp* contains the ip^r and ip^s locus for homologous integration and selection.

pMCH (Zahiri *et al*., submitted): Used to construct the *fox1:mcherry:ha* fusions.
A pMF3-h (Brachmann *et al*., 2004) derivative in which the *egfp* gene was removed and replaced with the 748 bp *Asc*I-*Sfi*I *mcherry:ha* fragment from p123-VCP1 (R. Kahmann and A. Djamei).

pJF1-FBD*mut:egfp*: Was used for the complementation of the *fox1* deletion by integration of a *fox1:egfp* where the following residues, asparagine at position 180 (N180), arginine at position 183 (R183) and histidine at position 184 (H184), were replaced with an alanine, glycine and alanine respectively, under the control of the

mig2-5-promoter into the *ip*-locus of SG200Δ*fox1* generating strain C4. PCR mutagenesis was implemented by amplifying the first half of the *fox1* ORF using primers fox1-NcoI-for and fox1-FBD-mutations-re, and the second half of the *fox1* ORF using primers fox1-FBD-mutations-for and fox1-NcoI-rev, where primers fox1-FBD-mutations-rev and fox1-FBD-mutations-for share overlapping sequences harboring the appropriate nucleotide substitutions resulting in residues N180, R183 and H184 to be mutated to an alanine, glycine and alanine respectively. The two amplicons were placed in the same PCR reaction along with primers fox1-NcoI-for and fox1-NcoI-rev to generate a 1,344 bp *fox1* gene without stop codon flanked by *Nco*I sites. The *Nco*I sites were digested and the amplicon integrated into the respective *Nco*I-sites of pJF1, linearized with *Ssp*I, and integrated into the *ip*-locus of strain SG200Δ*fox1* as described by Brachmann *et al*., (2001). Initiation and termination of transcription are mediated by the *mig2-5-fox1*-promoter and T*nos*-terminator respectively. pJF1- *fox1:egfp* contains the ip^r and ip^s locus for homologous integration and selection.

All plasmids in this study were analyzed by restriction digest and/or DNA sequencing.

Confirmed constructs were linearized by digesting with *Ssp*I and transformed into the *ip*-locus of *U. maydis* using the transformation protocol described in section 4.2.2. All transformants were analyzed by Southern blot for single integrations into the *ip*-locus.

4.2 Genetic, microbiology and cell biology methods

4.2.1 *Escherichia coli*

E. coli media and cultivation

E. coli was grown in dYT liquid medium or on YT solid medium. Liquid cultures were incubated at 37°C at 180 rpm. Solid media were incubated under aerobic condition at 37°C. For making frozen stocks exponentially growing cultures containing the appropriate antibiotic were mixed with dYT-glycerol at a 1:1 ratio and stored at -80°C.

Determination of *E. coli* cell density

E. coli liquid cultures were measured photometrically with a NovospecII photometer (Phamacia Biotech) at 600 nm. In order to obtain a linear reference for the measurement, *E. coli* cultures were diluted to a value of OD_{600} below 0.8. A

corresponding culture medium was used as a reference. A culture density of OD_{600} = 1 correlates to approximately 1.0 x 10^9 cells/ml.

Competent cell preparation and transformation of *E. coli* (Cohen *et al*., 1972)
Competent cell preparation (RbCl/CaCl*2*) and chemical transformation of *E. coli* were modified from Cohen *et al.* (1972). *E. coli* TOP10 cells were grown in 20 ml dYT medium at 37ºC and 200 rpm overnight and diluted 1:200 in 1000 ml dYT medium and continually grown to a cell density of OD600 of ~ 0.6. The culture was transferred to a microcentrifuge tube, incubated on ice for 30 min and centrifuged 4ºC for 8 min at 3000 rpm. The supernatant was discarded and cells were resuspended in 1/3 culture volume (330 ml) of pre-chilled RF1-solution and incubated for 30 min at 4ºC. The suspension was centrifuged at 4ºC for 8 min at 3000 rpm at 4ºC and the supernatant discarded. *E. coli* cells were resuspended in 1/20 culture volume (50 ml) of pre-chilled RF2-solution and incubated for 30 min on ice. Finally, 100 µl aliquots of competent cell suspension in 1.5-ml microcentrifuge tubes were kept on ice for direct use, or stored at - 80°C for later use.

RF1 solution
100 mM RbCl
50 mM $MnCl_2$ x 4 H_2O
30mM K-acetate
10 mM $CaCl_2$ x 2 H_2O
15% (v/v) glycerol
in H_2O_{bid}
pH was adjusted to 5.8 with NaOH and sterile filtered.

RF2 solution
10 mM MOPS
10mM RbCl
75 mM $CaCl_2$ x 2 H_2O
15% (v/v) glycerol
in H_2O_{bid}
pH was adjusted to 5.8 with NaOH and sterile filtered.

For the transforming *E. coli* by chemical transformation, 100 µl aliquots of chemically competent *E. coli* cells were thawed on ice for 2 min. Afterwards, 10-50 ng of plasmid DNA was added, gently mixed and incubated on ice for 15-30 min. *E. coli* cells were then heat shocked at 42°C for 30 sec and immediately cooled on ice for 5 min. For the recovery of the cells, 500 µl dYT medium was added and incubated at 200 rpm for 30 min at 37°C. Finally, the entire *E.coli* cell suspension was plated on YT-agar containing the appropriated antibiotic (100 µg/ml of ampicillin) and incubated at 37°C overnight.

4.2.2 *Ustilago maydis*

U. maydis media and cultivation

Liquid cultures were incubated at 28°C while shaking at 200 rpm. On solid media, *U. maydis* plates were incubated under aerobic condition at 28°C (or 22°C for charcoal containing solid media). For making frozen stocks exponentially growing cultures were mixed with NSY-glycerol at a 1:1 ratio and stored at -80°C.

Determination of _U. maydis_ cell density

U. maydis liquid cultures were measured photometrically with a NovospecII photometer (Phamacia Biotech) at 600 nm. In order to obtain a linear reference for the measurement, *U. maydis* cultures were diluted to a value of OD_{600} below 0.8. A corresponding culture medium was used as a reference. A culture density of OD600 = 1 correlates to approximately 1.5 x 10^7 cells/ml.

Induction of _U. maydis_

The use of inducible promoters enables the control of gene induction or repression by switching the cultivation media. The inducible promoter used in this study is the arabinose-inducible *crg1*-promoter (Brachmann *et al.*, 2001), which is repressed in media containing glucose. Inducible strains were grown in CM, NM or array-minimal media containing glucose as a sole carbon source. The cultures were grown at 28ºC and 200 rpm to a cell density of OD_{600} ~ 0.5. Afterwards, cells were harvested by centrifugation for 5 min at 3200 rpm. Cells were washed once in the corresponding arabinose containing media. Finally, the cells were shifted to CM, NM or array-minimal media containing 1% arabinose as the sole carbon source and grown at 28ºC and 200 rpm for 5-11 h. *U. maydis* strains FB2*Pcrg1fox1* and AB31*Pcrg1:fox1* were induced for 5-11 h in axenic culture to looking for any phenotypic alteration which may arise due to the induction of *fox1*. Strains FB2I*Pcrg1fox1:egfp* and AB31*Pcrg1:fox1:egfp* were induced for 5 h to determine Fox1:eGFP cellular localization.

Protoplast preparation and transformation of _U. maydis_ (Schulz *et al*., 1990)

Protoplast preparation and transformation of *U. maydis* strains was performed as described in Schulz *et al.* (1990). *U. maydis* cells were grown overnight in $YEPS_L$-medium at 28°C and 200 rpm to a cell density of OD600 0.8-1.0. Cells were harvested by centrifugation at 4°C for 5 min at 3200 rpm, washed in 25 ml SCS, and resuspended in 2 ml SCS containing 3.5 mg/ml Novozyme. Cells were incubated for

~10 min at room temperature to digest the cell wall, which was monitored under the microscope. Afterwards, *U. maydis* cells were washed three times with ice cold SCS and centrifuged at 2400 rpm for 8 min at 4°C. This was followed with an additional wash in ice cold STC and centrifugation step. Finally, protoplast pellets were resuspended in 0.5 ml of ice-cold STC, and 50 µl aliquots were made into pre-chilled 1.5 ml microcentrifuge tubes for immediate use, or stored at -80°C for later use.

For transformation of Protoplasts, 1 µl Heparin (1 mg/ml) and up to 10 µl of linearized DNA (3-5 µg) was added to the protoplast aliquot and incubated for 10 min on ice. Afterwards, 500 µl STC/PEG were added to the protoplasts, mixed gently, and incubated for another 15 min on ice. The transformation mix was plated on Regeneration-agar plates. Transformed colonies appeared after 5-7 days and were singled out and grown on PD-agar plates containing the appropriate antibiotic. Single colonies were picked and saved on PD-plates. The regeneration-agar plates were prepared by first pouring a bottom phase with 10 ml regeneration-agar containing the appropriate concentration of antibiotics (hygromycin: 400 µg/ml, carboxin: 4 µg/ml) was poured into plates and solidified. Afterwards, 10 ml of regeneration-agar without antibiotics was poured on top and solidified.

SCS
20 mM Na-citrate, pH 5.8
1 M Sorbitol
in H_2O, sterile filtered

STC
10 mM Tris-Cl, pH 7.5 100 mM $CaCl_2$
1 M Sorbitol in H_2O, sterile filtered

STC/PEG
15 ml STC
10 g PEG4000

4.2.3 Staining and microscopy

Chlorazole Black E (CBE) staining was performed as described (Brachmann *et al*., 2003). Infected leaf tissue was harvested from maize plants 1 to 9 dpi and cleared in ethanol overnight. The next day sampled were washed in water before being treat with 10% KOH at 90^{o}C for 3-4 h. Samples were then washed with water, incubated in CBE staining solution at 60^{o}C overnight, and destained in 50% glycerol for at least one day. Hyphae were visualized using an Axio Imager Z1 microscope (Carl Zeiss AG) in the DIC channel with AxioVision Rel. 4.7 software (Carl Zeiss AG). H_2O_2

accumulation was visualized by diaminobenzidine (DAB) staining as previously described (Molina and Kahmann, 2007). Infected leaf tissue was harvested from maize plants 2 dpi, and the detached side placed into 15 ml Greiner tubes containing 500 µl DAB staining solution (Diaminobenzidine (Sigma; D-8001) 1 mg/ml in H_2O) and incubated in the dark with high humidity overnight. Samples were then cleared in ethanol/chloroform (4:1) for 2 days at 4°C, and stored in 60% glycerol. H_2O_2 accumulation was visualized by bright field microscopy. Cellulose was stained using 0.1% aqueous methylene blue for 15 min, washed with dH_2O, and visualized by bright field microscopy. Visualization of callose using aniline blue was performed as described (Meyer *et al*., 2009). Infected leaf tissue was harvested 4 dpi, cleared in ethanol/acetic acid (3:1) for 24 h and stained with aniline blue in 150 mM KH_2PO_4 (pH 9.5). Callose was visualized through the DAPI channel. GFP fusion proteins were excited at 488 nm, and emission was detected at 495-530 nm. For staining of nuclei with DAPI, Vectashield H-1200 (Vector Laboratories) was used. For visualizing hyphae in the plant vasculature, fungal hyphae were stained with Fluorescein WGA (Vector Laboratories). Plant membranes were visualized using Propidium Iodide (Fluka). Samples were incubated in staining solution (10 µg/ml WGA, 1 µg/ml Propidium Iodide, 0.02% Tween20) for 15 min and washed in 1 x PBS. Confocal images were taken using a TCS-SP5 confocal microscopy (Leica).

4.2.4 Mating and filamentation assays (Schulz *et al*., 1990)

Compatible haploid mixtures FB1 x FB2 (wild-type crosses) and FB1Δ*fox1* x FB2Δ*fox1* (Δ*fox1* crosses), and solopathogenic strains SG200 (wild-type) and SG200Δ*fox1* (Δ*fox1*) were incubated at 28°C and 200 rpm until a cell density of OD_{600} 0.8-1.0 was reached, washed once with sterile water and adjusted to an OD_{600} of ~ 1.0 with sterile water. Compatible strains were equally mixed together. 5 µl of the FB1 x FB2 mixture or SG200 were spotted on charcoal containing CM-glucose solid media plates and incubated at 22°C for 2 days.

4.2.5 Plant infection assay

Pathogenic development of tested strains was assayed by infection of the corn variety Early Golden Bantam (Olds Seeds, Madison, Wins.). Kernels were sown (4 per pot) in potting soil (Fruhstorfer Pikiererde). Maize plants were grown in a Control Master growth chamber (GroBanks CLF Plant Climatics) under the following conditions: 15h/9 h light-dark cycle, with the light period initiating and ending with light intensity ramping for 1 h. Growth temperatures were 28^{o}C (light) and 20^{o}C (dark). *U. maydis* mutant strains and their respective progenitors were incubated at 28°C and 200 rpm until a cell density of OD600 0.8-1.0 was reached, washed once with ddH_2O and concentrated to an OD_{600} of 3.0 in ddH_2O. Compatible haploid strains were equally mixed prior to infection, and 1 ml of the respective cell suspension was injected into the basal stem of 7 day old seedlings using a 26G 3/8" syringe. The infected plants were grown in a phytochamber for an additional 7 days under the above-mentioned conditions. Disease symptoms were investigated 7 days after infection.

4.2.6 Anthocyanin measurement

Maize plants were infected with FB1Δ*fox1* x FB2Δ*fox1* and FB1 x FB2 as described above. At 7 dpi whole plant leaves were harvested in three different pools (8 leaves per falcon tube) and frozen with liquid nitrogen. Anthocyanin extraction and quantification was performed as described (Martin *et al*., 2002). Equal weighted amounts of frozen homogenized material was incubated overnight at 4°C with gentle shaking in 300 µl of 7% (v/v) HCl in methanol. The next day ddH_2O was added to the extract and mixed. Next, 500 µl of chloroform was added to each sample, mixed and centrifuged at 13, 000 rpm for 2 min. Approximately 400 µl of the top layer was transferred to a fresh 1.5-ml microcentrifuge tube along with 600 µl of 1% (v/v) HCl in methanol and centrifuged at 13,000 rpm for 2 min. Anthocyanin measurements were carried out by measuring the absorbency of the respective supernatants at A_{530} and A_{657} on a Ultraspec III (Pharmacia Biotech). Relative anthocyanin concentrations were calculated as absorbency OD_{530} minus OD_{657}. All anthocyanin concentrations were relative to the A_{530} minus A_{657} value obtained from mock-infected plant material.

4.3 Molecular biology standard methods

Standard molecular biology methods, such as purification, precipitation, electrophoresis of DNA or molecular cloning technique, are followed protocols described in Ausubel *et al*. (1987) and Sambrook *et al.*, (1989). The concentration of nucleic acids was determined by photometry. Photometric measurements were performed using a NanoDrop ND-1000 Spectrophotometer. The purity of nucleic acids was determined by the ratio of A_{260} to A_{280}. For purified DNA and RNA samples, the A_{260} to A_{280} ratios were ~1.8.

4.3.1 Isolation of nucleic acids

E. coli plasmid minipreparation

E. coli plasmid minipreparation was performed by "Lysis by Boiling" as previously described in Sambrook *et al.* (1989). *E. coli* culture grown at 37°C and 180 rpm overnight was transferred to a 1.5-ml microcentrifuge tube and centrifuged for 1 min at 13,000 rpm. The supernatant was discarded and the cell pellet was resuspended in 300 µl of STET and 20 µl of Lysozyme solution using a Vibrax-VXR shaker (IKA), and incubated for 1 min at 95°C. To pellet the cell debris, the *E. coli* lysate was centrifuged for 15 min at 13,000 rpm, and cell debris was removed using a sterile toothpick. To precipitate plasmid DNA, 40 µl of 3 M sodium acetate (pH 4.8) and 400 µl of isopropanol were added. The mixture was incubated at room temperature for 5 min followed by centrifugation for 5 min at 13,000 rpm. The supernatant was discarded and the DNA pellet was washed with 70% ethanol, and air dried for 5 min. The DNA pellet was dissolved in 100 µl TE buffer containing 20 µg/ml RNase A, and incubated at on a heating block at 50°C with gentle shaking for 10 min.

STET
50 mM Tris-CL, pH 8.0
50 mM Na_2-EDTA
8% (w/v) Sucrose
5% (v/v) Triton X-100
in H_2O

Lysozyme solution
10 mg/ml Lysozyme
10mM Tris-CL, pH 8.0
in H_2O

Isolation of genomic DNA from *U. maydis* (Hoffman and Winston, 1987)

U. maydis culture grown in YEPSL at 28°C and 200 rpm overnight were transferred to 2-ml microcentrifuge tubes containing 300 mg glass beads, and centrifuged for 2 min at 13,000 rpm. The supernatant was discarded and 400 µl of *Ustilago*-lysis buffer and 500 µl TE-phenol/chloroform was added and shaken for 6-10 min on a Vibrax-VXR shaker (IKA) set to 1,800. Next, samples were centrifuged for 15 min at 13,000 rpm, and 400 µl of the aqueous phase were transferred to new 1.5-ml microcentrifuge tubes. Afterwards, 1 ml of ethanol was added and mixed by inverting 2-3 times, and incubated at room temperature for 5 min. Subsequently the mixtures were centrifuged for 15 min at 13,000 rpm. The DNA pellets were washed once with 70% ethanol and air dried for 5-10 min. Finally, DNA pellets were dissolved in 50 µl TE buffer containing 20 µg/ml RNase A, and incubated at on a heating block at 50°C with gentle shaking for 10 min. Genomic DNA was stored at - 20°C.

***Ustilago*-lysis buffer**
50 mM Tris-Cl, pH 7.5
50 mM Na_2-EDTA
1% (w/v) SDS
in H_2O

TE-phenol/chloroform
Mixture of phenol (in TE-buffer) and chloroform in a 1:1 ratio

***U. maydis* total RNA isolation from axenic culture** (Invitrogen)

Trizol reagent (Invitrogen) was used for total RNA isolation as described by the manufacturer. For liquid cultures, 50 ml of *U. maydis* overnight culture having a cell density of OD600 0.8-1.0 was harvested by centrifugation at 3,200 rpm for 5 min. The pellet was resuspended in 1.0 ml Trizol reagent and transferred to 2-ml microcentrifuge tube containing 300 mg of glass beads and homogenized with a cell mill (Retsch MM200) for 5 min at 30 $_{S/1}$. Afterwards, samples were incubated for 5 min at room temperature, 200 µl of chloroform was added, shaken for 15 sec and incubated for an additional 2-3 min. Samples were centrifuged at 4°C for 15 min at 11,500 rpm. The upper aqueous phase (500 µl) was transferred to a 1.5-ml RNase free microcentrifuge tube. RNA was precipitated by addition of 500 µl isopropanol, and incubating for 10 min at room temperature. After centrifugation at 4°C for 10 min at 11,500 rpm, the pellet was washed once with 1 ml of 70% ethanol, centrifuged at 7,500g for 5 min and air dried. Finally, the RNA pellet was dissolved in 50 µl RNase-

free water and incubated on a heating block at 55°C with gentle shaking for 10 min.

Total RNA isolation from infected plant material (Invitrogen)

For the isolation of total RNA from *U. maydis*-infected plant tissue, tested strains were inoculated into the corn variety Early Golden Bantam (Olds Seeds, Madison, Wins.) as described in the section entitled **"Plant infection assay"**. Maize plants were grown in a phytochamber (Conviron; Model E15) under the following conditions: 15h/9 h light-dark cycle, with the light period initiating and ending with light intensity ramping for 1 h. Growth temperatures were 28°C (light) and 20°C (dark). Infected leaf tissue was harvested at 4 dpi and 5 dpi. In all cases, three independently conducted experiments (biological replicates) were carried out for RNA isolation. Infected leaf tissue were removed from plants, stored in 50 ml Falcon tubes, immediately ground in liquid nitrogen, and directly used for RNA isolation or stored at -80°C for later use. Total RNA was extracted from frozen homogenized infected plant tissue using Trizol reagent (Invitrogen) as described in the previous section **"*U. maydis* total RNA isolation from axenic culture"**.

4.3.2 Nucleic acid blotting and hybridization

DNA-blotting and hybridization (radioactive)

The following method is modified version from Southern (1975). 20-30 µg of genomic DNA was digested using 5-10 U of the respective restriction enzyme in a total volume of 30 µl overnight. Digestions were separated on a 1X TBE 0.8-1% agarose gel for 2 ½ hours at 90V. The gel was incubated in 0.25 M HCl for 15 min to depurinate the DNA, and neutralized in 0.4 M NaOH for an additional 15 min. The nucleic acid fragments were transferred to a nylon membrane (Hybond-XL, Amersham Pharmacia Biotech) by capillary blotting overnight with 0.4 M NaOH. The next day, DNA was cross-linked using a UV Stratalinker 1800 (Stratagene). To block non-specific binding of probe, the membranes were pre-hybridized in Southern-hybridization buffer for 1 h at 65°C. In parallel, 25-100 ng of DNA probe fragment was labeled by random priming with $P^{32}\alpha$-dCTP (Hartmann analytic). The DNA probe was denatured at 95°C for 5 min, quickly chilled on ice for an additional 5 min, and briefly centrifuged. Next, 5 µl labeling buffer (NEB), 6 µl dNTP (-dCTP), 5 µl $P^{32}\alpha$-dCTP and 1 µl (5U) klenow fragment (NEB) was added, gently mixed and incubated at 37°C for 1 h. Finally, the labeled probe was purified with a S-300 HR

Column (GE Healthcare) and denatured at 95°C for 5 min in 10 ml of Southern hybridization buffer. Hybridization was performed overnight at 65°C. The next day the membrane was washed twice with Southern-wash buffer at 65°C for 15 min, wrapped in a plastic bag and exposed to a phosphor screen (Molecular dynamics) for 12-24 h. The Analysis of the screen was performed using a Storm 840 scanner (Molecular dynamics) and processed with IMAGEQUANT (Molecular dynamics).

Southern-hybridization buffer
50 mM Na-phosphate buffer, pH 7.0
100 mM PIPES
100 mM NaCl
1 mM Na_2-EDTA
5% (w/v) SDS
in H_2O

Southern-wash buffer
1x SSC
0.1% (w/v) SDS
in H_2O

DNA-blotting and hybridization (non-radioactive)

A total of 20-30 µg of genomic DNA was digested using 5-10 U of the respective restriction enzyme in a total volume of 30 µl overnight. Digestions were separated on a 1X TBE 0.8-1% agarose gel for 2 ½ h at 90V. The gel was incubated in 0.25 M HCl for 20 min, rinsed briefly in water, incubated I DENAT-solution for 20 min, rinsed in H_2O, and finally incubated in RENAT-solution for 20 min. Labeling reactions were carried out as described in the DIG-High Prime protocol (Roche). The nucleic acid fragments were transferred to a positively charged nylon membrane (Hybond-N+, GE Healthcare) by capillary blotting overnight with 20x SSC. The next day, DNA was cross-linked using a UV Stratalinker 1800 (Stratagene). In parallel, 1.5 µg of DNA probe fragments (in a total volume of 10 µl) were denatured at 99°C for 10 min, briefly centrifuged and put on ice. Next, 1 µl 10x NEB Labeling buffer, 1 µl 10x BSA, 1 µl 10x DIG-dNTP-Mix (1 mM dATP, dCTP, dGTP, 0.65 mM dTTP, 0.35 mM DIG-dUTP) and 1 µl Klenow, and incubated at 37°C overnight. The reaction was stopped with 0.5 µl of EDTA (pH 8.0) and/or heat inactivation at 65°C for 10 min, and precipitated with 1.5 µl 4 M LiCl and 37.5 µl 100% ethanol for 2 h at -20°C. Next, the transfer membrane was prehybridized with 40 ml Southern-hybridization buffer at 65°C in a hybridization oven for 15-30 min. In parallel, the precipitated probe was centrifuged at 13,000 rpm for 15 min, supernatant was discarded, the pellet resuspended in 1 ml of Southern-hybridization buffer, and denatured at 95°C for 5-10

min. Next, the prehybridization solution was discarded, and the 1 ml of labeled probe in 15 ml of prewarmed Southern-hybridization buffer was added to the membrane, and incubated at 65°C overnight in a hybridization oven. The next day, the probe was discarded and the membrane was washed as followed; 2x 15 min with SSPE + 0.1% SDS-buffer at 65°C, 2x 15 min with 1x SSPE + 0.1% SDS-buffer at 65°C, 1x 15 min with 0.1x SSPE + 0.1% SDS-buffer at 65°C, and 1x 5 min with 20 ml DIG-Wash buffer (0.3% (v/v) Tween-20 in DIG1) at 25°C. The following incubation steps were carried out at 25°C: 1x 30 min with 25 ml DIG2 (10x blocking solution in DIG1 (1:10)), 1x 2 h with 10 ml Anti-DIG antibody solution (1:5000 in DIG2), 2x 15 min with DIG-Wash, 1x 5 min with 40 ml DIG3, 1x 5 min with 10 ml CDP-Star solution (100 µl CDP-Star in 10 ml DIG3 (1:100)). Finally, the membrane was sealed in a plastic bag and exposed to a phosphor screen for 1-5 min.

DENAT
1.5 M NaCl
0.4 M NaOH
in H_2O

RENAT
1.5 M NaCl
282 mM Tris-HCl
218 mM Tris-Base
in H_2O

20x SSC
3 M NaCl
0.3 M Na-citrate*2 H_2O
in H_2O, adjust to pH 7.0 with HCl

Southern-hybridization buffer
0.5 M Na-phosphate buffer, pH 7.0
7% (w/v) SDS
in H_2O, autoclave and store at 37°C

20x SSPE
3 mM NaCl
227 mM $Na_2H_2PO_4$*H_2O
20 mM Na_2-EDTA*2 H_2O
in H_2O, adjust to pH 7.4 with NaOH

DIG1 (1x)
0.1 M maleic acid
0.15 M NaCl
in H_2O, adjust pH to 7.5 with NaOH

DIG3 (1x)
0.1 M NaCl
0.05 M $MgCl_2$*6 H_2O
in H_2O, adjust to pH 9.5 with Tris-HCl
and sterile filter

RNA-blotting and hybridization (radioactive)

In order to determine the expression level of a specific gene, RNA blotting and hybridization was performed. Total RNA was denatured in 1X MOPS, 0.8 M glyoxal and 50% (v/v) DMSO, incubated at 50°C for 1 h, and separated by electrophoresis in a 1x MOPS 1% agarose gel for 3 h at 80V with circulated buffer reservoir. Next the RNA was transferred to a nylon membrane by capillary transfer. The capillary transfer of total RNA is similar to genomic DNA. The RNA gel was saturated in 20X SSC buffer for 1 h and blotted to a Hybond-NX membrane (Amersham Biosciences). The hybridization was similarly performed as described in **"DNA-blotting and hybridization"**, with the exception of Northern-hybridization and -wash buffer replacing the Southern-hybridization and -wash buffers. The probe was generated by PCR amplifying *fox1* from FB1 x FB2-infected tumor 5 dpi using primers fox1-NdeI-for and fox1-NotI-rev.

10x MOPS buffer
200 mM MOPS
80 mM Sodium acetate
10 mM Na_2-EDTA*2 H_2O
in H_2O, adjust to pH 7.0 with 5M NaOH

20x SSC buffer
3 M NaCl
0.3 M Na-citrate*2 H_2O
in H_2O, adjust to pH 7.0 with HCl

Northern-hybridization buffer
5% (v/v) 1 M Na-phosphate buffer, pH 7.0 (f.c. 50 mM)
5% (v/v) 1 M PIPES (f.c. 50 mM)
2% (v/v) 5 M NaCl (f.c. 100 mM)
25% (v/v) 20% SDS (f.c. 5%)
0.2% (v/v) 0.5 M EDTA, pH 8.0 (f.c. 1 mM)

Northern-wash buffer
5% (v/v) 20x SSC (f.c. 1x)
25% (v/v) 20% SDS (f.c. 5%)

4.3.3 PCR techniques

Polymerase Chain Reaction (PCR)

This method is modified from Innis *et al.* (1990). A standard PCR reaction consists of ~10 ng template DNA, 1 μM of a pair of primers, 200 μM dNTPs, 1-2 U *Taq* DNA polymerase, and 1 x PCR buffer (10 mM Tris-HCl, 1.5 mM MgCl2, 50 mM KCl, pH

8.3) in a 50 µl reaction. PCR cycling conditions were as follows: denaturation at 94°C for 2 min followed by, 1) 35 cycles of denaturation for 30 s at 94°C, 2) annealing for 30 s at 3 to 5°C lower than the melting temperature (T_m) of the primers, 3) extension (1 min / 1 kb of product at 72°C), repeat steps 1-3 for an additional 34 cycles, and final elongation at 72°C for 7 min, followed by a cooling down of the reaction to 4°C. All PCR reactions were performed using a Thermocycler PTC-100 or PTC-200 (MJ Research). PCR reactions with Phusion™ High-Fidelity DNA Polymerase were performed according to the manufacturer's protocol (Finnzymes).

PCR generation of gene deletion, truncation and *mcherry:ha* gene fusion constructs

The *fox1:mcherry:ha* gene fusion, *tr1*, *tr2* and *tr3* truncations, and gene deletion constructs of *um03046*, *um12258* and *um05027* were all generated by a PCR-based approach (Kämper, 2004). The left and right borders of the target genes were amplified by PCR with primers incorporating distinct *Sfi*I restriction sites for each fragment for site-specific directional ligations. The size of amplified left and right border fragments were ~1 kb for efficient recombination. The Phusion™ High-Fidelity DNA Polymerase was used to minimize the mutation rate. All PCR products were purified using the QiaQuick PCR Purification kit (Qiagen). Left and right border PCR products and the hygromycin resistance cassette (Hyg^R) with compatible *Sfi*I sites were digested with *Sfi*I, purified, and ligated together using T4 DNA Ligase (NEB) generating either a gene deletion, truncation or *mcherry:ha* gene fusion construct. Finally, the ligated products were PCR amplified using nested primer pairs. All PCR amplified constructs were transformed into *U. maydis* as described above. Primers for the left and right 1kb flanking regions and the nested primers for the amplification of the final product after ligation of the left and right border sequences to the hygromycin resistance cassette are given in Table 5.

***U. maydis* deletion strains**

The following gene deletion strains, SG200Δ*um03046,* SG200Δ*um12258* and SG200Δ*um05027* were generated using the PCR based approach described above. Primers for the left and right 1kb flanking regions and the nested primers for the amplification of the final product after ligation of the left and right border sequences to the hygromycin resistance cassette are given in Table 5. Deletion constructs were

transformed into the *U. maydis* solopathogenic strain SG200 as described in section 4.2.2.

fox1:mcherry:ha-gene fusion

To fuse *fox1* to *mcherry:ha*, the *mcherry:ha* was amplified from vector p123-VCP1 (kindly provided by R. Kahmann and A. Djamei) using primers mcherry-for and mcherry-rev. The 748 bp *Asc*I-*Sfi*I *mcherry:ha* fragment was ligated to the hygromycin cassette with compatible *Asc*I-*Sfi*I sites from the pMF3-h vector (Brachmann *et al*., 2004), and digested with *Sfi*I. The 3 kb *Sfi*I *mcherry:ha:hyg*^{R} fragment was then ligated to left (primers fox1-mch-lb-for and fox1-mch-lb-rev) and right border (primers fox1-mch-rb-for and fox1-mch-rb-rev) sequences with compatible *Sfi*I sites; the construct was finally amplified with nested primers fox1-mch-nested-for and fox1-mch-nested-rev, and transformed into the *U. maydis* solopathogenic strain SG200 as described in section 4.2.2.

fox1 truncations TR1, TR2 and TR3

Truncation mutants of the serine-rich region were generated using the above-mentioned PCR based approach. The same right border was used in all truncation constructs (primers TR-rb-for and TR-rb-rev). Primers for the left borders were as follows: TR1 (*fox1*-79aa): TR-lb-for and TR1-lb-rev; TR2 (*fox1*-139aa): TR-lb-for and TR2-lb-rev; TR3 (*fox1*-216aa): TR-lb-for and TR3-lb-rev. The respective left borders and right border were ligated to a 1,884 bp hygromycin resistance cassette with compatible *Sfi*I sites. All three final ligation products were amplified using nested primers TR-nested-for and TR-nested-for and transformed into strain SG200 as described in section 4.2.2.

Quantitative real-time PCR analysis (qRT-PCR)

First-strand synthesis was carried out using SuperScript III (Invitrogen) from 1 μg of total RNA. qRT-PCR was performed using a Bio-Rad iCycler along with Platinum SYBR Green qPCR SuperMix-UDG (Invitrogen). Cycling conditions were as follows: 95^{o}C for 2 min, followed by 45 cycles of 95^{o}C for 30 sec / 65^{o}C for 30 sec / 72^{o}C for 30 sec. To verify *fox1* (*um01523*) expression, qRT-PCR was performed on RNA isolated from SG200 infected leaf tissue at 1, 2, 4 and 8 dpi, and SG200 in axenic culture (liquid array medium: 6.25% (w/v) salt solution, 30mML-Gln, and

1%(w/v) glucose, pH 7.0 (filter-sterilized)). Primers used for *fox1* were rt-fox1-for and rt-fox1-rev (Table 5). The *U. maydis actin* gene (*um11232*) was used as a control (primers were rt-actin-for and rt-actin-rev; Table 5).

4.3.4 Sequence and structure analysis

DNA sequencing technique

DNA was sequenced using a ABI 377 Automated DNA Sequencer (Perkin Elmar). DNA samples to be sequenced were first purified using the QiaQuick PCR purification Kit (Qiagen). The principle of this sequencing technique is based on "DNA sequencing with chain-terminating inhibitors" (Sanger *et al.*, 1992) using the BigDye-Kit (ABI).

The sequencing reaction was performed as follows: BigDye Terminator v3.1 Cycle Mix 2 µl 5X dilution buffer 3 µl sequencing primer (5 pmol/ µl) 1 µl DNA (3-8 kb plasmid) 400 ng	Adjusted to 20 µl with H_2O Sequencing cycling condition: 96 °C for 1 min 30 cycles of 10 s at 96 °C 4 min at 60 °C

Sequencing reactions were precipitated using 10 µl 125 mM EDTA, 9 µl 3M sodium acetate (pH 4.6-4.8), 80 µl HPLC graded H_2O and 400 µl 96% ethanol per 20 µl reaction, centrifuged at 13,000 rpm for 20-30 min followed by two washing steps with 70% ethanol. The pellet was air dried and resuspended in 20 µl formamide with 25 mM Na_2-EDTA (pH 8.0).

Phylogenetic tree construction

Sequences of Fox1 and 58 forkhead proteins obtained through BlastP were aligned using the MAFFT version 6 global alignment G-INS-I strategy (http://align.bmr.kyushu-u.ac.jp/mafft/software/). Six homeodomain protein sequences were used as an out-group. A phylogenetic tree was generated using the all ungapped Neighbour Joining (NJ) method with a bootstrap value of 1000. MAFFT results were exported in Nexus format and visualized using FigTree (http://tree.bio.ed.ac.uk/software/figtree/).

Sequence and structure analyses

Vector NTI (version 11, Invitrogen)
Used for the analysis of genomic and plasmid DNA sequences, restriction analysis, developing cloning strategies, construct design, and primer design.

ApE
Used for the analysis of genomic and plasmid DNA sequences and restriction analysis.

SubLoc (Hua and Sun, 2001)
Used to determine the subcellular localization of a protein.

BlastP (NCBI)
Used to search the non-redundant protein database for similar sequences using a protein query sequence.

ELM server (Puntervoll *et al*., 2003)
Is a resource used to predict functional sites in eukaryotic proteins.

PROSITE (Sigrist *et al*., 2005)
Used to determine if a query sequence contains previously described protein domains and functional sites.

TargetP (version 1.1; Nielsen *et al*., 1997)
Used to determine the subcellular localization of proteins, and if the protein query contains a secretory pathway signal peptide.

MAFFT (version 6)
Used to align protein sequences, phylogenetic tree construction, and calculation of bootstrap 1000 values.

FigTree
Used for the visualization of phylogenetic trees.

Blast2Go (Conesa *et al*., 2005)
Used to carry out functional enrichment analysis on the differentially expressed genes identified on the *U. maydis* microarray experiments.

PageMan V 0.11
Used for the identification of biological processes that were significantly over-represented by differentially expressed genes in the maize microarray experiments

4.3.5 Molecular biology protein methods

Western blot analysis

Strains (FB2*Pcrg:fox1:egfp*, AB31*Pcrg:fox1:egfp*, FB2 and AB31) were grown in liquid minimal media (6.25% (w/v) salt solution, 30mML-Gln, 1%(w/v) glucose (pH 7.0), and filter-sterilized) to OD_{600} of 0.5, washed in ddH_2O, and induced in liquid array medium containing 1% arabinose for 5 h at 28°C. Induction was verified by fluorescence microscopy. 50 ml of each culture were centrifuged at 3200 rpm for 5 min in 50 ml falcon tubes, resuspended in 2 ml lysis buffer (50mM Tris-HCl, pH 7.5, 10% glycerol, 1mM EDTA, 200mMNaCl, along with protease inhibitors 2mM PMSF, 5mM Benzimidine and 1x Complete EDTA free (Roche)) and frozen using liquid nitrogen. The frozen pellet was homogenized using a Retsch MM200 cell homogenizer at maximum frequency for 5 min. Homogenized samples were centrifuged at 14000 rpm for 2 min at 4°C. Protein supernatant sample concentrations were determined using Bradford analysis, and equal amounts of protein were separated by SDS-PAGE and transferred to a PVDF membrane (Amersham) via electroblotting. The membrane was blocked in TBST (50mM Tris-HCL, pH 7.5, 150mM NaCl, 0.05% Tween20) containing 3% non-fat milk powder for 30 min at RT. For detection of Fox1:eGFP, an anti-GFP mouse IgG (Roche) was used as primary antibody (1:1000) in TBST+3% non-fat milk powder. For secondary antibody an anti-mouse IgG HRP conjugate (Promega) was used diluted (1:4000) in TBST+3% non-fat milk powder. Chemiluminescene detection was performed using ECL Plus Western Blot detection reagent (GE Healthcare) as described in the manufacturers protocol.

4.4 DNA microarray analyses

DNA microarray analysis of *fox1*-induction

U. maydis DNA microarray analyses were used to compare the transcriptome profiles of FB2 and FB2Δ*fox1* under uninduced and induced conditions.

Growth conditions

FB2 and FB2Δ*fox1* cultures were grown in array-minimal media containing 1% glucose (uninduced conditions) at 28ºC and 200 rpm to a cell density of OD_{600} ~ 0.5. Afterwards, cell cultures were split in half, and cells were harvested by centrifugation for 5 min at 3200 rpm. Cells were washed once in array-minimal media containing

either 1% glucose or 1% arabinose. Finally, the cells were shifted to array-minimal media containing 1% arabinose (induced conditions) or 1% glucose (uninduced conditions) as the sole carbon source and grown at 28ºC and 200 rpm for 5 h. Afterwards, cells were harvested by centrifugation for 5 min at 3200 rpm in 50 ml Falcon tubes, supernatant discarded, and the cell pellet immediately frozen in liquid nitrogen.

RNA isolation and purification

RNA isolation was performed as described in **"*U. maydis* total RNA isolation from axenic culture"**, and **"Total RNA isolation from infected plant material"**. All RNA to be used for subsequent microarray experiments was purified using the RNeasy Kit (Qiagen). Prior to first- and second-strand cDNA synthesis, RNA quality was determined using Bioanalyzer 2100 and RNA 6000 Nano reagent (Agilent).

cDNA synthesis via Affymetrix

First- and second-strand cDNA synthesis was performed as described in the "GeneChip®

Expression Analysis Technical Manual"

First-strand cDNA synthesis

U. maydis

For first-strand cDNA synthesis 5 µg of total RNA and 2 µl of 50 µM T7-oligo(dT) Primer in a 12 µl reaction was incubated at 70ºC for 10 min, quickly spun down and incubated on ice. Next, 4 µl 5X First-strand cDNA buffer, 2 µl 0.1 M DTT and 1 µl 10 mM dNTP mix was added and incubated at 42ºC for 2 min. Afterwards, 1 µl of SuperScript II RT (Invitrogen) was added to the reaction tube, mixed and incubated at 42ºC for 1 hour.

Z. mays (Affymetrix)

First-strand cDNA synthesis from *Z. mays* total RNA was carried out as described in the "GeneChip Expression Analysis" technical manual (Affymetrix). For first-strand cDNA synthesis 1 µg of total RNA and 2 µl of 50 µM T7-Oligo(dT) Primer in a 12 µl reaction was incubated at 70ºC for 10 min, briefly spun down and incubated at 4ºC for at least 2 min. Next, 7 µl of "First-Strand Master Mix" (4 µl 5x 1st Strand Reaction

Mix, 2 µl 0.1 M DTT, 1 µl 10 mM dNTPs) was added to each RNA/T7-Oligo(dT) Primer mix, mixed thoroughly, briefly centrifuged, and incubated at 42ºC for 2 min. Next, 2 µl of Superscript II was added to each reaction, mixed thoroughly, briefly centrifuged, incubated at 42ºC for 1 h, and cooled down for 2 min at 4ºC.

Second-strand cDNA synthesis

U. maydis

For second-strand cDNA synthesis 91 µl RNase free H_2O, 30µl 5X Second-Strand Reaction buffer, 3 µl 10 mM dNTP mix, 1 µl 10U/µl *E. coli* DNA Ligase, 4 µl 10U/µl *E. coli* DNA Polymerase I and 1 µl 2U/µl *E. coli* RNase H were added into the first strand cDNA reaction, spun down and incubated at 16ºC for 2 h. Afterwards, T4 DNA Polymerase was added and incubated at 16ºC for 5 min. Finally, the reaction was stopped by adding 10 µl of 0.5 M EDTA.

Z. mays (Affymetrix)

Second-strand cDNA synthesis from *Z. mays* total RNA was carried out as described in the "GeneChip Expression Analysis" technical manual (Affymetrix). For second strand cDNA synthesis 130 µl of "Second-Strand Master Mix" (91 µl RNase-free Water, 30 µl 5x 2nd Strand Reaction Mix, 3 µl 10 mM dNTPs, 1 µl *E. coli* DNA ligase, 4 µl *E. coli* DNA Polymerase I, and 1 µl RNase H) were added to the 20 µl first strand cDNA reaction and incubated at 16ºC for 2 h. Next, 2 µl of T4 DNA Polymerase was added to each reaction and incubated at 16ºC for 5 min. Finally, the reaction was stopped by adding 10 µl of 0.5 M EDTA.

Cleanup of double stranded cDNA

Cleanup of double stranded cDNA was performed using the components supplied in the GeneChip® Sample Cleanup Module (Qiagen). 600 µl cDNA Binding buffer was added to the 162 µl cDNA reaction, briefly mixed, applied to a cDNA Cleanup Spin Column, and centrifuged at 10,000 rpm for 1 min. The flow-through was discarded and 750 µl cDNA Wash Buffer was added and centrifuged at 10,000 rpm for 1 min. The flow-through was discarded, and the column centrifuged at 13,000 rpm for 5 min with an open cap to assist with drying. The column was transferred to 1.5-ml microcentrifuge tube, 14 µl Elution Buffer was applied to the column matrix, incubated for 1 min and centrifuged at 13,000 rpm for 1 min. The quality of the

cDNA was examined using the Bioanalyzer 2100 and the RNA 6000Nano reagent (Agilent).

cRNA Synthesis- in vitro transcription (IVT)

U. maydis

For cRNA Synthesis- *in vitro* transcription was performed using the Enzo® BioArrayTM HighYieldTM RNA Transcript labeling Kit (Enzo). 12 µl of double strand cDNA, 4 µl 10X HY Reaction Buffer, 4 µl 10X Biotin-Labeled Ribonucleotides ,4 µl DTT ,4 µl 10X RNase Inhibitor Mix and 2 µl 20X T7 RNA Polymerase were added to a reaction tube and the volume adjusted to 40 µl RNase-free H_2O. The reaction was gently mixed, briefly spun down, and incubated on a heating block at 37ºC for 16 h and 750 rpm for 30 min.

Z. mays (Affymetrix)

For IVT amplification of cRNA 30 µl of "First-Cycle, IVT Master Mix" (5 µl 10x Reaction Buffer, 5 µl ATP Solution, 5 µl CTP Solution, 5 µl UTP Solution, 5 µl GTP Solution, and 5 µl Enzyme Mix) was added to the 20 µl of purified cDNA, briefly centrifuged, and incubated at 37ºC for 16 h.

Cleanup of cRNA

Cleanup of cRNA was performed using the components supplied in the GeneChip® Sample Cleanup Module (Qiagen). 60 µl of RNase-free H_2O was added to the in vitro transcription reaction and mixed thoroughly for 3 sec. Next, 350 µl IVT cRNA Binding Buffer was added, thoroughly mixed, 250 µl of absolute ethanol added, mixed gently, applied to the IVT cRNA Cleanup Spin Column, and centrifuged at 10,000 rpm for 15 sec. Afterwards, 500 µl of 80% ethanol was added to the column and centrifuged at 10,000 rpm for 15 sec. The flow-through was discarded and the column centrifuged for at 13,000 rpm for 5 min with opened cap to assist with drying. The column was transferred to a 1.5-ml microcentrifuge tube and 11 µl RNase-free H_2O was added to the column matrix and centrifuged 13,000 rpm for 1 min. Next, an additional 10 µl of RNase-free H_2O was applied to the column matrix and centrifuged at 13,000 rpm for 1 min. The quality of the cRNA was assessed using a Bioanalyzer 2100 and RNA 6000Nano reagent (Agilent).

cRNA fragmentation for target preparation.

For the fragmentation of cRNA, 5X Fragmentation buffer supplied with the GeneChip® Sample Cleanup Module (Qiagen) was used. This step is critical in obtaining optimal assay sensitivity. 20 μg of cRNA (20μl) and 8 μl 5X Fragmentation buffer were added to a reaction tube and adjusted to 40 μl with RNase-free H_2O. The reaction was incubated at 94ºC for 35 min and stored on ice. The quality of fragmented-cRNA was examined using a 2100 Bioanalyzer and RNA 6000 Nano reagent (Agilent).

Microarray hybridization

For analysis of the *U. maydis* and *Z. mays* transcriptomes, Affymetrix Gene Chip^R *Ustilago* genome arrays and Affymetrix Gene Chip^R maize genome arrays were used respectively. For microarray hybridization, 15 μg fragmented cRNA were mixed with 15 μl 3 nM Control Oligonucleotide B2, 15 μl 20X Eukaryotic Hybridization Control, 3 μl Herring Sperm DNA (10 mg/ml), 3 μl acetylated BSA and 150 μl 2X Hybridization buffer and adjusted to 300μl with RNase-free H_2O. The hybridization cocktail was heated at 99ºC for 5 min, and incubated at 45ºC for 5 min. Next, the cocktail was centrifuged at 13,000 rpm for 5 min at room temperature. To equilibrate an array 200 μl 1X hybridization buffer was filled into the DNA chip and incubated at 45ºC for 10 min with rotation. After equilibration, the solution was removed and refilled with 250 μl of the hybridization cocktail. The array was placed into the hybridization oven and hybridized at 45ºC with 60 rpm for 16 h. The hybridization oven used during this study was the GeneChip® Hybridization Oven 640.

Microarray detection reaction

After 16 h of hybridization, the hybridization cocktail was removed from the array, and the array washed with 300 μl of Non-Stringent Wash Buffer (Wash Buffer A). The detection reaction was followed by washing and staining procedure 2: antibody amplification stain for eukaryotic target protocol (Affymetrix). The staining solution was composed of 300 μl 2x MES stain buffer, 24 μl BSA (50 mg/ml), 6 μl Streptavidin Phycoerythrin (1 mg/ml) in a final volume of 600 μl, and antibody solution composed of 300 μl 2x Stain Buffer, 24 μl BSA (50 mg/ml), 6 μl normal Goat IgG (10 mg/ml) and 3.6 μl biotinylated antibody (0.5 mg/ml). For the washing

and staining steps the Gene Chip Fluidics station 400 (program EukGe2V4) was used. All arrays were scanned on a Affymetrix GSC3000 Microarray Scanner.

Microarray analysis

Affymetrix Gene Chip^{R} *Ustilago* genome arrays were carried out in three biological replicates using Affymetrix protocols (staining: EukGe2V4 protocol on GeneChip Fluidics Station 400; scanning on Affymetrix GSC3000 Microarray Scanner). The image data produced by the microarray scanner was analyzed using Affymetrix Micro Array Suite 5.1(MAS 5.1), which normalized the data and generated expression values for each probe set. Further analysis was carried out using R bioconductor software (http://www.bioconductor.org/), which adjusts the *P*-value for each probe set using the false discovery rate (fdr) method (Benjamini and Hochberg, 1995). The data was then imported into dChip1.3 (http://biosun1.harvard.edu/complab/dchip/) as described (Eichhorn *et al*., 2006) in order to calculated mean expression and fold change values for each probe set. In addition dChip1.3 was also used to remove probe sets where the difference between mean expression values was < 50. Probe sets that were present in at least 2 of 3 biological replicates were considered expressed. Only genes that displayed fold changes > 2-fold with a difference between expression values >50 and a corrected *P*-value < 0.01 were considered as significant. Array data was submitted to GeneExpressionOmnibus (GEO: http://www.ncbi.nlm.nih.gov/geo/; accession GSE19591). Functional enrichment analysis was carried out using the Blast2Go (Conesa *et al*., 2005) Fisher's exact test. Enrichment analysis of secreted proteins was done by performing a hypergeometric distribution comparing the total present calls representing secreted proteins on the FB1Δ*fox1* x FB2Δ*fox1 in planta* arrays to that of the FB1 x FB2 *in planta* arrays. Affymetrix Gene Chip^{R} maize genome arrays were carried out in three biological replicates using RNA isolated from SG200Δ*fox1*-infected leaf tissue as described above. Array data were analyzed as described above. SG200Δ*fox1* array data were compared to SG200 array data published by Doehlemann *et al*., (2008). To identify over-represented biological processes, PageMan V 0.11 (http://mapman.mpimp-golm.mpg.de/pageman/index .shtml) was used. Subsequently, genes in the enriched biological processes were subjected to more stringent analysis. Genes with expression change > 2-fold with a difference between expression values >50 and a corrected *P*-value < 0.001 were considered significant. Array data were submitted to GEO (accession GSE19559).

5 Literature

Aist, J.R. (1976). Papillae and related wound plugs of plant cells. Annu. Rev. Phytopathol. **14,** 145-163.

Alvarez, M.E., Pennell, R.I., Meijer, P.J., Ishikawa, A., Dixon, R.A., and Lamb, C. (1998). Reactive oxygen intermediates mediate a systemic signal network in the establishment of plant immunity. Cell **92,** 773-784.

Appenzeller, L., Doblin, M., Barreiro, R., Wang, H., Niu, X., Kollipara, K., Carrigan, L., Tomes, D., Chapman, M., and Dhugga, K.S. (2004). Cellulose synthesis in maize: isolation and expression analysis od the cellulose synthase (*CesA*) gene family. Cellulose**,** 287-299.

Ausubel, M.A., Ausubel, M.A., Brent, R., Kingston, R.E., Moore, D.D., Seidmann, J.G., and Smith, J.A. (1987). Current protocols in molecular biology. (John Wiley & Sons, Inc.).

Banuett, F. (1992). *Ustilago maydis*, the delightful blight. Trends Genet. **8,** 174-180.

Banuett, F. (1995). Genetics of *Ustilago maydis*, a fungal pathogen that induces tumors in maize. Annu Rev Genet **29,** 179-208.

Banuett, F., and Herskowitz, I. (1989). Different *a* alleles of *Ustilago maydis* are necessary for maintenance of filamentous growth but not for meiosis. Proc. Natl. Acad. Sci. USA **86,** 5878-5882.

Bauer, R., Oberwinkler, F., and Vanky, K. (1997). Ultrastructural markers and systematics in smut fungi and allied taxa. Canadian Journal of Botany **75,** 1273-1314.

Benjamini, Y., and Hochberg, Y. (1995). Controlling the false discovery rate: A practical and powerful approach to multiple testing. J. R. Stat. Soc. Ser. **57,** 289-300.

Birch, P.R., Rehmany, A.P., Pritchard, L., Kamoun, S., and Beynon, J.L. (2006). Trafficking arms: oomycete effectors enter host plant cells. Trends Microbiol. **14,** 8-11.

Bölker, M., Urban, M., and Kahmann, R. (1992). The *a* mating type locus of *U. maydis* specifies cell signaling components. Cell **68,** 441-450.

Bölker, M., Genin, S., Lehmler, C., and Kahmann, R. (1995). Genetic regulation of mating, and dimorphism in *Ustilago maydis*. Can. J. Bot. **73,** 320-325.

Bolwell, G.P., Bindschedler, L.V., Blee, K.A., Butt, V.S., Davies, D.R., Gardner, S.L., Gerrish, C., and Minibayeva, F. (2002). The apoplastic oxidative burst in response to biotic stress in plants: a three-component system. J. Exp. Bot. **53,** 1367-1376.

Bottin, A., Kämper, J., and Kahmann, R. (1996). Isolation of a carbon source-regulated gene from *Ustilago maydis*. Mol. Gen. Genet. **253,** 342-352.

Boura, E., Silhan, J., Herman, P., Vecer, J., Sulc, M., Teisinger, J., Obsilova, V., and Obsil, T. (2007). Both the N-terminal loop and wing W2 of the forkhead domain of transcription factor Foxo4 are important for DNA binding. J. Biol. Chem. **282,** 8265-8275.

Bourguignon, C., Li, J., and Papalopulu, N. (1998). XBF-1, a winged helix transcription factor with dual activity, has a role in positioning neurogenesis in Xenopus competent ectoderm. Development **125,** 4889-4900.

Brachmann, A., Weinzierl, G., Kämper, J., and Kahmann, R. (2001). Identification of genes in the bW/bE regulatory cascade in *Ustilago maydis*. Mol. Microbiol. **42,** 1047-1063.

Brachmann, A., Schirawski, J., Müller, P., and Kahmann, R. (2003). An unusual MAP kinase is required for efficient penetration of the plant surface by *Ustilago maydis*. EMBO J **22,** 2199-2210.

Brachmann, A., König, J., Julius, C., and Feldbrügge, M. (2004). A reverse genetic approach for generating gene replacement mutants in *Ustilago maydis*. Mol. Genet. Genomics **272,** 216-226.

Brisson, L.F., Tenhaken, R., and Lamb, C. (1994). Function of Oxidative Cross-Linking of Cell Wall Structural Proteins in Plant Disease Resistance. Plant Cell **6,** 1703-1712.

Brunet, A., Bonni, A., Zigmond, M.J., Lin, M.Z., Juo, P., Hu, L.S., Anderson, M.J., Arden, K.C., Blenis, J., and Greenberg, M.E. (1999). Akt promotes cell survival by phosphorylating and inhibiting a Forkhead transcription factor. Cell **96,** 857-868.

Caderas, D., Muster, M., Vogler, H., Mandel, T., Rose, J.K., McQueen-Mason, S., and Kuhlemeier, C. (2000). Limited correlation between expansin gene expression and elongation growth rate. Plant Physiol. **123,** 1399-1414.

Campbell, P., and Braam, J. (1999). In vitro activities of four xyloglucan endotransglycosylases from Arabidopsis. Plant J. **18,** 371-382.

Carlsson, P., and Mahlapuu, M. (2002). Forkhead transcription factors: key players in development and metabolism. Dev. Biol. **250,** 1-23.

Catanzariti, A.M., Dodds, P.N., Lawrence, G.J., Ayliffe, M.A., and Ellis, J.G. (2006). Haustorially expressed secreted proteins from flax rust are highly enriched for avirulence elicitors. Plant Cell **18,** 243-256.

Chisholm, S.T., Coaker, G., Day, B., and Staskawicz, B.J. (2006). Host-microbe interactions: shaping the evolution of the plant immune response. Cell **124,** 803-814.

Christensen, J.J. (1963). Corn smut induced by *Ustilago maydis*. Amer Phytopathol Soc. Monogr. **2**.

Clark, K.L., Halay, E.D., Lai, E., and Burley, S.K. (1993). Co-crystal structure of the HNF-3/fork head DNA-recognition motif resembles histone H5. Nature **364,** 412-420.

Cohen, S.N., Chang, A.C., and Hsu, L. (1972). Nonchromosomal antibiotic resistance in bacteria: genetic transformation of *Escherichia coli* by R-factor DNA. Proc. Natl. Acad. Sci. U S A **69,** 2110-2114.

Conesa, A., Gotz, S., Garcia-Gomez, J.M., Terol, J., Talon, M., and Robles, M. (2005). Blast2GO: a universal tool for annotation, visualization and analysis in functional genomics research. Bioinformatics **21,** 3674-3676.

Cosgrove, D.J., Bedinger, P., and Durachko, D.M. (1997). Group I allergens of grass pollen as cell wall-loosening agents. Proc. Natl. Acad. Sci. U S A **94,** 6559-6564.

Darieva, Z., Bulmer, R., Pic-Taylor, A., Doris, K.S., Geymonat, M., Sedgwick, S.G., Morgan, B.A., and Sharrocks, A.D. (2006). Polo kinase controls cell-cycle-dependent transcription by targeting a coactivator protein. Nature **444,** 494-498.

Darieva, Z., Pic-Taylor, A., Boros, J., Spanos, A., Geymonat, M., Reece, R.J., Sedgwick, S.G., Sharrocks, A.D., and Morgan, B.A. (2003). Cell cycle-regulated transcription through the FHA domain of Fkh2p and the coactivator Ndd1p. Curr. Biol. **13,** 1740-1745.

Doehlemann, G., Wahl, R., Vranes, M., de Vries, R.P., Kämper, J., and Kahmann, R. (2008a). Establishment of compatibility in the *Ustilago maydis*/maize pathosystem. Journal of plant physiology **165,** 29-40.

Doehlemann, G., Wahl, R., Horst, R.J., Voll, L.M., Usadel, B., Poree, F., Stitt, M., Pons-Kuhnemann, J., Sonnewald, U., Kahmann, R., and Kämper, J. (2008b). Reprogramming a maize plant: transcriptional and metabolic changes induced by the fungal biotroph *Ustilago maydis*. Plant J.

Eichhorn, H., Lessing, F., Winterberg, B., Schirawski, J., Kämper, J., Müller, P., and Kahmann, R. (2006). A ferroxidation/permeation iron uptake system is required for virulence in Ustilago maydis. Plant Cell **18,** 3332-3345.

Encina, A., and Fry, S.C. (2005). Oxidative coupling of a feruloyl-arabinoxylan trisaccharide (FAXX) in the walls of living maize cells requires endogenous hydrogen peroxide and is controlled by a low-Mr apoplastic inhibitor. Planta **223,** 77-89.

Farfsing, J.W., Auffarth, K., and Basse, C.W. (2005). Identification of cis-active elements in *Ustilago maydis mig2* promoters conferring high-level activity during pathogenic growth in maize. Mol. Plant Microbe Interact. **18,** 75-87.

Ferrer, J.L., Austin, M.B., Stewart, C., Jr., and Noel, J.P. (2008). Structure and function of enzymes involved in the biosynthesis of phenylpropanoids. Plant Physiol. Biochem. **46,** 356-370.

Flor-Parra, I., Vranes, M., Kämper, J., and Perez-Martin, J. (2006). Biz1, a zinc finger protein required for plant invasion by *Ustilago maydis,* regulates the levels of a mitotic cyclin. Plant Cell **18,** 2369-2387.

Freyaldenhoven, B.S., Freyaldenhoven, M.P., Iacovoni, J.S., and Vogt, P.K. (1997). Avian winged helix proteins CWH-1, CWH-2 and CWH-3 repress transcription from Qin binding sites. Oncogene **15,** 483-488.

Gillissen, B., Bergemann, J., Sandmann, C., Schröer, B., Bölker, M., and Kahmann, R. (1992). A two-component regulatory system for self/non-self recognition in *Ustilago maydis*. Cell **68,** 647-657.

Govrin, E.M., and Levine, A. (2000). The hypersensitive response facilitates plant infection by the necrotrophic pathogen *Botrytis cinerea*. Curr. Biol. **10,** 751-757.

Hanchey, P., and Wheeler, H. (1971). Pathological changes in ultrastructure: tobacco roots infected with *Phytophthora parasilica var. nicotianae.* Phytopathology**,** 33-39.

Hatfield, R., and Nevins, D.J. (1986). Purification and properties of an endoglucanase isolated from the cell walls of Zea mays seedlings. Carbohydr. Res. **148,** 265-278.

Hatfield, R., and Nevins, D.J. (1987). Hydrolytic Activity and Substrate Specificity of an Endoglucanase from Zea mays Seedling Cell Walls. Plant Physiol. **83,** 203-207.

Heath, M.C., and Heath, I.B. (1971). Ultrastructure of an immune and susceptible reaction of cowpea leaves to rust infection. Physiol. Mol. Plant Pathol. **1,** 277-287.

Hellqvist, M., Mahlapuu, M., Blixt, A., Enerback, S., and Carlsson, P. (1998). The human forkhead protein FREAC-2 contains two functionally redundant activation domains and interacts with TBP and TFIIB. J. Biol. Chem. **273,** 23335-23343.

Hipskind, J.D., Nicholson, R.L., and Goldsbrough, P.B. (1996). Isolation of a cDNA encoding a novel leucine-rich repeat motif from *Sorghum bicolor* inoculated with fungi. Mol. Plant Microbe Interact. **9,** 819-825.

Hoffman, C.S., and Winston, F. (1987). A ten-minute DNA preparation from yeast efficiently releases autonomous plasmids for transformation of *E. coli*. Gene **57,** 267-272.

Hoi, J.W., Herbert, C., Bacha, N., O'Connell, R., Lafitte, C., Borderies, G., Rossignol, M., Rouge, P., and Dumas, B. (2007). Regulation and role of a

STE12-like transcription factor from the plant pathogen Colletotrichum lindemuthianum. Mol. Microbiol. **64,** 68-82.

Hollenhorst, P.C., Pietz, G., and Fox, C.A. (2001). Mechanisms controlling differential promoter-occupancy by the yeast forkhead proteins Fkh1p and Fkh2p: implications for regulating the cell cycle and differentiation. Genes Dev. **15,** 2445-2456.

Holliday, R. (1974). *Ustilago maydis*. In Handbook of Genetics, R.C. King, ed (New York, USA: Plenum Press), pp. 575-595.

Hua, S., and Sun, Z. (2001). Support vector machine approach for protein subcellular localization prediction. Bioinformatics **17,** 721-728.

Hückelhoven, R. (2007). Cell wall-associated mechanisms of disease resistance and susceptibility. Annu. Rev. Phytopathol. **45,** 101-127.

Hückelhoven, R., and Kogel, K.H. (2003). Reactive oxygen intermediates in plant-microbe interactions: who is who in powdery mildew resistance? Planta **216,** 891-902.

Innis, M.A., Gelfand, D.H., Sninsky, J.J., and White, T.J. (1990). PCR Protocols: a guide to methods and applications. (San Diego, USA, Academic Press).

Inouhe, M., and Nevins, D.J. (1991). Auxin-Enhanced Glucan Autohydrolysis in Maize Coleoptile Cell Walls. Plant Physiol. **96,** 285-290.

Jacobs, A.K., Lipka, V., Burton, R.A., Panstruga, R., Strizhov, N., Schulze-Lefert, P., and Fincher, G.B. (2003). An Arabidopsis Callose Synthase, GSL5, Is Required for Wound and Papillary Callose Formation. Plant Cell **15,** 2503-2513.

Kahmann, R., and Kämper, J. (2004). *Ustilago maydis*: how its biology relates to pathogenic development. New Phytologist **164,** 31-42.

Kamoun, S. (2006). A catalogue of the effector secretome of plant pathogenic oomycetes. Annu. Rev. Phytopathol. **44,** 41-60.

Kamoun, S. (2007). Groovy times: filamentous pathogen effectors revealed. Curr Opin. Plant. Biol. **10,** 358-365.

Kämper, J. (2004). A PCR-based system for highly efficient generation of gene replacement mutants in *Ustilago maydis*. Mol. Genet. Genomics **271,** 103-110.

Kämper, J., Reichmann, M., Romeis, T., Bölker, M., and Kahmann, R. (1995). Multiallelic recognition: nonself-dependent dimerization of the bE and bW homeodomain proteins in *Ustilago maydis*. Cell **81,** 73-83.

Kämper, J., Kahmann, R., Bölker, M., Ma, L.J., Brefort, T., Saville, B.J., Banuett, F., Kronstad, J.W., Gold, S.E., Müller, O., Perlin, M.H., Wösten, H.A., de Vries, R., Ruiz-Herrera, J., Reynaga-Pena, C.G., Snetselaar, K., McCann, M., Perez-Martin, J., Feldbrugge, M., Basse, C.W., Steinberg,

G., Ibeas, J.I., Holloman, W., Guzman, P., Farman, M., Stajich, J.E., Sentandreu, R., Gonzalez-Prieto, J.M., Kennell, J.C., Molina, L., Schirawski, J., Mendoza-Mendoza, A., Greilinger, D., Münch, K., Rössel, N., Scherer, M., Vranes, M., Ladendorf, O., Vincon, V., Fuchs, U., Sandrock, B., Meng, S., Ho, E.C., Cahill, M.J., Boyce, K.J., Klose, J., Klosterman, S.J., Deelstra, H.J., Ortiz-Castellanos, L., Li, W., Sanchez-Alonso, P., Schreier, P.H., Häuser-Hahn, I., Vaupel, M., Koopmann, E., Friedrich, G., Voss, H., Schlüter, T., Margolis, J., Platt, D., Swimmer, C., Gnirke, A., Chen, F., Vysotskaia, V., Mannhaupt, G., Güldener, U., Münsterkotter, M., Haase, D., Oesterheld, M., Mewes, H.W., Mauceli, E.W., DeCaprio, D., Wade, C.M., Butler, J., Young, S., Jaffe, D.B., Calvo, S., Nusbaum, C., Galagan, J., and Birren, B.W. (2006). Insights from the genome of the biotrophic fungal plant pathogen *Ustilago maydis*. Nature **444,** 97-101.

Kangatharalingam, N., Pierce, M.L., Bayles, M.B., and Essenberg, M. (2002). Epidermal anthocyanin production as an indicator of bacterial blight resistance in cotton. Physiol. Mol. Plant Pathol. **61**, 189-195.

Kaufmann, E., Müller, D., and Knochel, W. (1995). DNA recognition site analysis of Xenopus winged helix proteins. J. Mol. Biol. **248,** 239-254.

Khan, R., Tan, R., Mariscal, A.G., and Straney, D. (2003). A binuclear zinc transcription factor binds the host isoflavonoid-responsive element in a fungal cytochrome p450 gene responsible for detoxification. Mol. Microbiol. **49,** 117-130.

Kim, S.H., Virmani, D., Wake, K., MacDonald, K., Kronstad, J.W., and Ellis, B.E. (2001). Cloning and disruption of a phenylalanine ammonia-lyase gene from *Ustilago maydis*. Curr. Genet. **40,** 40-48.

Kimura, S., Laosinchai, W., Itoh, T., Cui, X., Linder, C.R., and Brown, R.M. (1999). Immunogold labeling of rosette terminal cellulose-synthesizing complexes in the vascular plant vigna angularis. Plant Cell **11,** 2075-2086.

Kops, G.J., and Burgering, B.M. (1999). Forkhead transcription factors: new insights into protein kinase B (c-akt) signaling. J. Mol. Med. **77,** 656-665.

Koranda, M., Schleiffer, A., Endler, L., and Ammerer, G. (2000). Forkhead-like transcription factors recruit Ndd1 to the chromatin of G2/M-specific promoters. Nature **406,** 94-98.

Kothe, E. (1996). Tetrapolar fungal mating types: sexes by the thousands. FEMS Microbiol. Rev. **18,** 65-87.

Kuzniak, E., and Urbanek, H. (2000). The involvement of hydrogen peroxide in plant responses to stresses. Acta. Physiol. Plant **22,** 195-203.

Lee, D., and Douglas, C.J. (1996). Two divergent members of a tobacco 4-coumarate:coenzyme A ligase (4CL) gene family. cDNA structure, gene inheritance and expression, and properties of recombinant proteins. Plant Physiol. **112,** 193-205.

Li, D., Sirakova, T., Rogers, L., Ettinger, W.F., and Kolattukudy, P.E. (2002). Regulation of constitutively expressed and induced cutinase genes by different zinc finger transcription factors in Fusarium solani f. sp. pisi (Nectria haematococca). J. Biol. Chem. **277,** 7905-7912.

Mahlapuu, M., Pelto-Huikko, M., Aitola, M., Enerback, S., and Carlsson, P. (1998). FREAC-1 contains a cell-type-specific transcriptional activation domain and is expressed in epithelial-mesenchymal interfaces. Dev. Biol. **202,** 183-195.

Martin, T., Oswald, O., and Graham, I.A. (2002). Arabidopsis seedling growth, storage lipid mobilization, and photosynthetic gene expression are regulated by carbon:nitrogen availability. Plant. Physiol. **128,** 472-481.

Mateo, A., Muhlenbock, P., Rusterucci, C., Chang, C.C., Miszalski, Z., Karpinska, B., Parker, J.E., Mullineaux, P.M., and Karpinski, S. (2004). *LESION SIMULATING DISEASE 1* is required for acclimation to conditions that promote excess excitation energy. Plant. Physiol. **136,** 2818-2830.

McQueen-Mason, S., Durachko, D.M., and Cosgrove, D.J. (1992). Two endogenous proteins that induce cell wall extension in plants. Plant Cell **4,** 1425-1433.

Meyer, D., Pajonk, S., Micali, C., O'Connell, R., and Schulze-Lefert, P. (2009). Extracellular transport and integration of plant secretory proteins into pathogen-induced cell wall compartments. Plant J. **57,** 986-999.

Micheli, F. (2001). Pectin methylesterases: cell wall enzymes with important roles in plant physiology. Trends Plant Sci. **6,** 414-419.

Mielnichuk, N., Sgarlata, C., and Perez-Martin, J. (2009). A role for the DNA-damage checkpoint kinase Chk1 in the virulence program of the fungus *Ustilago maydis*. J. Cell Sci. **122,** 4130-4140.

Molina, L., and Kahmann, R. (2007). An *Ustilago maydis* gene involved in H2O2 detoxification is required for virulence. Plant Cell **19,** 2293-2309.

Morgan, W., and Kamoun, S. (2007). RXLR effectors of plant pathogenic oomycetes. Curr. Opin. Microbiol. **10,** 332-338.

Muller, B., Bourdais, G., Reidy, B., Bencivenni, C., Massonneau, A., Condamine, P., Rolland, G., Conejero, G., Rogowsky, P., and Tardieu, F. (2007). Association of specific expansins with growth in maize leaves is maintained under environmental, genetic, and developmental sources of variation. Plant Physiol. **143,** 278-290.

Müller, O., Kahmann, R., Aguilar, G., Trejo-Aguilar, B., Wu, A., and de Vries, R.P. (2008). The secretome of the maize pathogen Ustilago maydis. Fungal Genet. Biol. **45 Suppl 1,** S63-70.

Nielsen, H., Engelbrecht, J., Brunak, S., and von Heijne, G. (1997). Identification of prokaryotic and eukaryotic signal peptides and prediction of their cleavage sites. Protein Eng. **10,** 1-6.

O'Connell, R.J., and Panstruga, R. (2006). Tete a tete inside a plant cell: establishing compatibility between plants and biotrophic fungi and oomycetes. New. Phytol. **171,** 699-718.

Overdier, D.G., Porcella, A., and Costa, R.H. (1994). The DNA-binding specificity of the hepatocyte nuclear factor 3/forkhead domain is influenced by amino-acid residues adjacent to the recognition helix. Mol. Cell. Biol. **14,** 2755-2766.

Pani, L., Overdier, D.G., Porcella, A., Qian, X., Lai, E., and Costa, R.H. (1992). Hepatocyte nuclear factor 3 beta contains two transcriptional activation domains, one of which is novel and conserved with the Drosophila fork head protein. Mol. Cell Biol. **12,** 3723-3732.

Pedley, K.F., and Walton, J.D. (2001). Regulation of cyclic peptide biosynthesis in a plant pathogenic fungus by a novel transcription factor. Proc. Natl. Acad. Sci. U S A **98,** 14174-14179.

Pic-Taylor, A., Darieva, Z., Morgan, B.A., and Sharrocks, A.D. (2004). Regulation of cell cycle-specific gene expression through cyclin-dependent kinase-mediated phosphorylation of the forkhead transcription factor Fkh2p. Mol. Cell. Biol. **24,** 10036-10046.

Pierrou, S., Hellqvist, M., Samuelsson, L., Enerback, S., and Carlsson, P. (1994). Cloning and characterization of seven human forkhead proteins: binding site specificity and DNA bending. EMBO J. **13,** 5002-5012.

Pondugula, S., Neef, D.W., Voth, W.P., Darst, R.P., Dhasarathy, A., Reynolds, M.M., Takahata, S., Stillman, D.J., and Kladde, M.P. (2009). Coupling phosphate homeostasis to cell cycle-specific transcription: mitotic activation of *Saccharomyces cerevisiae* PHO5 by Mcm1 and Forkhead proteins. Mol. Cell Biol. **29,** 4891-4905.

Puntervoll, P., Linding, R., Gemünd, C., Chabanis-Davidson, S., Mattingsdal, M., Cameron, S., Martin, D.M., Ausiello, G., Brannetti, B., Constantini, A., Ferre, F., Maselli, V., Via, A., Cesareni, G., Diella, F., Super-Furga, G., Wyrwicz, L., Ramu, C., McGuigan, C., Gudavalli, R., Letunic, I., Bork, P., Rychlewski, L., Küster, B., Helmer-Citterich, M., Hunter, W.N., Aasland, R., and Gibson, T.J. (2003). ELM server: A new resource for investigating short functional sites in modular eukaryotic proteins. Nucleic Acids Res. **31,** 3625-3630.

Purugganan, M.M., Braam, J., and Fry, S.C. (1997). The Arabidopsis TCH4 xyloglucan endotransglycosylase. Substrate specificity, pH optimum, and cold tolerance. Plant Physiol. **115,** 181-190.

Qian, X., and Costa, R.H. (1995). Analysis of hepatocyte nuclear factor-3 beta protein domains required for transcriptional activation and nuclear targeting. Nucleic Acids Res. **23,** 1184-1191.

Ramberg, J.E., and McLaughlin, D.J. (1979). Ultrastructural study of promycelial development and basidiospore initiation in *Ustilago maydis*. . Can. J. Bot. **58,** 1548-1561.

Reynolds, D., Shi, B.J., McLean, C., Katsis, F., Kemp, B., and Dalton, S. (2003). Recruitment of Thr 319-phosphorylated Ndd1p to the FHA domain of Fkh2p requires Clb kinase activity: a mechanism for CLB cluster gene activation. Genes Dev. **17,** 1789-1802.

Ridout, C.J., Skamnioti, P., Porritt, O., Sacristan, S., Jones, J.D., and Brown, J.K. (2006). Multiple avirulence paralogues in cereal powdery mildew fungi may contribute to parasite fitness and defeat of plant resistance. Plant Cell **18,** 2402-2414.

Roux, J., Pictet, R., and Grange, T. (1995). Hepatocyte nuclear factor 3 determines the amplitude of the glucocorticoid response of the rat tyrosine aminotransferase gene. DNA Cell. Biol. **14,** 385-396.

Salas Fernandez, M.G., Becraft, P.W., Yin, Y., and Lübberstedt, T. (2009). From dwarves to giants? Plant height manipulation for biomass yield. Trends Plant Sci. **14,** 454-461.

Sambrook, J., Frisch, E.F., and Maniatis, T. (1989). Molecular Cloning: A Laboratory Manual. (Cold Spring Harbor, New York: Cold Spring Harbor Laboratory Press).

Sampedro, J., and Cosgrove, D.J. (2005). The expansin superfamily. Genome Biol. **6,** 242.

Sanger, J., Nicklen, S., and Coulson, A.R. (1992). DNA sequencing with chain-terminating inhibitors. Biotechnology **24,** 104-108.

Scherer, M., Heimel, K., Starke, V., and Kämper, J. (2006). The Clp1 protein is required for clamp formation and pathogenic development of *Ustilago maydis*. Plant Cell **18,** 2388-2401.

Schuddekopf, K., Schorpp, M., and Boehm, T. (1996). The whn transcription factor encoded by the nude locus contains an evolutionarily conserved and functionally indispensable activation domain. Proc. Natl. Acad. Sci. U S A **93,** 9661-9664.

Schulz, B., Banuett, F., Dahl, M., Schlesinger, R., Schäfer, W., Martin, T., Herskowitz, I., and Kahmann, R. (1990). The *b* alleles of *U. maydis*, whose combinations program pathogenic development, code for polypeptides containing a homeodomain-related motif. Cell **60,** 295-306.

Smith, R.C., and Fry, S.C. (1991). Endotransglycosylation of xyloglucans in plant cell suspension cultures. Biochem. J. **279 (Pt 2),** 529-535.

Snetselaar, K.M., and Mims, C.W. (1993). Infection of maize stigmas by *Ustilago maydis*: Light and electron microscopy. Phytopathology **83,** 843.

Snetselaar, K.M., and Mims, C.W. (1994). Light and electron microscopy of *Ustilago maydis* hyphae in maize. Mycol. Res. **98,** 347-355.

Snetselaar, K.M., Bölker, M., and Kahmann, R. (1996). *Ustilago maydis* mating hyphae orient their growth toward pheromone sources. Fungal Genetics and Biology **20,** 299-312.

Snyder, B.A., and Nicholson, R.L. (1990). Synthesis of Phytoalexins in *Sorghum* as a Site-Specific Response to Fungal Ingress. Science **248,** 1637-1639.

Spellig, T., Bölker, M., Lottspeich, F., Frank, R.W., and Kahmann, R. (1994). Pheromones trigger filamentous growth in *Ustilago maydis*. EMBO J. **13,** 1620-1627.

Spellman, P.T., Sherlock, G., Zhang, M.Q., Iyer, V.R., Anders, K., Eisen, M.B., Brown, P.O., Botstein, D., and Futcher, B. (1998). Comprehensive identification of cell cycle-regulated genes of the yeast Saccharomyces cerevisiae by microarray hybridization. Mol. Biol. Cell **9,** 3273-3297.

Sigrist, C.J., De Castro, E., Langendijk-Genevaux, P.S., Le Saux, V., Bairoch, A., and Hulo, N. (2005). ProRule: a new database containing functional and structural information on PROSITE profiles. Bioinformatics **21,** 4060-4066.

Sutton, J., Costa, R., Klug, M., Field, L., Xu, D., Largaespada, D.A., Fletcher, C.F., Jenkins, N.A., Copeland, N.G., Klemsz, M., and Hromas, R. (1996). Genesis, a winged helix transcriptional repressor with expression restricted to embryonic stem cells. J. Biol. Chem. **271,** 23126-23133.

Talarczyk, A., and Hennig, J. (2001). Early defense responses in plants infected with pathogenic organisms. Cell Mol. Biol. Lett. **6,** 955-970.

Tan, P.B., Lackner, M.R., and Kim, S.K. (1998). MAP kinase signaling specificity mediated by the LIN-1 Ets/LIN-31 WH transcription factor complex during *C. elegans* vulval induction. Cell **93,** 569-580.

Tanaka, K., Murata, K., Yamazaki, M., Onosato, K., Miyao, A., and Hirochika, H. (2003). Three distinct rice cellulose synthase catalytic subunit genes required for cellulose synthesis in the secondary wall. Plant Physiol. **133,** 73-83.

Taylor, N.G., Laurie, S., and Turner, S.R. (2000). Multiple cellulose synthase catalytic subunits are required for cellulose synthesis in *Arabidopsis*. Plant Cell **12,** 2529-2540.

Taylor, N.G., Scheible, W.R., Cutler, S., Somerville, C.R., and Turner, S.R. (1999). The irregular xylem3 locus of *Arabidopsis* encodes a cellulose synthase required for secondary cell wall synthesis. Plant Cell **11,** 769-780.

Taylor, N.G., Howells, R.M., Huttly, A.K., Vickers, K., and Turner, S.R. (2003). Interactions among three distinct CesA proteins essential for cellulose synthesis. Proc. Natl. Acad. Sci. U S A **100,** 1450-1455.

Thordal-Christensen, H., Zhang, Z., Wei, Y., and Collinge, D.B. (1997). Subcellular localization of H_2O_2 in plants. H_2O_2 accumulation in papillae and hypersensitive response during the barley-powdery mildew interaction. Plant Journal **11,** 1187-1194.

Tsukuda, T., Carleton, S., Fotheringham, S., and Holloman, W.K. (1988). Isolation and characterization of an autonomously replicating sequence from *Ustilago maydis*. Mol. Cell. Biol. **8,** 3703-3709.

Turner, S.R., and Somerville, C.R. (1997). Collapsed xylem phenotype of Arabidopsis identifies mutants deficient in cellulose deposition in the secondary cell wall. Plant Cell **9,** 689-701.

Urban, M., Kahmann, R., and Bölker, M. (1996). The biallelic *a* mating type locus of *Ustilago maydis*: remnants of an additional pheromone gene indicate evolution from a multiallelic ancestor. Mol. Gen. Genet. **250,** 414-420.

van Dongen, M.J., Cederberg, A., Carlsson, P., Enerback, S., and Wikstrom, M. (2000). Solution structure and dynamics of the DNA-binding domain of the adipocyte-transcription factor FREAC-11. J. Mol. Biol. **296,** 351-359.

Wahl, R., Zahiri, A., and Kämper, J. (2010). The *Ustilago maydis b* mating type locus controls hyphal proliferation and expression of secreted virulence factors in planta. Mol. Microbiol. **75,** 208-220.

Weigel, D., Jurgens, G., Kuttner, F., Seifert, E., and Jackle, H. (1989). The homeotic gene fork head encodes a nuclear protein and is expressed in the terminal regions of the Drosophila embryo. Cell **57,** 645-658.

Wu, Y., Meeley, R.B., and Cosgrove, D.J. (2001). Analysis and expression of the alpha-expansin and beta-expansin gene families in maize. Plant Physiol. **126,** 222-232.

Xu, W., Purugganan, M.M., Polisensky, D.H., Antosiewicz, D.M., Fry, S.C., and Braam, J. (1995). Arabidopsis TCH4, regulated by hormones and the environment, encodes a xyloglucan endotransglycosylase. Plant Cell **7,** 1555-1567.

Zheng, Y., Kief, J., Auffarth, K., Farfsing, J.W., Mahlert, M., Nieto, F., and Basse, C.W. (2008). The *Ustilago maydis* Cys2His2-type zinc finger transcription factor Mzr1 regulates fungal gene expression during the biotrophic growth stage. Mol. Microbiol. **68,** 1450-1470.

Zhong, R., Morrison, W.H., 3rd, Freshour, G.D., Hahn, M.G., and Ye, Z.H. (2003). Expression of a mutant form of cellulose synthase AtCesA7 causes dominant negative effect on cellulose biosynthesis. Plant. Physiol. **132,** 786-795.

6 Supplementary Material

Data CD: The data CD contains one folder entitled Microarray Data which contains the following files:

Supplemental Table 1.xls: DNA microarray data of *Zea mays* genes differentially expressed during *in planta* development of SG200Δ*fox1*-hyphae 4 days post infection.

Supplemental Table 2.xls: DNA microarray data of *Ustilago maydis* genes differentially expressed during *in planta* development of FB1Δ*fox1* x FB2Δ*fox1*-hyphae 5 days post infection.

7 Acknowledgments

First and foremost I would like to thank my supervisor Prof. Dr. Jörg Kämper for giving me the opportunity to come to Germany and do a PhD in his lab. I would also like to thank you for all of the support and encouragement you have provided me throughout the past few years. Not only have you been an excellent supervisor, you have also been a very dear friend to me, and I will always remember all you have done for me. I am also very grateful to my PhD committee members Prof. Dr. Michael Bölker, Prof. Dr. Renate Renkawitz-Pohl and Dr. Martin Thanbichler for their suggestions and guidance.

I would like to thank Ramon for all of the good times, colorful discussions and all the great laughs we shared together. I will never forget the year we spent living at Kaiserallee 40, those days will be missed. I would also like to thank my friends and labmates Miro, Kai, Sarah and Dave for all of the great times we spent together. Without you guys, the lab would not be the same, and the nights spent at the Stövchen will always be remembered.

I would also like to thank Prof. Dr. Regine Kahmann and the Max-Planck-Institute for Terrestrial Microbiology, Marburg, Germany, for their generous support, Volker Vincon for technical assistance, Armin Djamei for plasmid p123-VCP1, Christoph Basse for plasmid pJF1, Magnus Rath for his consultation in plant staining techniques, and the International Max-Planck Research School and Karlsruhe Institute of Technology for funding.

I would like to express my deepest appreciation and love to my parents and my brother for providing me with much support, encouragement, and love. Even though we have been through tough times lately, I am hopeful that the future will prove to be very bright. I love you all very much, and will always have a place for you in my thoughts and my heart.

Finally I would like to thank my girlfriend Steffi for all of the support, encouragement, laughter and love. You have been the source of my energy during the tough times. I love you very much, and look forward to a bright future with you by my side.

8 Curriculum Vitae

Personal Information

Alexander Zahiri

Date of Birth:	July 14th,1979
Place of Birth:	London, England
Gender:	Male
Nationality:	Canadian

Education

09/1986- 06/1991	Elementary school: Hawthorn Elementary, Mississauga, Ontario, Canada.
09/1991- 06/1998	High school: The Woodlands Secondary School, Mississauga, Ontario, Canada. Graduated with honours.

Undergraduate Studies

09/1998- 04/2003	hBSc from The University of Toronto. Specialist: Biology Undergraduate Thesis: "Disruption of a novel MAP3K gene in *Ustilago maydis*."

Graduate Studies

09/2003- 07/2005	MSc in Cell and Systems Biology from The University of Toronto Supervisor: Prof. Dr. Barry Saville Thesis: "Differential gene expression during *Ustilago maydis* teliospore germination."
10/2006- 04/2008	Doctoral studies were initiated at the Max-Planck Institute for Terrestrial Microbiology in Marburg
04/2008- 04/2010	Doctoral studies were continued at the Karlsruhe Institute of Technology at the Karlsruhe Institute of Technology
04/2010	Dissertation at the faculty in Biology of the Philipps-University in Marburg Supervisor: Prof. Dr. Jörg Kämper Thesis: **"**The *Ustilago maydis* forkhead transcription factor Fox1 is involved in the regulation of genes required for the attenuation of plant defenses during pathogenic development "